University Of Alberta

Fibre Type Specific Nuclear Localisation Patterns of NFAT-isoforms in CLFS-Induced Skeletal Muscle Adaptations

By

Pamela Caitlin McDonald

A thesis submitted to the faculty of Graduate Studies and Research

in partial fulfillment of the requirement for the degree of

Master of Science

Faculty of Physical Education and Recreation

Spring 2014

Edmonton, Alberta

ABSTRACT

The purpose of this investigation was to characterize the nuclear localisation patterns of NFAT-c1, -c2, -c3, and -c4 in relation to chronic low-frequency stimulation induced fibre type transitions. A model has been suggested to describe the roles of all 4 NFAT isoforms in activity-dependent skeletal muscle fibre transformation. The findings of the present study are consistent with different yet related roles for the NFAT isoforms in *fast-to-slow* fibre type transformation. NFAT-c1 nuclear expression was associated with transition toward slower fibre types (type-I, type-IIA, type-IID(X)), whereas NFAT-c3 nuclear expression was associated with transformations surrounding the type-IIA fibres. The nuclear expression patterns of NFAT-c2 and NFAT-c4 are consistent with their involvement in fibre maintenance and cell survival.

ACKNOWLEDGEMENTS

I would like to thank first and foremost, my supervisor, Dr. Ted Putman for his patience, expert guidance and overall support. In addition, I would like to express my sincere gratitude to Karen Martins who first piqued my interest in this area and has lent her expertise on more than one occasion. Thank you to Ian MacLean and Karen Martins for all of their technical assistance, without which this document would not be complete. Furthermore, thank you to Stephen Ogg and Arlene Oatway for all of their guidance in microscopy. Lastly, I would like to thank my committee Dr. Walter Dixon and Dr. Darren Delorey for their time and direction throughout. This work was funded by the Natural Sciences and Engineering Council of Canada, Alberta Innovates – Health Solutions, and the University of Alberta.

TABLE OF CONTENTS

LIST OF TABLES

CHAPTER TWO

LIST OF FIGURES

CHAPTER ONE

CHAPTER TWO

CHAPTER THREE

LIST OF SYMBOLS, NOMENCLATURE, AND ABBREVIATIONS

Ach	Acetylcholine
Ad Libitium	At ones leisure
Akt	Protein kinase B
AMPK	Activated protein kinase
ATCC	American type culture collection
ATP	Adenosine Triphosphate
ATPase	Adenosine Triphosphatase
BS-1	Blocking Solution 1
BS-2	Blocking Solution 2
BSA	Bovine serum albumin
Ca^{2+}	Calcium
CaMK	Calmodulin dependent kinase
CCAC	Canadian Council for Animal Care
cGMP	Cyclic guanosine monophosphate
CK1/2	Casein kinase
CLFS	Chronic low-frequency stimulation
Cn	Calcineurin
CnAα	Calcineurin A catalytic subunit alpha
CnAβ	Calcineurin A catalytic subunit beta
CnAγ	Calcineurin A catalytic subunit gamma
CnB1	Calcineurin B regulatory subunit
CnB2	Calcineurin B regulatory subunit
COX	Cytochrome c oxidase
CRM1	Chromosome region maintenance 1
CS	Citrate synthase
CsA	Cyclosporin A
CRM1	Chromosome region maintenance 1
DNA	Deoxyribonucleic acid
DYRK	Dual-specificity tyrosine kinase

EDL	Extensor Digitorum Longus muscle
FG	Fast Glycolytic
FIRE	Troponin I fast intronic regulatory element
FO	Fast Oxidative
FOG	Fast Oxidative Glycolytic
GAPDH	Glyceraldehyde phosphate dehydrogenase
GSK-3β	Glycogen synthase kinase-3
h	Hour(s)
HCl	Hydrogen Chloride
HDAC	Histone deacetylases
Hz	Hertz
JNK	c-jun terminal kinase
kDa	Kilodalton
kg	Kilogram
m.	Muscle
mc	Monoclonal
MEF2	Myocyte Enhancer Factor 2
mg	Milligram
min	Minute
MRF	Muscle Regulatory Factor
mRNA	Messenger ribonucleic acid
mTOR	Mammalian target of rapamycin
Myf-5	Myogenic factor 5
MyHC	Myosin Heavy Chain
MyoD	Myogenic Differentiation 1
*Myoz*1	Myozenin 1
NADH-TR	nicotinamide adenine dinucleotide tetrazolium reductase
NFAT-c1,-c2,-c3,-c4	Nuclear Factor of Activated T-cells
NHR	NFAT homology region

NLS	Nuclear localisation sequence
NMJ	Neuromuscular junction
NO	Nitric Oxide
P13k	Phosphatidylinositide 3-kinases
p38	p38 MAP kinase
PBS	Phosphate buffered saline
pc	Polyclonal
PFK	Phosphofructokinase
PGC-1α	Peroxisome proliferator-activated receptor gamma coactivator 1-alpha
PKA	Protein kinase A
PL	Peroneus Longus muscle
PPAR	Peroxisome proliferator-activated receptor
RHR/RHD	Rel-homology region (domain)
RNA	Ribonucleic acid
SEM	Standard error of the mean
SERCA	Sarcoplasmic reticulum Ca^{2+}-ATPase
SO	Slow Oxidative
TA	Tibialis anterior muscle
TAD	Transactivation domain
TET_f	Tetanic force generation
TnIf	Troponin I fast
wgt	Weight

CHAPTER ONE

INTRODUCTION AND REVIEW OF LITERATURE

1.1 Thesis Overview

This study investigated aspects of Calcineurin (Cn)-Nuclear Factor of Activated T-cells (NFAT) signalling within rat mixed fast-twitch *peroneus longus* muscle (*m.*), in response to Chronic Low-Frequency stimulation (CLFS)-induced *fast-to-slow* fibre type transformations. A previous study by Calabria *et al.*, (2009) showed differential patterns of NFAT-isoform nuclear-cytoplasmic localisation in adult rat muscle fibres, as well as differential sensitivity to electrical activity of the sarcolemma. Maintenance of myosin-heavy-chain(MyHC)-based slow type-I fibres was transcriptionally dependent on NFAT-c1, but also required the presence of NFAT-c2, NFAT-c3 and NFAT-c4. By comparison, maintenance of the fast type-IIA or type-IID(X) fibres demonstrated transcriptional dependence on NFAT-c2 and NFAT-c3, in the presence of NFAT-c4, whilst fast type-IIB fibres were transcriptionally dependent on NFAT-c4 alone. Acute (*i.e.*, 2 hours) experimental exposure of the fast-twitch rat *extensor digitorum longus m.* to a slow motoneuron pattern of 20 Hz electrical stimulation induced translocation of NFAT-c1, NFAT-c2 and NFAT-c3 into the nuclear compartment of muscle fibres. In contrast, the application of a fast-motoneuron pattern of 100 Hz induced nuclear translocation of only NFAT-c2 and NFAT-c3. Thus, it was proposed that different combinations of NFAT-family members control transcriptional regulation of slow and fast fibre genes.

The principal objective of this study was to investigate the time-dependent nuclear localisation of NFAT-c1, NFAT-c2, NFAT-c3 and NFAT-c4 within pure (*i.e.*, type-I, type-IIA, type-IID(X), type-IIB fibres) and hybrid fibre (*i.e.*, fibres expressing 2 or more MyHC-isoforms) types in a rodent model of muscle training. The present study tested the hypothesis that activity-induced *fast-to-slow* fibre type transitions occurring within rat fast-twitch *peroneus longus m.* are preceded by changes in the combinatorial patterns of NFAT isoform nuclear localisation that correspond to the new

slower fibre type. *Fast-to-slower* fibre type transitions were induced by applying Chronic Low-Frequency electrical Stimulation (CLFS – 10 Hz for 12 hours/day) for 0-, 5- , 10- , or 21-days. CLFS was chosen as the experimental model of muscle training because it has proven to be highly reproducible, inducing rapid, time-dependent *fast-to-slower* fibre type transitions in rat skeletal muscles that proceed sequentially in the direction of IIB → IID(X) → IIA → I, passing through many transitional hybrid fibre types according to the *"next-nearest neighbour rule"* (Ljubicic *et al.*, 2005;Pette & Staron, 1997;Pette & Vrbová, 1999). CLFS has the added advantage of inducing muscle fibre adaptation that is devoid of fibre injury and compensatory regeneration (Putman*, et al.*, 1999, 2000; Putman*, et al.*, 2001). It also has been shown to induce low-amplitude biphasic intracellular Ca^{2+}-transients (Carroll, S. L.*, et al.*, 1999) sufficient for Cn-activation (Healy*, et al.*, 1997), and to up-regulate MyHC-I in a manner that is dependent on nuclear import of NFAT-c1.

The present study used immunohistochemical staining of all four fibre types as well as nuclear stains of the four NFAT-c isoforms to match the localisation of each NFAT isoform with each fibre type. Changes in myonuclear content were enumerated. The absolute and relative changes in myonuclei that stained positive for the various NFAT-c isoform were also quantified. CLFS induced *fast-to-slower* fibre transformations, as evidenced by a significant increase in the proportion of fibres expressing MyHC-IIa at 5- , 10- and 21-days. Most of the increase in MyHC-IIa expression resulted from time-dependent increases in the hybrid type-IIA/IID(X) and type-IIA/IID(X)/IIB fibres. CLFS induced *fast-to-slower* fibre transformations were also indicated by significant decreases in the proportions of pure type-IID(X) and type-IIB fibres, and of hybrid type-IID(X)/IIB fibres. As the first study of this kind to examine the *peroneus longus m.*, a muscle also targeted by CLFS, the present study also reports unique phenotypic properties compared to the *tibialis anterior m.* and *extensor digitorum longus m.* that

were investigated in previous reports. Unique properties of the *peroneus longus m.* include the expression of a significantly greater proportion of hybrid fibres at rest (*i.e.,* 30±6%), and a comparatively faster rate of fibre transformation.

The results of this study indicate an important role for NFAT-c1 in mediating the intracellular signal of a slow motoneuron pattern of stimulation, evidenced by the increase in overall number of NFAT-c1 positive nuclei at 5-days, especially within myonuclei of type-I and of type-IIA/D(X) fibres, the latter preceding a significant increase in the proportion of type-IIA/D(X) fibres present in the muscle. The results also support the involvement of NFAT-c2 in fibre type maintenance at rest, due to the high initial level of NFAT-c2 and the overall decrease with stimulation and fibre type transition, particularly in type-IID(X) fibres, which subsequently decrease. On the other hand, the frequency of NFAT-c3 nuclear localisation tended to increase during 10-days of CLFS, being significantly elevated in hybrid type-IIA/D(X) fibres after 5-days of CLFS, and in hybrid type-I/IIA and -IIA/D(X) fibres after 10-days of CLFS; the increase in NFAT-c3 nuclear localisation within hybrid type-IID(X)/B fibres preceded the detection of MyHC-IIa within this fibre population after 21-days of CLFS. Thus, the results are consistent with the involvement of NFAT-c3 in regulating the transition of the fastest type-IIB fibres toward slow, oxidative type-IIA fibres, by positively regulating MyHC-IIa expression and/or negatively regulating MyHC-IIb expression. The frequency of nuclear NFAT-c4 localisation remained consistent throughout stimulation with CLFS, which reinforces the notion that NFAT-c4 is a common requirement for the maintenance of all muscle fibre types. The collective findings of this study are consistent with distinct roles for the four NFAT-c isoforms that form important foundations for the maintenance of fibre type heterogeneity, and muscle fibre plasticity.

1.2 Limitations

The use of a rat model to investigate aspects of Cn-NFAT signalling in both steady-state control muscles and during CLFS-induced *fast-to-slow* fibre type transitions limits the extent to which the research outcomes may be extrapolated to other tissues within the rat, and to other vertebrate species. Compared with muscles of larger vertebrate species, rat fast-twitch muscles are unique in several respects that are relevant to the present study. Firstly, type-IIB fibres are abundantly expressed in muscles of rats and smaller rodents but not in much larger species, such as humans. This would seem to have important implications for understanding fundamental aspects of Cn-NFAT signalling that involve NFAT-c4. Secondly, compared with larger vertebrates, rat muscles do not develop muscle fibre damage in response to CLFS (Pette & Staron, 1997), and demonstrate substantial resistance to undergo full transition to type-I fibres that appears to result from greater capacity to meet the metabolic demands at the onset of CLFS (Green*, et al.*, 1992; Green & Pette, 1997; Hicks*, et al.*, 1997). The resulting fundamental intracellular differences (*e.g.*, [Ca^{2+}], NO*) would thus differently influence the intracellular signalling properties of NFAT-c1, and possibly related components of Cn-NFAT signalling.

Thirdly, previous studies of Cn-NFAT signalling that investigated the mixed fast-twitch *extensor digitorum longus m.* (Calabria*, et al.*, 2009), and *plantaris m.* (Dunn*, et al.*, 2000; Dunn & Michel, 1999; Dunn*, et al.*, 2002) of rat and mouse hindlimb used an overload model, which is known to induce fibre damage. Because the present study examined rat *peroneus longus m.,* which possessed a greater proportion of hybrid fibres, and because CLFS induces faster and more extensive adaptive transformation, without injury (Martins*, et al.*, 2012), it is reasonable to expect quantitative and qualitative differences in Cn-NFAT signalling when directly compared.

Finally, most of the research investigating Cn-NFAT signalling has been completed using other tissues (*e.g.,* T-Cells, neurons) (Li, H.*, et al.*, 2011; Oh-hora & Rao, 2009; Wu*, et al.*, 2007). This is an important consideration pertinent to interpreting the results of the present study. Cn-NFAT signalling has been identified as a signalling pathway of ancient origins that is ubiquitously expressed within vertebrate tissue (Crabtree, 1999; Wu*, et al.*, 2007), and has demonstrated regulation over a diverse range of biological processes (Armstrong, S. P.*, et al.*, 2009; Sitara & Aliprantis, 2010). Thus, variations in signalling between tissues may be dependent on the cellular environment in which Cn-NFAT signalling operates, determining operational parameters such as, up-stream activators, thresholds of activation, and down-stream targets. Indeed the recent identification of novel targets for both Cn-enzyme complex and NFAT-isoforms suggests that a number of Cn-NFAT signalling targets remain to be identified within mammalian skeletal muscle (Li, H.*, et al.*, 2011; Oh-hora & Rao, 2009; Wu*, et al.*, 2007).

1.3 Skeletal Muscle Fibre Diversity and Plasticity

Adult skeletal muscle is a post-mitotic, heterogeneous, multinucleated tissue that consists of a spectrum of fibre types ranging from slow-twitch fibres, with a high potential for oxidative ATP production, to fast-twitch fibres that possess high potential for glycolytic ATP production (Bass*, et al.*, 1969; Pette & Staron, 1997). The initial discovery of two distinct fibre types came in 1873 with the characterization of “white” and “red” muscle by Louis Ranvier in rabbit and ray (Ranvier, 1873). The next notable finding occurred in 1960 with the classic cross re-innervation study of Buller, Eccles & Eccles (1960), who demonstrated the fundamental nature of the innervating motor nerve on muscle fibre phenotype. When a previously denervated fast-twitch muscle was re-innervated with the nerve of a slow-twitch muscle it underwent a *fast-to-slow* fibre type transformation. On the other hand, when they denervated a slow-twitch muscle and subsequently re-innervated it

with the nerve from a fast-twitch muscle it underwent a *slow-to-fast* fibre type transformation.

Pioneering studies conducted by Salmons & Vrbova (1967, 1969), and by Pette, *et al.* (1976; 1973) further revealed that application of electrical stimulation to intact nerves altered the fundamental phenotypic properties of the target muscles, such as contraction speed, metabolic capacity and fibre types. More recent research revealed the large inherent adaptability, or plasticity, of adult skeletal muscle was largely dictated by the specific impulse patterns delivered by motoneuron to its target muscle (*For reviews see Pette, et al., 1990, 1992, 1997, 1999, 2001, & 2002*). For example, slow specific motoneurons deliver a tonic low-frequency stimulation pattern (*i.e.*, 10-30 Hz) (Hennig & Lømo, 1985), whereas fast motoneurons produce a phasic high-frequency stimulation pattern (*i.e.*, 80-150 Hz) (Hennig & Lømo, 1985). Discharge patterns have since been correlated with fatigue resistance, fibre types and contractile properties (*as recently reviewed by Schiaffino & Reggiani, 2011*).

The classical determination of fibre types was based on differences in the pH lability and sulfhydryl dependence of myosin ATPase within the various MyHC isoforms, which allowed the histochemical identification of 3 fibre types (Brooke & Kaiser, 1970). Functional studies have since established that the MyHC isoform determines the rate of force development and the maximum shortening velocity (Bottinelli, Betto*, et al.*, 1994a, 1994b; Bottinelli, Canepari*, et al.*, 1994; Bottinelli*, et al.*, 1991) providing further rationale for the nomenclature that described slow-twitch type-I fibres, fast-twitch type-IIA and fast-twitch type-IIB fibres. Thus, the myosin content became the primary basis for muscle fibre nomenclature and an important basis for investigating muscle fibre diversity and plasticity. Often supported by the histochemical co-determination of glycolytic enzyme activity (Martin*, et al.*, 1985) and oxidative enzyme activity (Martin*, et al.*, 1985; Skorjanc*, et*

al., 1997), myosin ATPase histochemistry also formed the basis for a complementary classification system for the 3 fibre types: Slow-Oxidative (SO), Fast-Oxidative (FO), Fast-Glycolytic (FG).

Refinements to SDS-PAGE analysis and in MyHC isolation procedures (Bar & Pette, 1988) and the development of isoforms specific anti-MyHC monoclonal antibodies (Schiaffino*, et al.*, 1989) eventually led to the independent discovery of a fourth major MyHC isoform. Using SDS-PAGE, Bar & Pette (1988) discovered a new fast MyHC isoform, which they named MyHC-IId; they also named the corresponding histochemically identified fibre "type-IID." Schiaffino *et al.* (1989) created a panel of monoclonal anti-MyHC antibodies which when applied to mammalian muscle led to the immunohistochemical identification of a new fibre type, which they named type-IIX. Numerous studies that followed determined these two isoforms to be one and the same, and that type-IID(X) fibres possess significant amounts of both oxidative and glycolytic enzyme activities (Hämalainen & Pette, 1993, 1995), establishing it also as the FOG fibre type. In recognition of these discoveries, the nomenclature MyHC-IId(x) is typically used to refer to the protein, while type-IID(X) refers to the corresponding fibre type. Present day fibre type nomenclature is based on the prevalent MyHC isoform present, as determined by immunocytochemical analyses of serial sections. This includes "pure" fibres expressing only one MyHC isoform, such as slow-twitch type-I and fast-twitch type-IIA, type-IID(X), and type-IIB, which contain the corresponding MyHC isoforms listed in increasing order of shortening velocity: MyHC-I (encoded by MYH7 gene), MyHC-IIa (encoded by MYH2 gene), MyHC-IId(x) (encoded by MYH1 gene), and MyHC-IIb (encoded by MYH4 gene). The application of several isoform-specific anti-MyHC monoclonal antibodies on serial sections also has revealed a spectrum of transitional hybrid fibres (*i.e.,* those expressing two or more MyHC isoforms simultaneously) that emerge in response to chronic changes in the pattern of muscle contractile activity.

1.3.1 Skeletal muscle adaptation in response to exercise training

Activity patterns largely dictate adaptations in contractile machinery, membrane properties, Ca^{2+} shuttling mechanisms (Gundersen*, et al.*, 1988; Lynch*, et al.*, 1993), metabolic profile and the structure of the cytoskeleton. The features of training adaptation are specific to the type of training stimulus, including the intensity, volume and duration. Motor unit recruitment with training follows a specific pattern, called Henneman's size principle. Henneman *et al.* (1974, 1985) found that at low forces only small motor units are recruited, as the force increases, the size of the motor unit recruited increases. Therefore, the protein signalling as well as metabolic pathways, and cytoskeletal properties initiated by exercise will depend on which motor units are recruited. Shifts in MyHC content that occur with strength and endurance training vary in direction and intensity (Salmons, 1994). Salmons (1994, 2009) suggested there is a threshold at which each fibre type will transform to the next slowest fibre type. This threshold appears to correlate with the Ca^{2+} transients that are released in response to different types of stimuli. Employing different exercise models provides insight into the different Ca^{2+} transients released during exercise, in addition to other downstream factors involved in skeletal muscle adaptation.

The response of skeletal muscle to resistance training and high-frequency sprint training has demonstrated unique adaptations in mammalian skeletal muscle. High load resistance training, for example, causes an initial decrease in type-IID(X) fibres, with a subsequent increase in cross sectional area, along with capillarisation (angiogenesis) to maintain capillary density (Green*, et al.*, 1998). Generally resistance training has been shown to cause early changes within the type-II fibres, namely increased expression of MyHC-IIa (Carroll, T. J.*, et al.*, 1998; Hather*, et al.*, 1991; Staron*, et al.*, 1990; Williamson*, et al.*, 2001). High intensity exercise has similar effects with a trend toward the IIA fibre type (Jansson*, et al.*, 1990), with

recovery being dependent on the oxidative potential of the muscle (Jansson*, et al.*, 1990). Sprint trained athletes seem to have greater rates of force development and relaxation than their endurance trained counterparts (Carrington*, et al.*, 1999; Maffiuletti*, et al.*, 2001). In regards to fibre type transition, the literature is not consistent whether sprint training causes fibre adaptation in a certain direction, however it is hypothesized that there is an overall shift toward a type-IIA fibre (Andersen*, et al.*, 1994; Esbjornsson, Hellsten-Westing*, et al.*, 1993). Exercise models tend to be intermittent and milder than the application of chronic electrical stimulation, and can dilute single fibre results when studied at the whole muscle level because analytical measures also include inactive fibres (Salmons, 2009). Thus, the confounding influence of inactive fibres seems to explain much of the uncertainty with regards to sprint training adaptations.

Some interesting examples of the combined effects of environmental perturbations and exercise training further illustrate the scope of muscle plasticity. To determine the influence of intracellular energetics on muscle phenotype, creatine supplementation was studied in rats who completed 91 consecutive days of voluntary wheel running of a phasic, high-frequency nature. When rat *plantaris m.* was creatine loaded by oral supplementation before and during long-term voluntary exercise training, the expected activity-induced increases in the proportion of type-IIA fibres did not occur; the major adaptive responses were greater proportions and cross-sectional areas of type-IID(X) and type-IIB fibres (Gallo*, et al.*, 2006). Consequently creatine-loaded muscles displayed greater power output, as demonstrated by an 18% increase in tetanic force generation (TET_f) and a 10% increase in fatigue resistance, compared with controls (Gallo*, et al.*, 2006). Long-term creatine loading also seems to relieve the need for parvalbumin-dependent facilitated diffusion of Ca^{2+}, by retaining the high glycolytic potential typical of type-IIB fibres, while also benefitting from a 70% increase in the capacity for oxidative ATP production (Gallo*, et al.*, 2008). Collectively the adaptive

changes observed appear to support greater power output while also increasing fatigue resistance. A second example is exercise training under hypoxic conditions. Training under hypoxic conditions causes an increase in fatigue resistance through an increase in aerobic capacity and oxygen carrying capacity of the muscle (Abdelmalki*, et al.*, 1996; Esbjornsson, Jansson*, et al.*, 1993). When subjects are sedentary under the same conditions, there are contradictory findings, namely a decrease in type-II fibre size as well as a reduced oxidative capacity (Abdelmalki*, et al.*, 1996). Thus, training under ischemic conditions causes a change in the muscle metabolic profile in a direction facilitating aerobic metabolism.

In response to endurance exercise, which induces a slow motoneuron activity pattern, *fast-to-slow* fibre type transformation occurs according to the "next-nearest neighbour rule" (Pette & Staron, 2000, 2001). According to this rule, hybrid fibres (*i.e.,* fibres expressing more than one MyHC isoform) bridge the gap between pure fibres (*i.e.,* fibres expressing one MyHC isoform), following a predictable pattern of transformation based on co-expression of MyHC isoforms as follows.

IIb ↔ IId(x)/IIb ↔ IId(x) ↔ IIa/IId(x) ↔ IIa ↔ I/IIa ↔ I

Hybrid fibres expressing three or more isoforms have also been observed in both transforming and normal muscle. It should be noted that suggestions have been made that there is a limited range through which fibres can transition. For example, fibres derived from a slow developmental lineage can only transition between type-I↔IIA↔IID(X) fibres (Ausoni*, et al.*, 1990). Similarly, fibres derived from a fast developmental lineage can only transition between type-IIA↔IID(X)↔IIB fibres (Ausoni*, et al.*, 1990). With stimulation, a fibre can only shift to certain neighbour fibre types and not through the entire continuum (Ausoni*, et al.*, 1990; Jaschinski*, et al.*, 1998). Challengers of the next-nearest neighbour rule have stated that fibres can

express two non-neighbour MyHC isoforms at the same time without expressing the middle one (*i.e.,* MyHC-I/IId(x)) (Caiozzo*, et al.*, 2003) however, no fibres of this nature were found in this investigation.

Concurrent with the switch to a slower phenotype, an increase in capillarisation, as well as oxidative enzyme activity occurs with endurance training (Hermansen & Wachtlova, 1971; Holloszy, 1967). In addition, the Ca^{2+} activated contractile characteristics of muscle are modified (Lynch*, et al.*, 1993). An intense bout of endurance exercise (*i.e.,* marathon) (Staron*, et al.*, 1989) can decrease the lipid content in muscle and cause it to remain lower than pre-marathon for 7 days after. In regard to the characteristics of specific fibre types, endurance training causes an increase in power output of type-I and type-IIA fibres, when compared to recreational individuals (Harber & Trappe, 2008).

By examining a variety of exercise training models the inherent plasticity of skeletal muscle can be readily observed. In addition, environmental changes further influence aspects of muscle adaptation and plasticity. These two factors form the basis for muscle fibre plasticity, acting cooperatively to regulate adaptive response, which may encompass all aspects involved in muscle structure and function. However, the use of exercise training models to study the cellular and molecular mechanisms that underlie skeletal muscle plasticity have two major limitations. First, such models introduce muscle damage and thus the effects of muscle regeneration cannot be separated from training effects. Second, since motor units are recruited according to exercise demand, the resultant exercise effects are diminished by the inclusion of motor units that are not recruited.

1.3.2 Chronic Low Frequency Stimulation as a Model of Muscle Training

Chronic Low Frequency Stimulation (CLFS) is a rodent model of endurance training, which causes a phenotypic transition toward a slower fibre type.

CLFS produces a sustained tonic pattern of neuromuscular activity that mimics the pattern of slow motoneurons, innervating slow-twitch muscles but not necessarily mimicking voluntary muscle action (Ljubicic*, et al.*, 2005; Pette & Vrbova, 1999). In rat tissue, CLFS induces maximal *fast-to-slow* fibre type transformation with an absence of muscle damage (Putman*, et al.*, 1999, 2000; Putman*, et al.*, 2001) that is inherent to exercise models (Faulkner*, et al.*, 1993). The absence of damage allows exercise effects to be isolated without the confounding influence of muscle fibre regeneration. The *fast-to-slow* transformation that occurs in response to electrical stimulation is well defined, predictable and reproducible, which makes it easier to study other treatments in conjunction. Knowing the predictable time course of CLFS and that the *fast-to-slow* signalling pathways are activated before transition is detected, allows for the study of the mechanisms that regulate *fast-to-slow* transformation, and thus fundamental aspects of muscle plasticity.

There are some key differences between voluntary exercise and CLFS. Firstly, with voluntary action motor units are recruited sequentially in a hierarchical order from smallest to largest according to Henneman's Size Principle (Henneman, 1985), alternatively with CLFS all motor units are stimulated simultaneously. In addition, motor units fire asynchronously and at different frequencies during voluntary activity. CLFS, however, activates all sizes of motor units maximally and synchronously with the pattern of a slow motoneuron. Thus, the CLFS model of endurance muscle training maximally challenges the adaptive potential of muscle fibres. Maximal, synchronized activity, whilst not characteristic of voluntary muscle action, allows for a reproducible, predictable model to study adaptations to activity.

A second advantage of CLFS, is that localized cellular changes occur without many systemic effects. The neuromuscular junction is remodelled (Figure 1.1) to support the signals of a slower phenotype, by a reduction in the acetylcholine (Ach) vesicle pool size in fast-twitch fibres (Reid*, et al.*,

2003). In stimulated fast muscles, acetylcholinesterase (AChE) mRNA levels decrease and become similar in those present in slow *soleus m.* (Sketelj*, et al.*, 1998). Taken together, in response to CLFS, the neuromuscular junctions of the fast fibres appear as they would within slow fibres.

A third advantage of CLFS is that contractile proteins gradually transition toward slower phenotypes, as shown in Figure 1.1 and described in Section 1.3.1. During this transition, intermediate hybrid fibres that express two or more MyHC-isoforms begin to appear. Hybrid fibres are indicative of fibre transformation and increase substantially with stimulation. Coordinately with a change in MyHC, many other myofibrillar proteins adapt to a slower isoform including myosin light chains (Leeuw & Pette, 1996), troponin (Hartner*, et al.*, 1989; Hartner & Pette, 1990; Leeuw & Pette, 1993), and tropomyosin (Schachat*, et al.*, 1988).

CLFS is known to induce changes in Ca^{2+} kinetics, as illustrated in Figure 1.1. Firstly, the uptake characteristics of the sarcoplasmic reticulum adapt to stimulation. Secondly, the amount of Ca^{2+}-binding proteins in the cytosol changes with CLFS, including the upregulation of phospholamban, a protein of the sarcoplasmic recticulum Ca^{2+} -ATPase (SERCA), and the slow SERCA2a isoform (Hu*, et al.*, 1995; Ohlendieck*, et al.*, 1991). There is a concurrent down regulation of the fast SERCA1 isoform and Ca^{2+} binding protein parvalbumin (Klug*, et al.*, 1988). In addition, the ryanodine receptor, dihydropyridine receptor, and triadin exhibit considerable reductions in muscles stimulated with CLFS (Ljubicic*, et al.*, 2005). Such adaptations lead to the production of low amplitude Ca^{2+} transients (Carroll, S. L.*, et al.*, 1999), in comparison to the phasic high amplitude Ca^{2+} transients in fast muscles, that mimic those of endurance exercise and consequently cause activation of slow fibre specific pathways (Figure 1.1). The slow biphasic pattern of Ca^{2+} transients is known to activate certain downstream signalling pathways

including the Cn- NFAT pathway (Chin*, et al.*, 1998; Martins*, et al.*, 2012; Wu*, et al.*, 2000).

Additionally, CLFS induces changes in the metabolic pathways of ATP production that are characterised by increased expression and activity of mitochondrial enzymes that catalyse terminal glucose and fat oxidation (Figure 1.1)(Putman*, et al.*, 2004); this adaptive change is a direct function of mitochondrial genesis (Ljubicic*, et al.*, 2005). CLFS also induces a concurrent decrease in the expression and activity of glycolytic enzymes (Hood*, et al.*, 1989; Pette & Vrbova, 1999). The change in oxidative enzyme activity in response to CLFS has been inversely correlated with basal levels of a muscle (Ljubicic*, et al.*, 2005). In other words, muscles that already report high levels of oxidative activity at rest do not show as great of an increase as highly glycolytic muscles.

An increase in capillary density (Putman*, et al.*, 2001; Skorjanc*, et al.*, 1998) and myoglobin content (Kaufmann*, et al.*, 1989) occur quite rapidly in response to CLFS, providing vascular support for the new, smaller, more oxidative, fibres as illustrated in Figure 1.1. Slower fibres (*e.g.,* type-I), in general, have a smaller cross sectional area than the larger fast fibres (*e.g.,* type-IIB). For the muscle to be able to support the smaller cross sectional area of the new slower fibres, muscle satellite cells are known to actively cycle and form the basis for creation of new myonuclei (Martins*, et al.*, 2006; Martins*, et al.*, 2009; Putman*, et al.*, 1999, 2000). As well, achieving a threshold myonuclear domain seems to be required to allow for fibre type transition to proceed (Pavlath*, et al.*, 1989). The combination of a smaller cross sectional area and an increased capillary density, seem to be required to support the new slower-phenotype (Brown*, et al.*, 1976; Pette*, et al.*, 1975; Skorjanc*, et al.*).

Therefore, by using CLFS as a model of muscle training the inherent plasticity of skeletal muscle can be readily observed. The chronic nature of CLFS provides a predictable environment that stimulates metabolic, structural, enzymatic, and conformational changes of the muscle. Encompassing all aspects involved in muscle structure and function. The use of CLFS to study the cellular and molecular mechanisms that underlie skeletal muscle plasticity removes the two major limitations of exercise training models. First, muscle damage is not a factor with CLFS in rat. Second, motor units are recruited maximally and synchronously, which involves inducing muscle changes in all fibres.

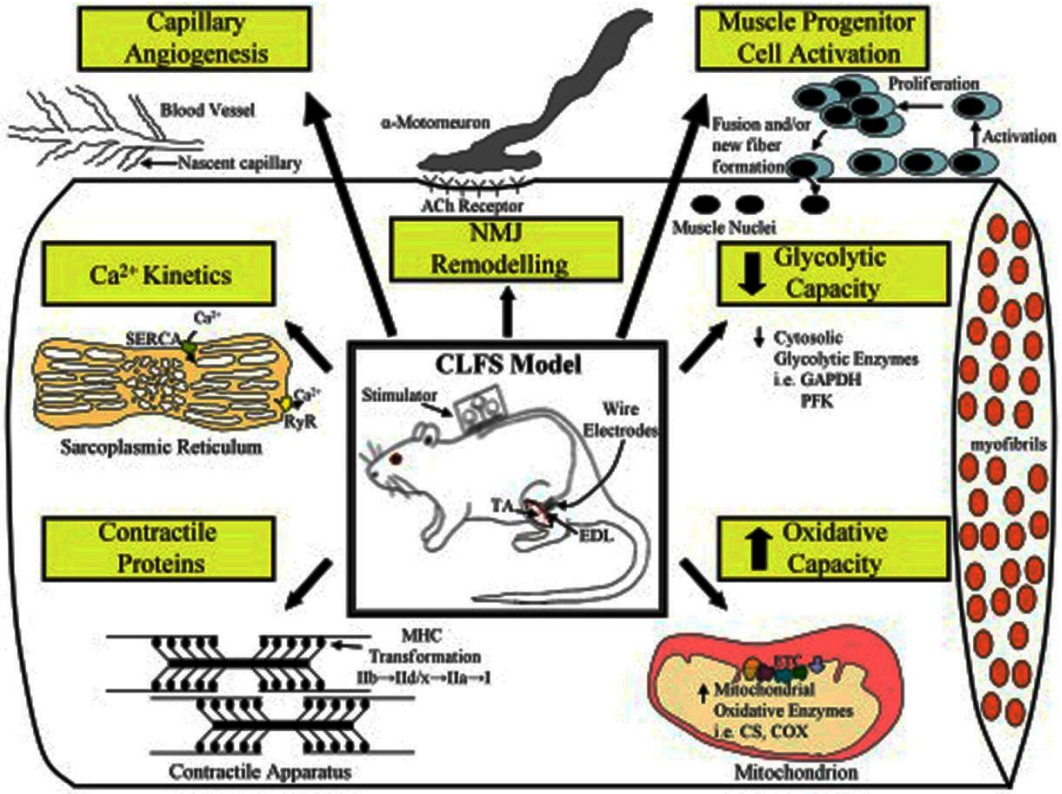

Figure 1.1 The CLFS model and a summary of the CLFS-induced adaptations. Ach=acetylcholine; Ca^{2+}=calcium; CLFS=chronic low-frequency stimulation; CS=citrate synthase; COX=cytochrome c oxidase; EDL=extensor digitorum longus; GAPDH=glyceraldehyde phosphate dehydrogenase; NMJ=neuromuscular junction; PFK= phosphofructokinase; TA=tibialis anterior. *With permission from Ljubicic et al. 2005 .*

1.4 Intracellular Signals Regulating CLFS-Induced *Fast-to-slow* Fibre Type Transitions

The underlying signalling mechanisms that link slow tonic motor nerve activity to shifts in fibre type specific gene expression (*i.e.*, MyHC), have yet to be fully elucidated. Slow motoneuron activity is known to trigger sustained, low-amplitude increases in intracellular Ca^{2+} transients, which not only result in contractile activity but also stimulate a number of transcriptional factors and co-activators. The two major pathways that are known to be activated by slow motoneuron activity are Myocyte Enhancer Factor (MEF)2-Class II histone deacetylase proteins (HDAC), and the focus of this investigation, the Cn-NFAT pathway. It has been postulated that these pathways interact in the cell to activate slow specific genes in response to low-frequency stimulation.

Ca^{2+} concentration inside the cell is controlled largely by the sarcoplasmic reticulum through calcium release and uptake systems in skeletal muscle. Ca^{2+} transient kinetics have a direct effect on fibre properties, indicated by the higher level of cytosolic free Ca^{2+} concentration in slow muscles (Carroll, S. L.*, et al.*, 1997), as well as the lower peak and slower decline of Ca^{2+} transients in slow muscles. One explanation for the contrast in $[Ca^{2+}]$ between fibre types is a more developed, larger sarcoplasmic reticulum terminal cisternae in fast muscles leading to a higher amplitude Ca^{2+} influx with excitation. One similarity between fibre types is the rate of decline of amount of Ca^{2+} released in subsequent action potentials. Overall, Ca^{2+} kinetics differ between fast and slow muscles as well as with different types of stimuli (*i.e.,* endurance vs. resistance training), in turn activating different pathways and promoting different gene programs. (*For a recent review see Schiaffino & Reggiani, 2011*).

With chronic stimulation of skeletal muscle there is a sustained influx of intracellular Ca^{2+}, which in turn causes the phosphorylation of Class II HDAC proteins by nuclear calmodulin dependent kinase (CaMK). Subsequently, HDAC binds to 14-3-3 protein and moves out of the nucleus into the cytoplasm (McKinsey*, et al.*, 2001), this removes the inhibition of MEF2 and allows transcriptional activity to occur. Two additional proteins have been shown to cause slow gene upregulation as well as the activation of MEF2, AMPK (activated protein kinase) and Calcineurin (Cn) (as shown by MEF2 blockage caused cyclosporine A (Wu*, et al.*, 2000)). The specific downstream pathways of MEF2 are still largely unknown. However, it has been elucidated that MEF2 binds to an A/T-rich DNA sequence that is in the control regions of numerous muscle specific genes, particularly in the same regions of slow fibre specific genes (similar to NFAT). (*For recent review see Bassel-Duby & Olson, 2006*).

The same chronic influx of Ca^{2+} that activates HDAC also stimulates calmodulin and the B subunit of Cn, which in turn dephosphorylates nuclear factor of activated T-cells (NFAT), and subsequently translocates into the nucleus (McCullagh*, et al.*, 2004). Once in the nucleus, NFAT binds to specific sequences on the promoter regions of specific target genes that induce a slower fibre-specific gene program (Liu, Y.*, et al.*, 2005)(Figure 1.2). The activity-induced up-regulation of slow fibre specific genes is dependent on Cn-activation and NFAT-c1 nuclear import. This pathway also demonstrates properties that implicate Ca^{2+} signalling in mediating the adaptive response. Carroll *et al.* (1999) reported that transforming single fibres exposed to CLFS displayed $[Ca^{2+}]_i$ transients typical of slow-twitch fibres, with characteristic biphasic low-amplitude contraction-dependent changes in intracellular Ca^{2+} concentration ($[Ca^{2+}]_{intracellular}$) on the order of 1.2-1.5 μM. This $[Ca^{2+}]_{intracellular}$ coincides with the concentration that is required for half-maximal activation of Cn-NFAT signalling pathway by $[Ca^{2+}]_{intracellular}$ (Healy*, et al.*, 1997). Indeed a previous study from our laboratory (Martins*, et al.*,

2012) confirmed that activity-induced up-regulation of MyHC-I expression was dependent on Cn-activation and NFAT-c1 nuclear import (As seen in Figure 1.2).

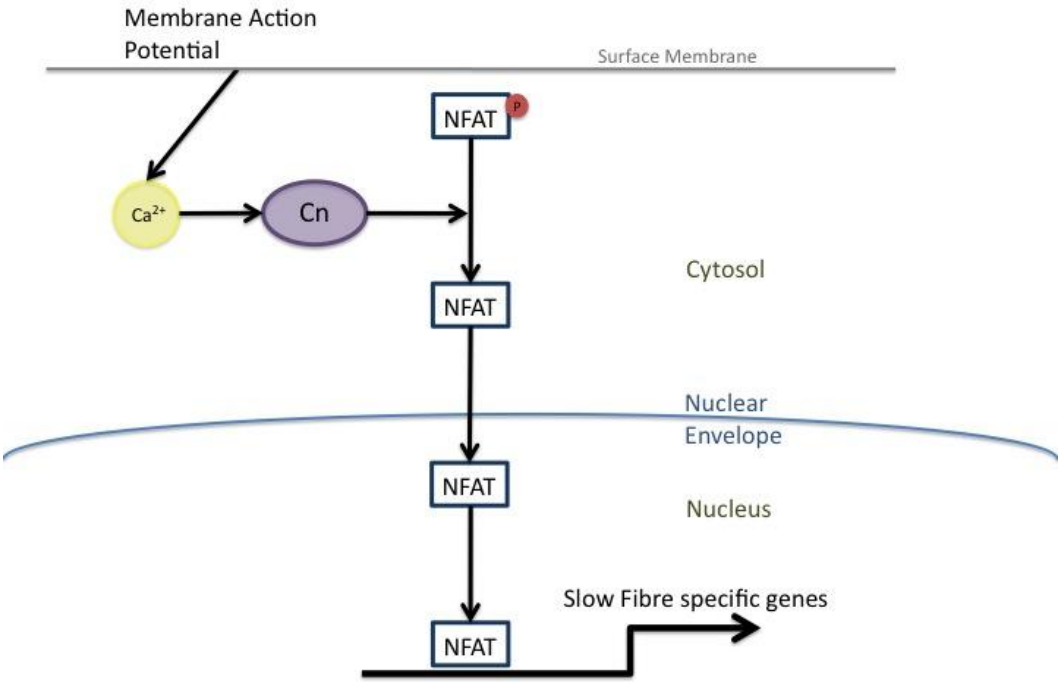

Figure 1.2 A simplified diagram of the Ca^{2+}/calcineurin/NFAT pathway for activation of slow skeletal muscle fibre gene expression. An action potential in the external membranes causes elevated cytosolic Ca^{2+}, which then activated Cn, which subsequently dephosphorylates cytoplasmic NFAT. NFAT is then permitted to enter the nucleus, leading to the activation of slow fibre genes by nuclear NFAT.

1.4.1 Calcineurin

Calcineurin (Cn), a cyclosporine-sensitive, Ca^{2+}-regulated serine/threonine phosphatase, is a heterodimer of a calmodulin-binding catalytic subunit (CnA) (59 to 62 kDa) and a Ca^{2+}-binding regulatory subunit (CnB) (19 kDa), each with various isoforms that are transcribed from different genes (Parsons*, et al.*, 2003). Three catalytic genes (CnAα, CnAβ & CnAγ) have been discovered, however only two are expressed in skeletal muscle (CnAα and CnAβ) (Parsons*, et al.*, 2003). Whilst two regulatory subunits (CnB1 & CnB2) have been discovered, only one is expressed in skeletal muscle (CnB1) (Parsons*, et al.*, 2004).

In response to a sustained low-amplitude increase in intracellular Ca^{2+} transients, as seen in response to sub-maximal exercise and CLFS, Ca^{2+} binds with the CnB subunit and assists in the sub-maximal activation of the CnA subunit. The same Ca^{2+} transients reportedly free calmodulin to bind Ca^{2+} at high affinity sites, and subsequently to an auto-inhibitory region near the C-terminus of Cn-Aα, thereby fully activating the enzyme complex. Once activated, the Cn-enzyme complex proceeds to bind to and dephosphorylate multiple phospho-serine and phospho-threonine residues on local *NFAT-isoforms*, thereby facilitating their translocation into the nucleus (Figure 1.3) (Al-Shanti & Stewart, 2009). Once in the nuclear compartment an NFAT isoform may cooperatively bind to promoter regions with other transcription factors [*e.g.,* Myocyte Enhancer-Factor 2 ($MEF2_{A\text{-}D}$); Muscle Regulatory Factors (MRF's: MyoD, Myf-5, myogenin)] and cofactors (*e.g.,* E12, E47, p300) that determine slow or fast muscle fibre phenotypes. Evidence to date would seem to indicate that within both the Cn-enzyme complex and its target NFAT-isoforms there is considerable potential for graded responses to activity-dependent variations in $[Ca^{2+}]_i$ that might account for precise adjustments in Cn-NFAT signalling and control MyHC-based muscle fibre types, especially during CLFS-induced *fast-to-slow* fibre type transformations.

Calsarcins (Frey*, et al.*, 2008; Frey*, et al.*, 2000) are a family of sarcomeric proteins that tether Cn to the α-actinin at the z-line of the contractile apparatus, and regulate Cn activity. There are three calsarcin isoforms, (calsarcin-1, calsarcin-2 and calsarcin-3) each having slightly different roles in skeletal muscle. Calsarcin-2, and calsarcin-3 are specifically expressed in fast-twitch muscle, whereas Calsarcin-1 is only expressed in cardiac and slow skeletal muscle. Calsarcin-2 knockout caused an increase in slower phenotype muscles as well as increased running distance in mice (Frey*, et al.*, 2008). Thus, Calsarcins seem to position Cn in a unique position near a large intracellular Ca^{2+} pool to foster their activation with many up and downstream factors, whilst hindering Calcineurins activity by tethering it to the z-line, rendering it unable to translocate.

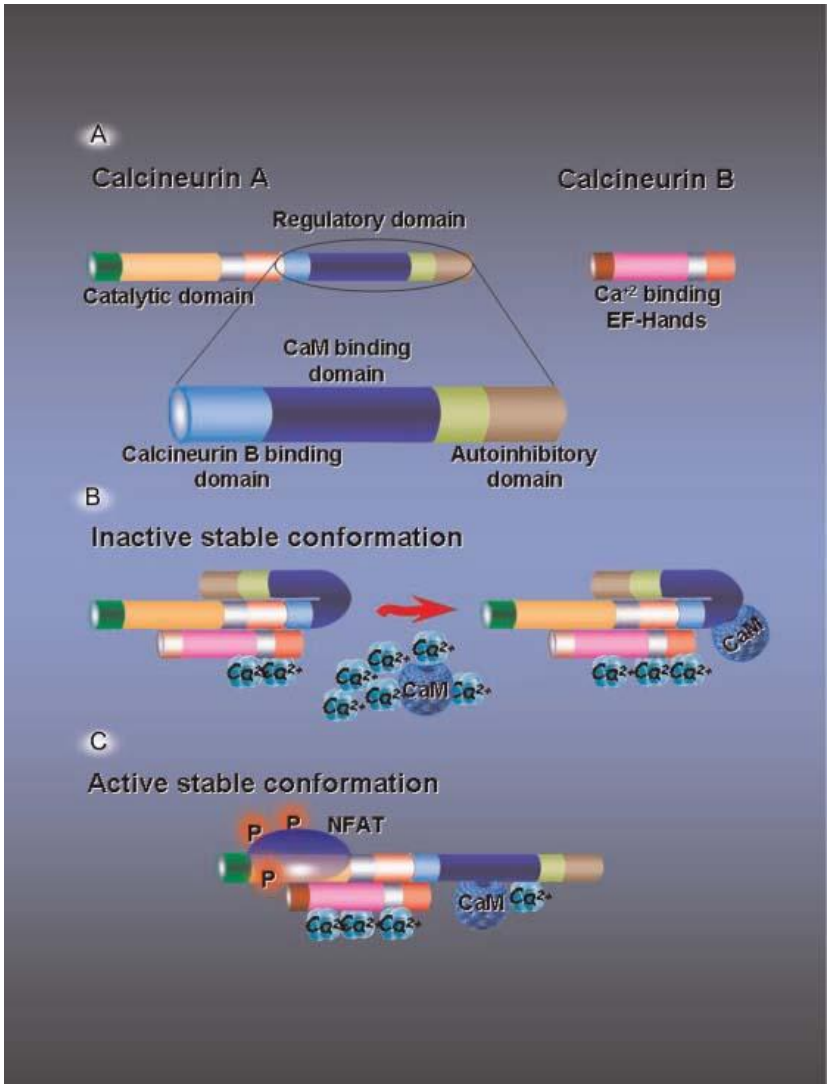

Figure 1.3 The structure of calcineurin and its enzymatic activation.

(A) Calcineurin consists of two subunits: catalytic-regulatory subunit (calcineurin A) containing the N-terminal catalytic and C-terminal regulatory domains. The C-terminal regulatory domain consists of three domains, which are the calcineurin binding site, calmodulin binding site and an auto-inhibitory site; and the Ca^{2+}-binding regulatory subunit (calcineurin B).

(B) In resting skeletal muscle cells the intracellular Ca^{2+} level is low, and therefore the heterodimeric structure of calcineurin is in an inactive conformational state. In response to physical activity and exercise intracellular Ca^{2+} levels increase and activate calmodulin, which, in turn, binds to the heterodimer calcineurin, inducing its active conformational changes.

(C) In its active stable conformational state the autoinhibitory domain has been displaced from the catalytic domain where the nuclear factor of activated T-cell (NFAT) protein binds. The binding of Ca^{2+} to the binding regulatory subunit, calcineurin B, stabilizes active Cn. With permission *from* (Al-Shanti & Stewart, 2009).

1.4.2 Review of Nuclear Factor of Activated T-cells (NFAT)

1.4.1.1 *STRUCTURE*

NFAT was first discovered in T-cells as a rapidly inducible transcription factor regulated by Ca^{2+}-activated signalling pathways (Shaw*, et al.*, 1988). Historically related to REL-nuclear factor-κB (REL-NF-κB) family of transcription factors, NFAT has since been shown to have a contrary role in T-cells. The Ca^{2+}-regulated isoforms of NFAT seem to play a role in T-cell apoptosis (Lee, H.*, et al.*, 2005), whilst NF-κB is active in cell reproduction. There are four isoforms of calcium activated NFAT: NFAT-c1 (also known as NFAT2 or NFATc); NFAT-c2 (also known as NFAT1 or NFATp); NFAT-c3 (also known as NFAT4 or NFATx); NFAT-c4 (also known as NFAT3). There is a fifth isoform (NFAT5) that has a structure 40% similar to the Ca^{2+}-activated NFAT isoforms (Lopez-Rodriguez*, et al.*, 1999), but is activated in response to osmotic stress and has not been found active in the pathways being investigated. Throughout, NFAT will refer to the four calcium activated NFAT isoforms.

Structurally the four NFAT isoforms are quite alike (Figure 1.4). They contain a high degree of similarity among the RHR (Rel-homology region), which includes the regulatory region (Luo*, et al.*, 1996) and the DNA binding region (Jain*, et al.*, 1995), suggesting common DNA binding specificities and partner interactions. Many of the RHR-C interface residues observed in NFAT-c2 are conserved in NFAT-c1 and NFAT-c3. NFAT-c4, however, seems to have different residues in many of those positions (Hogan*, et al.*, 2003). The similarities between NFAT-c1, -c2, and -c3 might explain the redundancy in some NFAT related functions. It has been suggested that regulating the balance between specific NFAT isoforms occupying a specific promoter at any given time may be controlling some function. The N-terminal and C-terminal transactivation domains, on the other hand, vary between isoform. There has been an abundance of research showing distinct roles for each

NFAT isoform in many different cell types (*For a review see Rao et al., 1997*) leading to the idea that each isoform would have different roles in skeletal muscle. Within the regulatory region of NFAT there are 13 activation sites (Okamura*, et al.*, 2000). Due to the number of phosphorylation sites, multisite phosphorylation (Hogan*, et al.*, 2003) could increase the sensitivity of each NFAT isoform to stimuli through the varying thresholds of activation of the many serine residues on the different NFAT isoforms. This variance in activation sites as well as the differences in C-terminus and N-terminus regions could explain the difference in response to stimulation and Ca^{2+} influx.

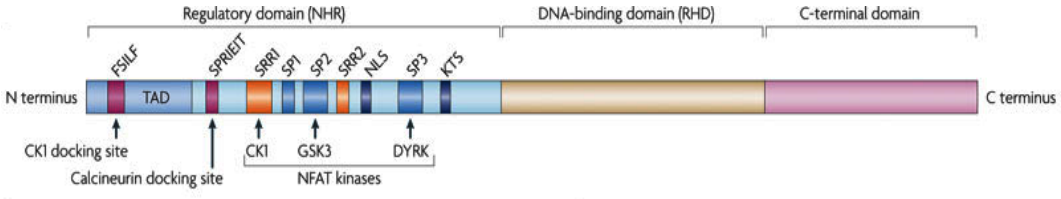

Figure 1.4 The General structure of nuclear factor of activated T cells (NFAT) transcription factors. NFAT proteins consist of an amino-terminal regulatory domain (also known as an NFAT homology region (NHR)), a DNA-binding domain (also known as a REL-homology domain (RHD)) and a carboxy-terminal domain. The regulatory domain contains an N-terminal transactivation domain (TAD), as well as a docking site for for casein kinase 1 (CK1), termed FSILF, and for calcineurin, termed SPRIEIT. It also includes multiple serine-rich motifs (SRR1, SP1, SP2, SRR2, SP3 and KTS) and a nuclear localisation sequence (NLS). With permission from (Muller & Rao, 2010).

1.4.1.2 FUNCTION

The four calcium activated NFAT isoforms exhibit varying actions throughout the body, including cell differentiation, growth promotion, cell apoptosis and cell production. All NFAT isoforms are dephosphorylated by a Ca^{2+}-Cn dependent pathway, and at least one isoform is active in most cell types. Specifically, NFAT-c2 controls bone resorption by stimulating the differentiation and functioning of osteoclasts (Ikeda*, et al.*, 2006). In melanoma cells, NFAT-c2 has an anti-apoptotic effect (Perotti*, et al.*, 2012). Whereas, NFAT-c2 deletion reduces cytokine production by mast cells (Solymar*, et al.*, 2002; Tsytsykova & Goldfeld, 2000). In adult rat joints, NFAT-c2 acts as a negative regulator to promote appropriate cartilage formation (Horsley and Pavlath 2002). The rate limiting step of NFAT-c2 with Ca^{2+} activation is its nuclear export, slow deactivation causes sustained responses after termination of initial signal (Kar*, et al.*, 2011). Overall, NFAT-c2 seems to have functions ranging from pro- to anti-apoptotic, however in general seems to be involved in cell regulation.

Similar to NFAT-c2, NFAT-c1 seems to have a predominant role in the differentiation of osteoclasts from monocyte precursors (Takayanagi*, et al.*, 2002) and the differentiation of Th2 cells from antigen- "naive" T-cells. (*for review see Glimcher & Murphy, 2000*). NFAT-c1 is the only isoform that is regulated by a positive auto-regulation loop (Zhou*, et al.*, 2002), and as such could explain why it is the most commonly identified regulator in many cell types. Deletion of NFAT-c1 causes defects in cardiac valve formation and lethality (de la Pompa*, et al.*, 1998; Ranger*, et al.*, 1998). NFAT-c1 is unable to promote apoptosis in T-cells by itself (Chuvpilo*, et al.*, 2002). NFAT-c1's transcriptional activity could, in turn, be dependent on the other isoforms activity in addition to its own.

Disruption of NFAT-c4 causes no known phenotype to develop in vascular tissue (Graef*, et al.*, 2001). In other tissues NFAT-c4 has been shown to be involved in cell survival (Vashishta*, et al.*, 2009) which could be the case in skeletal muscle as well. In other tissue types, NFAT-c4 has been implicated in cell apoptosis (Li, L.*, et al.*, 2013), and may underlie activity-dependent neuronal plasticity throughout the adult brain (Bradley*, et al.*, 2005). In regards to kinase activity, the knockdown of GSK3β significantly increased depolarization induced nuclear translocation of NFAT-c4 in neurons, while inhibition of mTOR and p38 had no effect and nuclear localisation only occurred after prolonged Ca^{2+} increases. When NFAT-c4 protein is ubiquitinated, decreases in protein levels and transcriptional activity occur. Additionally, GSK3β enhanced ubiquitination and decreased transactivation in cardiac tissue (Fan*, et al.*, 2008), revealing a possible mechanism by which NFAT-c4 is controlled.

NFAT-c3 is rapidly dephosphorylated and translocated into the nucleus in response to Ca^{2+} in neuronal cells (Ulrich*, et al.*, 2012), which seems to be the case in most cell types. In response to induced hypoxia, which causes an increase in arterial reactive oxygen species, NFAT-c3 activates and there is increase in Ca^{2+} and vasoconstrictor reactivity (Friedman*, et al.*, 2013). High extracellular Ca^{2+} induces activation and expression of NFAT-c1, which in turn increases NFAT-c3 expression and activity in osteoblasts (Lee, H. L.*, et al.*, 2011). There are some additional instances where two or more NFAT isoforms work together or have redundant roles. For instance, deletion of both NFAT-c1 and NFAT-c2 causes loss of cytokine production in T-cells (Peng*, et al.*, 2001). Also, in T-cells NFAT-c2 and NFAT-c3 have very similar responses to Ca^{2+} influx and inhibition. (Rao*, et al.*, 1997).

In resting skeletal muscle, inactive NFAT is heavily phosphorylated and, for the most part, located in the cytoplasm. NFAT is dephosphorylated

by the Cn-enzyme complex, which binds to the conserved regulatory domain, followed by translocation into the nucleus where it co-ordinately binds with other transcription factors, and to specific promoter regions that up-regulate skeletal muscle specific genes (Meissner, Umeda*, et al.*, 2007). NFAT protein activation closely follows the activation pattern of Cn. NFAT-c1 is the most studied isoform in skeletal muscle to date. It has been found to be involved in the transition to a slower phenotype, especially to the slowest (*ie.,* type-I) fibres. Research has been completed on the varying roles of NFAT in the growth and development of skeletal muscle. Knockout mice have been a common model used to study each NFAT isoform separately. NFAT-c2 knockout has been shown to effect fibre cross sectional area during muscle growth, as well as myonuclear number (Horsley*, et al.*, 2001). NFAT-c3 knockout, on the other hand, reduced number of fibres in developing muscle (Kegley*, et al.*, 2001). Other knockout models have shown to be lethal and therefore not possible to test in this manner.

Recently, using sodium bicarbonate buffering and heat in cultured human muscle cells, Yamaguchi, *et al*. (2013) found contradictory results to many of the previous studies. While, bicarbonate buffering and increased heat have been found to cause an increase in slower muscle fibres, Yamaguchi, *et al.* (2013) found an increase in NFAT-c2 and NFAT-c4 concurrent with an increase in the slower fibre types under these conditions. Differences between this study and others could be due to the model used; some studies have shown the coordinate increase in calcium with the decrease of proteins that shuttle NFAT out of the nucleus is needed to discover a substantial increase. Other pathways could be the major regulator to adaptations with heat and bicarbonate buffering.

NFAT is rephosphorylated by several protein kinases such as glycogen synthase kinase-3 (GSK-3β)(Beals, Sheridan*, et al.*, 1997), protein kinase A (PKA), casein kinase (CK1/2), p38 MAP kinase (p38), and c-jun terminal

kinase (JNK) (Chow, *et al.*, 2000), which promote its nuclear exit (Shen, *et al.*, 2006). Some act as export kinases, some as maintenance and some as both. CK1, for example, docks at a conserved motif near the N terminus and acts as a maintenance and export kinase for SRR1. GSK3β, on the other hand, functions as an export kinase for the SP1 motif of NFAT-c2, and the SP2 and SP3 motifs of NFAT-c1 (Beals, Clipstone, *et al.*, 1997). It has been suggested that with NFAT-c1, substrate sites for GSK3β might only be created after previous phosphorylation of SP1 by cyclic-AMP-dependent protein kinase (PKA) (Sheridan, *et al.*, 2002) or dual-specificity tyrosine-phosphorylation-regulated kinase (DYRK)-2 (Muller, *et al.*, 2009). In addition, Drenning *et al.* (2009) illustrated that calcium-dependent Nitric Oxide (NO) inhibits GSK-3β in a cGMP/PI3K/Akt dependent manner, and in turn assists in NFAT-c1's function. Martins *et al.* (2012) corroborated these findings in showing that a reduction in NFAT-c1 activity is caused by obstructing GSK-3β dephosphorylation through the inhibition of NO.

Variations in resting nuclear influx and efflux have been found between the different NFAT isoforms. NFAT-c1, for example, has been shown to shuttle in and out of nucleus under resting conditions, and accumulate in the nucleus with the blockage of chromosome region maintenance 1 (CRM1) (Shen, *et al.*, 2006). NFAT-c1 nuclear import and exit occurred even in the presence of other kinase inhibitors, and the blockage of Cn (Shen, *et al.*, 2006). Shen *et al.* (2006) suggests that resting shuttling of NFAT-c1 is constantly occurring regardless of phosphorylation status, whilst NFAT-c3 does not accumulate in the nucleus even with the blockage of CRM1 (Shen, *et al.*, 2006). Furthermore, it could be suggested that either a different pathway regulates nuclear efflux, or simply there is limited resting shuttling of NFAT-c3. MAPKs have been postulated to differentially phosphorylate the first serine of SRR1 depending on NFAT isoform. For example, p38 MAPK has been show to selectively phosphorylate NFAT-c2 (Gomez del Arco, *et al.*,

2000), whilst JNK phosphorylates NFAT-c1 and NFAT-c3 (Chow*, et al.*, 1997). Selective action of the various NFAT phosphorylation kinases could be one major factor in the different actions and functions demonstrated by the different NFAT isoforms. Overall, many factors effect each NFAT isoform leading to distinct downstream pathways in skeletal muscle. (*For a review see Hogan et al., 2003).*

1.4.2 The Calcineurin-NFAT Pathway

The Cn-NFAT pathway has been shown to play a key role in fibre type regulation, particularly *fast-to-slow* transformation. Chin *et al.* (1998) provided initial evidence through the use of skeletal myocytes that were transfected with a constitutively active (*) form of Cn*. The activation of Cn resulted in the selective upregulation of slow fibre specific gene promoters, which were mediated by NFAT. Conversely, the inhibition of Cn activity, by exposure to the Cn-inhibitor cyclosporine A (CsA), caused the opposite *slow-to-fast* fibre type transformation (Chin*, et al.*, 1998). Numerous studies have subsequently corroborated the involvement of the Cn-NFAT pathway in the promotion of the slow fibre-specific gene program *in vitro* (Delling*, et al.*, 2000; Higginson*, et al.*, 2002; Meissner, Umeda*, et al.*, 2007; Naya*, et al.*, 2000; Torgan & Daniels, 2001) and *in vivo* (McCullagh*, et al.*, 2004; Serrano*, et al.*, 2001; Talmadge*, et al.*, 2004). For example, Meissner, *et al.* (2007) demonstrated that exposure of differentiated C2C12 myotubes to a Ca^{2+}-ionophore or transfection with constitutively active NFAT-c1 induced increases in MyHC-Iβ promoter activity, whilst exposure of these same myotubes to CsA blocked MYHC-Iβ promoter activity. Similarly, studies by Talmadge, *et al.* (2004) revealed that the *diaphragm* muscles of transgenic mice that expressed high levels of constitutively active Cn (MCK-Cn* mice) had elevated expression levels of MyHC-I and lower expression levels of both MyHC-IIa and MyHC-IId(x). These collective results support a role for the Cn-NFAT pathway in regulating of slow fibre gene programs.

The Cn-NFAT pathway has also been implicated in *fast-to-slow* fibre transformation within the subpopulations of *fast* fibres (Dunn*, et al.*, 1999). For example, (Allen, David L.*, et al.*, 2001) observed that the over-expression of Cn in C2C12 myotubes promoted MyHC-IIa expression; the over-expression of NFAT-c also induced MyHC-IIa expression, but was further associated with lower expression levels of MyHC-IId(x) and MyHC-IIb. Allen & Leinwand (2002) later showed that exposure of C2C12 myotubes to a Ca^{2+}-ionophore activated the MyHC-IIa promoter to a much greater extent than the promoters regulating MyHC-IId(x) or MyHC-IIb expression. Thus, Ca^{2+}-ionophore treated myotubes clearly showed a shift toward a slower phenotype within fast muscle fibres in response to changes in intracellular concentrations of Ca^{2+} that were typical of slow type stimulation. The results of those studies also provide substantial evidence that Cn and NFAT-c are downstream regulatory targets and critical regulatory steps in mediating *fast-to-slow* fibre type transitions.

Dunn *et al.* (2000) uses a transgenic mouse model of Cn overexpression (CnA*) as well as, cyclosporine A administration (CsA; which blocks Cn) and overload of the mouse *plantaris m*. by synergist ablation to study *fast-to-slow* fibre type transformation. The overloaded mice, regardless if they were CnA* or wild type, were shown to have an increase in fibres expressing MyHC-IIa and MyHC-I isoforms, as well as an increase in slow fibre genes there was a concurrent decrease in fast fibre genes. Which was confirmed by Rana et al (2008), who found a NFAT binding site on the troponin I fast (TnIf) intronic regulatory element (FIRE). Conversely, with CsA administration the Cn-NFAT pathway was blocked, evidenced by the decrease in NFAT-c1 in this group, which causes a blockage of the *fast-to-slow* conversion that regularly occurs. Together, the results of Dunn, *et al.* (2000) support a role for the Cn-NFAT in *fast-to-slow* transformation within the fast population, as well as the final *fast-to-slow* transformation (MyHC-IIa to MyHC-I) in the *plantaris m.* Dunn, *et al.* performed similar experiments in

(1999) and (2001) which produced the same findings as the 2000 paper. Altogether, the Ca^{2+}-Cn-NFAT pathway is shown to contribute to the *fast-to-slow* myosin heavy chain transformation that occurs in response to exercise in the fast population. Most recently, Vechetti-Junior, *et al.* (2013) reported an increase in NFAT-c1, -c2, and -c3 without a concurrent increase in Cn activity with 8-weeks of aerobic training. One explanation for this could be the fact that they are looking at Cn mRNA levels after 8-weeks of training, and Cn has been shown to be a precursor to NFAT activity as well as fibre type transition. That late of a time point with training the majority of the adaptation should have already occurred.

A recent study reported that the four Ca^{2+}-Cn dependent NFAT isoforms (NFAT-c1, NFAT-c2, NFAT-c3, and NFAT-c4) are responsible for activating different fibre type genes and act co-ordinately with each other downstream of Cn (Figure 1.5) (Calabria*, et al.*, 2009). Using a loss-of-function approach by mRNA-*inhibition* (RNA*i*) in rats, Calabria *et al.* (2009) found that all four NFAT isoforms were necessary for MyHC-I expression. In contrast, the expression of MyHC-IIa and MyHC-IId(x) required only three NFAT isoforms (*i.e.*, NFAT-c2, -c3, and -c4). Notably there was a stronger relative influence of NFAT-c3 on MyHC-IIa expression than on MyHC-IId(x) expression. Finally, NFAT-c4 alone was required for MyHC-IIb expression. Examination of rodent muscles at rest has revealed distinct expression pattern of NFAT isoforms within muscle fibres. Fractionation experiments (Calabria*, et al.*, 2009) using muscles composed of different fibre types (*i.e.*, *soleus m.* and *extensor digitorum longus m.*) provide evidence that NFAT-c4 resides in a predominately nuclear location in all fibre types. By comparison, NFAT-c2 and -c3 display low but detectable nuclear signals in both muscles, whilst NFAT-c1 is in a predominately nuclear position in the *soleus m.* but not in the *extensor digitorum longus m.* A more detailed analysis by Mutungi (2008) found that NFAT-c1 occupies a mainly cytoplasmic location in type-IIA fibres in both mixed fast-twitch *extensor digitorum longus m.* and slow-

twitch *soleus m.* of rat. In the type-I fibres NFAT-c1 was found to primarily reside within a nuclear position, again regardless whether the fibres were in a mainly fast or slow muscle.

In addition, Calabria *et al.* (2009) applied stimulation to their samples, the slow pattern of stimulation (200 pulses, 20 Hz every 30 seconds) caused nuclear accumulation of NFAT-c1, -c2, and -c3, where NFAT-c4 was already nuclear in location. The fast pattern of stimulation (25 pulses, 100 Hz every 60 seconds) caused nuclear accumulation of NFAT-c4, -c3 and in some cases -c2. The patterns of NFAT nuclear accumulation that are caused by particular patterns of stimulation are consistent with earlier findings in resting muscle linking specific NFAT isoforms with certain MyHC isoforms (Calabria*, et al.*, 2009). The dephosphorylation and translocation of NFAT-c1 by a chronic low-frequency pattern of stimulation has been demonstrated previously (McCullagh*, et al.*, 2004) but the translocation of the specific NFAT isoforms in relation to fibre type has yet to be elucidated.

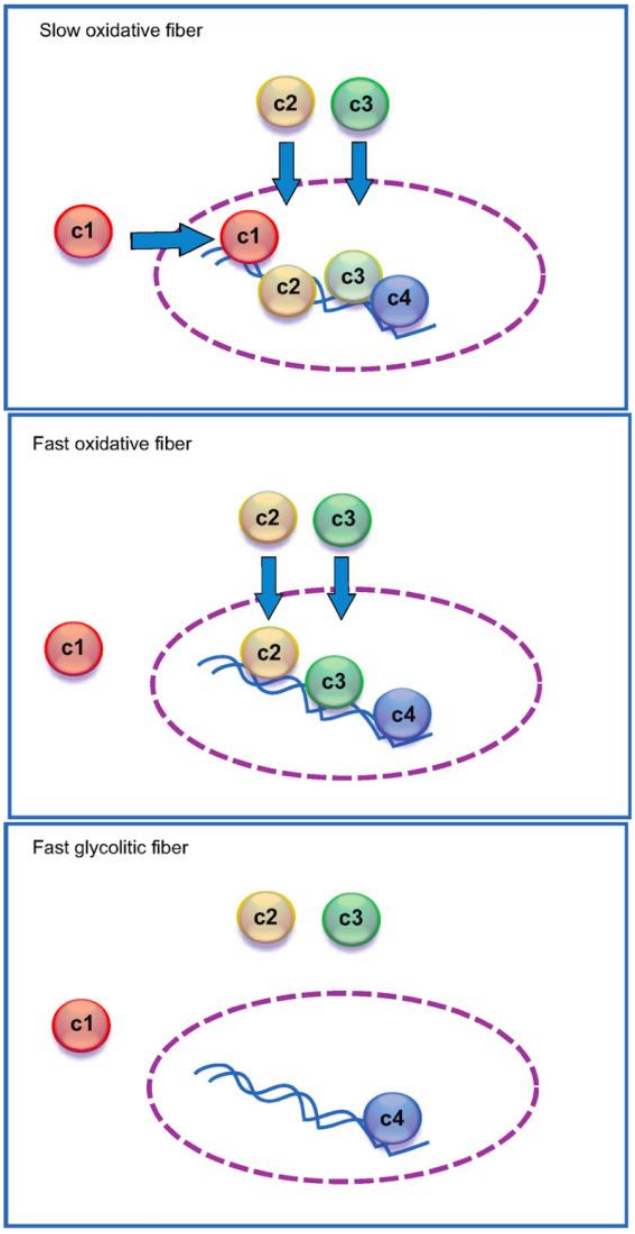

Figure 1.5 A graded nuclear recruitment of NFAT transcription factors in response to activity/exercise changes the expression of MyHC isoforms. c1=NFAT-c1, c2=NFAT-c2, c3=NFAT-c3, c4=NFAT-c4. A slow pattern of activity induces the nuclear translocation and activation of all 4 NFAT isoforms, which are necessary for the transcription of MyHC-I. NFAT-c1, in particular, only translocates to the nucleus in response to slow-type activity (Serrano*, et al.*, 2001), (Naya*, et al.*, 2000) and switches the specificity of the transcriptional machinery toward slow MyHC; by inhibiting fast MyHC expression (Chin*, et al.*, 1998), it also ensures that the fast and slow gene programs are mutually exclusive. In fast-oxidative (IIA/IIX) fibres, NFAT-c1 is mostly cytosolic and NFAT-c2 and -c3 are transcriptionally active; thus, contributing to the transcriptional activation of MyHC-IIa and -IIx. In fast-glycolytic fibres, where MyHC-IIB is the only transcribed isoform, only NFAT-c4 is nuclear and transcriptionally active. With permission *from Calabria et al., 2009*.

1.5 Thesis Objectives

Using selective molecular RNA$_i$ knockdown approach Calabria*, et al.* (2009) reported that fast-glycolytic type-IIB fibres are only transcriptionally dependent on *NFAT-c4*, whilst expression of fast-oxidative-glycolytic (FOG) type-IID/X, or fast-oxidative (FO) type-IIA fibre phenotypes was permissively dependent on *NFAT-c4* but transcriptionally dependent on both *NFAT-c3* and *NFAT-c2*. They further reported that slow-oxidative (SO) type-I fibres were only transcriptionally dependent on *NFAT-c1*. However, physiological studies conducted by this group could only demonstrate that myonuclear export of *NFAT-c1* was stimulated by fast motor-unit like direct nerve stimulation (*i.e.,* 100 Hz), whilst *NFAT-c1* myonuclear import was stimulated by slow motor-unit like direct nerve stimulation (*i.e.,* 20 Hz). Indeed, other studies have confirmed that *NFAT-c1* nuclear translocation and transcriptional activation are required for activity-induced *fast-to-slow* fibre type conversions (Chin*, et al.*, 1998; Martins*, et al.*, 2012). These collective findings suggest different roles for the various *NFAT-isoforms* in determining muscle fibre types, and possibly in regulating activity-induced *fast-to-slow* fibre type transformations that are dependent on Cn activation.

The present study tested the following hypotheses:

A. Within unstimulated rat *peroneus longus m.*: (1) type-I fibres will uniquely display the greatest NFAT-c1 myonuclear localisation, but will also express NFAT-c2, -c3, -c4 at levels similar to all other fibre types; (2) type-IIA, and -IID/X fibres will display the greatest frequency of NFAT-c2 and NFAT-c3 myonuclear localisation, but will also express NFAT-c4 similar to type-IIB fibres. (3) type-IIB fibres will only display NFAT-c4 nuclear localisation.

B. Application of CLFS to the *peroneus longus m.* will induce sequential step-wise *fast-to-slow* fibre type transitions in the direction of IIB→IID/X→IIA→I and will correspond to the *NFAT-isoform* profile unique to the slower fibre type at each transitional junction according to the next-nearest neighbour rule. *(1)* CLFS-induced up-regulation of MyHC-IIa and -IId(x) within transforming fibres will be preceded by greater myonuclear localisation of NFAT-c2 and NFAT-c3. (2) CLFS-induced up-regulation of MyHC-I within transforming fibres will be preceded by greater myonuclear localisation of NFAT-c1.

CHAPTER TWO

MATERIALS AND METHODS

2.1 Materials

Standard lab reagents were purchased from Fisher Scientific (Ontario, Canada), Sigma-Aldrich Canada (Oakville, ON, Canada), Vector Laboratories, Inc. (Burlingame, CA, USA). All other materials are listed in the following:

Table 2.1 Primary Monoclonal Anti-Myosin Heavy Chain Antibodies Harvested from Mouse Hybridoma Cells Obtained From the American Type Culture Collection (ATCC)

Antibody Clone Number	Antibody Specificity
BA-D5	IgG - anti-MyHC-I
SC-71	IgG - anti-MyHC-IIa
BF-F3	IgM - anti-MyHC-IIb
BF-45	IgG - anti-MyHC-embryonic
BF-35	IgG - all MyHC isoforms but not MyHC-IIx (IId)

Table 2.2 Monoclonal (mc) and Polyclonal (pc) Primary Antibodies Used for Immunohistochemistry

Antibody	Clone/Product Number – Class – Source
mc anti-dystrophin	DYS2 (Dy8/6C5) – IgG_1 – Novocastra Laboratories, Newcastle, UK
pc anti-laminin	68125 – IgG – ICN Biomedicals Inc., Aurora, OH, USA
pc anti-NFAT-c1	H-110, sc-13033 – IgG – Santa Cruz Biotechnology, CA, USA
pc anti-NFAT-c2	M-300, sc-13034 – IgG – Santa Cruz Biotechnology
pc anti-NFAT-c3	M-75, sc-8321 – IgG – Santa Cruz Biotechnology
pc anti-NFAT-c4	H-74, sc-13036 – IgG – Santa Cruz Biotechnology

Table 2.3 Affinity-Purified Biotinylated Secondary Antibodies Used for Immunohistochemistry

Antibody	Species Host	Clone/Product Number – Source
anti-mouse IgG *(rat-absorbed)*	horse	BA-2001 – Vector Laboratories, Inc. (Burlingame, CA, USA)
anti-mouse IgM	goat	BA-2020 – Vector Laboratories, Inc. (Burlingame, CA, USA)
anti-rabbit IgG	horse	BA-1000 – Vector Laboratories, Inc. (Burlingame, CA, USA)

Table 2.4 Software

Name	Source
Pette Program	Dirk Pette (Konstanz, Germany)
Statistica 8	Statsoft Inc. (CA, USA)
Sigma Plot 12.5	Systat Software, Inc. (CA, USA)

Table 2.5 Miscellaneous

Name	Source
Avidin-D Biotin Blocking Kit	Vector Laboratories, Inc. (Burlingame, CA, USA).
Vectastain kit	Vector Laboratories, Inc. (Burlingame, CA, USA).

2.2 Methods

2.2.1 Animal Care

The *peroneus longus* muscles used in the present study were previously excised during two experiments (Martins*, et al.*, 2006; Martins*, et al.*, 2009). Twenty-four Male Wistar Rats were previously acquired from Charles River Laboratories (Montreal, PQ, Canada). All animal procedures were carried out in accordance with the guidelines of the Canadian Council for Animal Care (CCAC) and received ethical approval from the University of Alberta. Animals were individually housed under controlled environmental conditions (*i.e.*, 22°C with alternating 12 h light and dark cycles) and received standard rat chow and water *ad libitum*. Animals were randomly assigned to one of the following four groups receiving: sham operation of the left leg only (0-day control); 5-days, 10-days or 21-days of CLFS (n = 6, animals each group)(See Martins, *et al. 2006, 2009* for details). It should be noted that the application of CLFS tended to elicit a compensatory effect in the contralateral control muscles due to increased weight bearing, as previously observed (Martins*, et al.*, 2012; Putman*, et al.*, 2000; Putman*, et al.*, 2001). Therefore, comparisons were evaluated against the 0-day animals.

2.2.2. Chronic Low Frequency Stimulation

Bipolar electrodes were implanted under general anaesthesia [75mg (kg body wgt)-1 ketamine and 10mg (kg body wgt)$^{-1}$ xylezine with 0.5mg (kg body wgt)-1 acepromazine maleate] lateral to the common peroneal nerve of the left hindlimb, externalized at the dorsal intrascapular region, and connected to a small, portable stimulator. To ensure complete recovery from surgery, a latent period of one week was allowed before CLFS was initiated. CLFS (10Hz, impulse width 380μs, 12h day) was applied for 5-days, 10-days, or 21-days consecutively. Strong persistent dorsiflexion was observed in the left legs twice daily throughout the study; muscle activity was confirmed in

both the anterior and lateral crural compartments by palpation. 0-day controls received a sham operation of the left leg.

The time points of stimulation for the study were chosen based on the time course of the *fast-to-slow* transformation of skeletal muscle. At 5-days mRNA and protein changes toward a slower phenotype are observed (Jaschinski*, et al.*, 1998; Martins*, et al.*, 2006; Martins*, et al.*, 2009). The final time point of 10-days for the NFAT-isoform analysis was chosen due to the finding of NFAT-c1 activity increases and subsequently decreases by this time (Martins*, et al.*, 2012). The final time point for the analysis of MyHC transition was selected because fibre type transformations are essentially 80-90% complete after 21-days of CLFS, at both the protein and mRNA levels (Jaschinski*, et al.*, 1998).

2.2.3 Muscle Sampling

Upon cessation of stimulation the animals were deeply anaesthetized and the peroneus longus muscles were excised from both hindlimbs, quickly fixed in a slightly longitudinally stretched position and frozen in melting isopentane (-159°C). Muscles were stored in liquid nitrogen (-196°C). Animals were then euthanized with an overdose of Sodium Pentobarbital [Somnotol or Euthanyl [100 mg (kg body wt)$^{-1}$] (Bimedia-MTC Animal Health Inc., Cambridge, ON, Canada)], followed by exsanguination.

2.2.4 Fibre Type Immunohistochemistry

Frozen *peroneus longus* muscles were mounted in embedding medium (Tissue-Tek O.C.T. Compound) at -20°C; 10 μm-thick frozen sections were collected from the mid belly of each *peroneus longus* muscle by sectioning in the Cryostat, also at -20°C. The muscle cross-sectional area of each individual muscle ranged from 0.5 mm^2 to 2.0 mm^2. Serial sections were then immunostained for the various MyHC isoforms (*i.e.*, BA-D5, SC-71, BF-

35, BF-45), Dystrophin and Laminin. Laminin sections were counterstained with Hemotoxylin.

Immunostaining was completed according to established protocols for MyHC isoforms (Martins*, et al.*, 2006; Martins*, et al.*, 2009; Martins*, et al.*, 2012; Putman, Jones*, et al.*, 2003; Putman*, et al.*, 2001). The sections were removed from the freezer, allowed to air dry for 30 minutes, double circled with an ImmEdge Pen (Vector Laboratories), washed once in PBS-T and twice with PBS. Sections were then incubated for 15 min in 3% (v/v) H_2O_2 in methanol and washed as before. Serial sections that were stained for BA-D5, SC-71, BF-35, or Dystrophin were incubated for 1 h at room temperature in a blocking solution [BS-1: 1%(w/v) bovine serum albumin, 10% (v/v) horse serum in PBS-T, pH 7.4] containing 4 drops of avidin- D blocking reagent (Vector Laboratories Inc.) per milliliter of solution. Sections being stained for BF-F3 and laminin were incubated in a corresponding blocking solution [BS-2: 1%(w/v) bovine serum albumin, 10% (v/v) goat serum in PBS-T, pH 7.4], containing 4 drops of avidin-D blocking reagent (Vector Laboratories Inc.) per milliliter of solution, for 1 hour at room temperature, all followed by 2 washes of PBS. Sections were incubated overnight at 4°C with a primary antibody diluted in blocking solution containing biotin blocking reagent (Vector Laboratories Inc.). The next day the sections were again washed 1 time with PBS-T and 2 times with PBS, and incubated for 1 h with biotinylated-horse-anti-mouse-IgG (BA-D5; SC-71; BF-35: Dystrophin) or biotinylated-goat-anti-mouse-IgM (BF-F3; Laminin) (Vector Laboratories Inc.). After several washings, sections were incubated with Vectastain ABC Reagent according to the manufacturer's instructions (Vector Laboratories Inc.) and reacted with 0.07% (w/v) diaminobenzidine, 0.05% (v/v) H_2O_2 and 0.03% (w/v) $NiCl_2$ in 50 mM Tris-HCl (pH 7.5). All sections were subsequently dehydrated, cleared, and mounted in Entellan (Merck, Darmstadt, Germany).

2.2.5 NFAT Immunohistochemistry

Frozen *peroneus longus* muscles were mounted in embedding medium (Tissue-Tek O.C.T. Compound) at -20°C; 10 μm-thick frozen sections were collected from the mid belly of each *peroneus longus* muscle by sectioning in the Cryostat, also at -20°C. Immunostaining was completed according to a modified protocol for myogenin nuclear staining (Martins*, et al.*, 2006; Martins*, et al.*, 2009; Putman*, et al.*, 2000; Putman, Jones*, et al.*, 2003; Putman*, et al.*, 2001). Sections were removed from the freezer, allowed to air dry for 30 min and subsequently fixed in acetone in a whatman dish on a shaker at -20°C for 10 min. Sections were removed from acetone, allowed to air dry and then double circled with an ImmEdge Pen (Vector Laboratories Inc.). Sections were washed once in PBS-T, twice with PBS and then incubated for 15 min in 3% (v/v) H_2O_2 in methanol, followed by another wash of PBS-T and 2 washes of PBS. Sections were then incubated for 1 h at room temperature in blocking solution (10% goat serum, 1% BSA in PBS-T, pH 7.4) containing 4 drops of avidin-D blocking reagent (Vector Laboratories Inc.) per milliliter of solution, followed by 2 washes of PBS. Sections were incubated overnight at 4°C with a primary antibody diluted in blocking solution and containing biotin blocking reagent (Vector Laboratories Inc.). The next day sections were again washed 1 time with PBS-T and 2 times with PBS, and incubated for 1 h with biotinylated-goat-anti-rabbit-IgG (Vector Laboratories Inc.) diluted in blocking solution. After several washings, sections were incubated with Vectastain ABC Reagent according to the manufacturer's instructions (Vector Laboratories Inc.) and reacted with 0.07% (w/v) diaminobenzidine, and 0.05% (v/v) H_2O_2 in 50 mM Tris-HCl (pH 7.5). All sections were subsequently dehydrated, cleared, and mounted in Entellan (Merck, Darmstadt, Germany).

2.2.6 MyHC Immunohistochemical Analysis

MyHC isoform semi-quantitative analyses was completed with a Olympus IX70 inverted microscope (Olympus Canada Inc, Ontario, Canada) fitted with a SPOT-RT Camera (Diagnostic instruments inc., Michigan, USA). Pictures (see figure 3.1) were taken at 20x magnification and subsequently loaded into a custom-designed analytical program (Putman*, et al.*, 2000) (See figure 2.1). An area of 0.39mm^2 was examined from each muscle for the various MyHC isoforms from a representative cross-sectional area of the *peroneus longus* muscles. Type-I, type-IIA, and type-IIB fibres were identified by positive staining and type-IID(X) fibres were identified by the absence of staining, with all antibodies directed against the various MyHC isoforms.

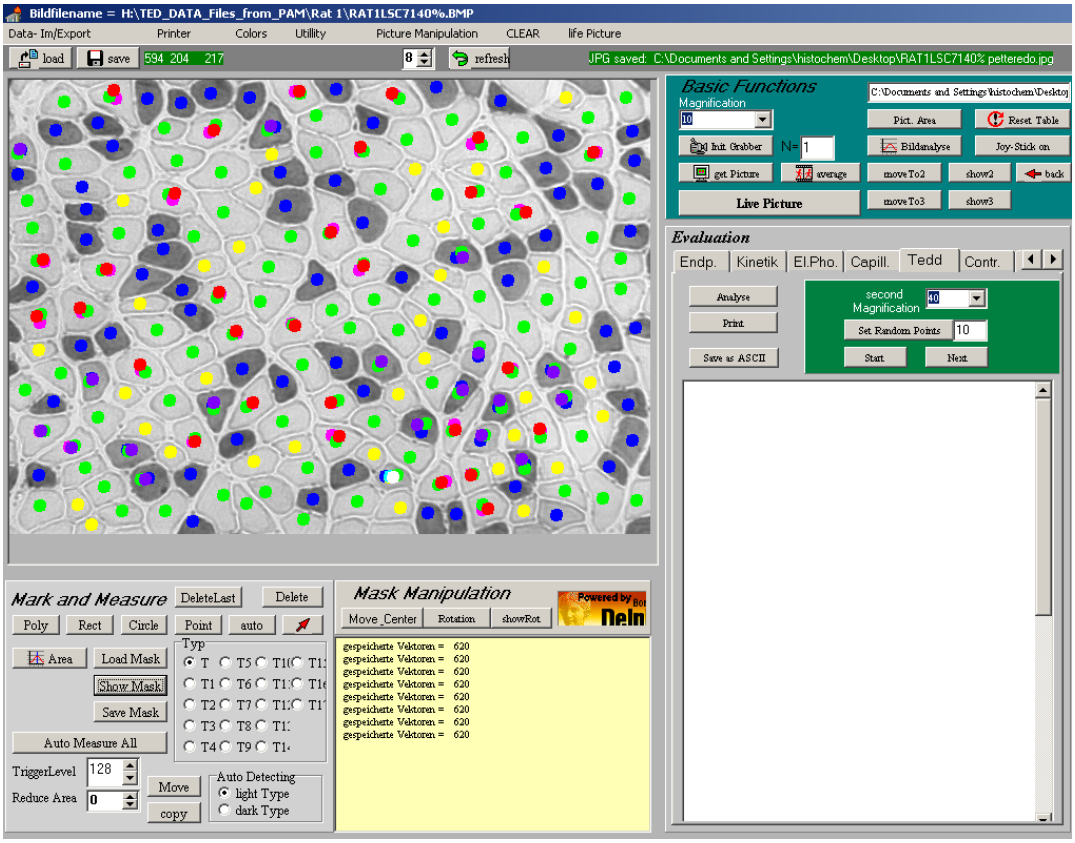

Figure 2.1 Example of custom designed fibre type analysis software. (Pette program)(Putman*, et al.*, 2000). Coloured dots represent different fibre types.

2.2.7 NFAT Immunohistochemical Analysis

Pictures were taken of representative areas on a Leica DMRXA Compound Light Microscope (Leica Microsystems Inc, Ontario, Canada) with a QI Click™ Digital Camera (Qimaging, BC, Canada) and Q Capture Pro 7 Software (Qimaging, BC, Canada) at 100x magnification (Figures 3.5, 3.6, 3.8, 3.9, 3.10 & 3.11). Criteria for inclusion of positively stained myonuclei were established by examining previous publications and only nuclei that stained strong positive were enumerated. For all NFAT isoforms a nucleus was considered positive when it appeared to be wholly or partially within the cell. Further criteria differed between isoforms due to varying staining patterns as seen in Calabria *et al.* (2009). NFAT-c1 and -c4 showed very strong staining along the nuclear envelope and within the nucleus. Therefore positive nuclei were those that had a clearly stained nuclear envelope in addition to staining within the cell (Figures 3.6, 3.8. & 3.11). NFAT-c2 and -c3 on the other hand displayed strong staining along the nuclear membrane, but not within the nucleus. As such, a positive nucleus was counted when a clearly stained membrane was identified (Figures 3.6, 3.9 & 3.10). See figure 3.5 for positive standards of myonuclear staining, which were described as a hemotoxylin stained nucleus that was within the anti-laminin stained basement membrane of the cell. Carl Zeiss Binocular Microscope (Carl Zeiss Canada Ltd, Ontario, Canada) fitted with a 100x oil lens was used for total nuclear counts as well as specific area counts. A total cross-sectional area of 1.043 mm^2 was analyzed on each individual muscle in order to quantify myonuclear counts. Numbers found for specific area counts were then matched with MyHC analysis (Figures 3.8, 3.9, 3.10 & 3.11) using the same custom-designed analytical program (Figure 2.1) (Putman*, et al.*, 2000). An area of 0.39mm^2 was examined from each muscle for the various NFAT isoforms.

Nuclear counts where specific area counts were performed by two observers; an additional observer assisted with nuclear counts. Myonuclear counts and NFAT-c2 nuclear counts were performed by observer one. NFAT-c1 and NFAT-c4 nuclear counts were completed by observer two and NFAT-c3 nuclear counts were completed by observer three. Specific area counts of NFAT-c1 and NFAT-c4 were completed by observer two, while NFAT-c2 and NFAT-c3 specific area counts were completed by observer one. Patterns of strong, positive staining were established as the uniform standard across all stains prior to analysis. Pilot analysis determined inter-observer reliability was 98%.

It is important to note that the hybrid type-IIA/D(X)/B fibres were rarely observed in the 0-day control muscles (see Figure 3.4); the frequency of NFAT-c1, –c2, -c3 and -c4 nuclear staining at 0-day within this fibre population was too low to conduct statistical analysis (i.e., the 4 type-IIA/D(X)/B fibres were not positive for NFAT-c1; one of the 4 type-IIA/D(X)/B fibres was positive for NFAT-c2; one of the 4 type-IIA/D(X)/B fibres was positive for NFAT-c3; all of the 4 type-IIA/D(X)/B fibres were not positive for NFAT–c4). Similarly, the pure type-IIB fibres were rarely observed at all time points (see Figure 3.4). Thus the frequency of NFAT-c1, –c2, -c3 and -c4 nuclear staining within pure type-IIB fibres was too low to conduct statistical analysis. In the 0-day control muscles 1 out of 4 fibres was positive for NFAT-c1, at 5-days 2 out of 12 fibres were positive for NFAT-c1 and at 10-days the one pure type-IIB fibre observed did not express NFAT-c1. In the 0-day control muscles 2 out of 4 fibres were positive for NFAT-c2, at 5-days 9 out of 12 fibres were positive for NFAT-c2 and at 10-days the one pure type-IIB fibre observed did not express NFAT-c2. In the 0-day control muscles 3 out of 4 fibres was positive for NFAT-c3, at 5-days 10 out of 12 fibres were positive for NFAT-c3 and at 10-days the one pure type-IIB fibre observed did not express NFAT-c3. In the 0-day control muscles 1 out of 4 fibres were positive for NFAT-c4, at 5-days 4 out of 12 fibres were

positive for NFAT-c4 and at 10-days the one pure type-IIB fibre observed did not express NFAT-c4. Graphs representing the small number of type-IIB as well as type-IIA/D(X)/B fibres expressing NFAT-c1, -c2, -c3 and -c4 are shown in Figure 3.12.

2.2.8 Statistics

Data were summarized as means ± SEM. Differences between group means were assessed using a one-way Analysis of Variance (ANOVA) [i.e. MyHC I x Time (0, 5, 10 day Stimulated)]. When a significant *F*-ratio was found, differences were located using the Least Significant Difference post-hoc analysis for planned comparisons. Differences were considered significant at $P < 0.05$. Data was considered a trend at $P<0.10$.

CHAPTER THREE

RESULTS

3.1 Animal Weights

Animals initially weighed 306±6g (mean ± SEM) and at the end of the experiment weighed 332±6g. Weight change throughout the experiment was similar between groups (i.e., 0-day sham operated 326±10g to 339±7g; 5-day 318±5g to 346±12g; 10-day 312±10g to 338±12g; 21-day 267±4g to 307±8g). Variations in initial weight between 21-day rats (Martins*, et al.*, 2006), and those studied at 0-, 5- and 10-days (Martins*, et al.*, 2009) reflect different initial ages of the animals, which were 3 months old (Martins*, et al.*, 2006) and 4 months (Martins*, et al.*, 2009).

3.2 Fibre Type Transformation in the *peroneus longus m.*

The fibre type characteristics of the *peroneus longus m.* have not yet been fully characterized. Armstrong and Phelps (1984) reported that the fibre composition of *peroneus longus m.* of adult Sprague-Dawley rats was 48±8% FG, 41±7% FOG and 11±2% SO. In that study they also evaluated the oxidative capacity of fibres, using nicotinamide adenine dinucleotide tetrazolium reductase (NADH-TR) histochemical staining, and differentiated fibre type using myosin ATPase histochemistry. In contrast, the present study employed more precise immunohistochemical methods and isoform-specific MyHC antibodies to identify muscle fibre types, as shown in Figure 3.1. The proportions of FG, FOG and SO fibres reported by those authors corresponds to type-IIB, type-IIA and type-I fibres quantified in the present study. However, the immunohistochemical method used in the present study allowed precise identification of type-IID/X fibres.

The proportion of pure type-IIB fibres observed in the present study was 0.4% (Figure 3.4), which appears very low by comparison. It is, however, important to note that myosin-ATPase histochemistry does not distinguish between type-IIB and –IID/X fibres. Therefore, for the purpose of comparison it seems reasonable to consider the sum of pure type-IIB (0.4%),

hybrid fibre types-IID/IIB (15.3%) and -IIA/IID/IIB (0.3%) (Figures 3.2 and 3.4), plus type-IID fibres (24%) (Figure 3.4). The resultant 40% of total fibres is similar to that reported by Armstrong and Phelps (1984). The present study extends and clarifies their earlier findings by clearly identifying and quantifying the two fastest fibre populations within the *peroneus longus m.*

In order to compare the proportion of FOG fibres reported by Armstrong and Phelps (1984) to the corresponding fibre population reported in the present study, it is important to apply up-to-date nomenclature. The FOG fibre population used in that study is more appropriately termed FO and corresponds to those fibres expressing MyHC-IIa in the present study (Figures 3.1 & 3.2). The previously reported value of 41% (Armstrong, R. B. & Phelps, 1984) is similar to the value of 45% observed in the present study (Figures 3.1 & 3.2). Similarly, the proportion of pure type-I fibres quantified in the present study (i.e., 15%) (Figure 3.4) compares very closely to the proportion of SO fibres previously reported (Armstrong, R. B. & Phelps, 1984).

A novel finding of the present study was that 30±6% of all fibres observed with the *peroneus longus m.* of 0-day controls were classified as *hybrid fibres* (Figure 3.3). The co-expression of two or more MyHC-isoforms within such a large proportion of fibres appears to be unique to the *peroneus longus m.* when compared with other rat hindlimb muscles that are located within the anterior, posterior and lateral crural compartments. Previous studies conducted within the same laboratory that investigated mixed fast-twitch rat *tibialis anterior m.* (Martins*, et al.*, 2006; Martins*, et al.*, 2009; Putman, Kiricsi*, et al.*, 2003), *extensor digitorum longus m.* (Putman*, et al.*, 2000; Putman*, et al.*, 2001) or *plantaris m.* (Gallo*, et al.*, 2008) observed a very small proportion of hybrid fibres (1-4%) within 0-day control muscles.

This important difference appears to be the result of greater daily recruitment of the *peroneus longus m.,* as discussed in section 4.2.

CLFS induced a *fast-to-slow*er phenotypic transition (Figures 3.1, 3.2 & 3.4). Specifically, the proportion of fibres expressing MyHC-IIa increased in response to CLFS ($P<0.002$) (Figure 3.2). This was largely due to a decrease in the proportion of IID fibres ($P<0.0003$) which transitioned into type-IIA/IID hybrid fibres, as shown by progressive increases of 2.5-, 3.0- and 4.0-fold after 5-, 10- and 21-days, respectively ($P<0.03$) (Figure 3.4). After 21-days of CLFS the proportion of type-I/IIA fibres was significantly decreased, when compared with 5- and 10-days ($P<0.02$); which would suggest they are transitioning toward the Type-1 fibres (Figure 3.4). The proportion of pure type-IIB fibres was low at 0-day and did not change in response to CLFS (i.e., 1.2% at 5-days, 0.1% at 10-days and 0.1% at 21-days) (Figure 3.4).

CLFS-induced fibre type transitions seem to have largely occurred after 5-days, which is earlier than previously demonstrated in the *extensor digitorum longus m.* (Putman*, et al.*, 1999, 2000) and *tibialis anterior m.* (Martins*, et al.*, 2006). Considering the large proportion of hybrid fibres that exist within the *peroneus longus m.* prior to the application of CLFS (Figure 3.3), an accelerated response of this muscle to stimulation is not surprising. Another divergent finding when compared to previous studies (Martins*, et al.*, 2006; Putman*, et al.*, 1999, 2000) is the change in overall proportion of hybrid fibre types. While there were significant changes in specific hybrid fibre types, increases in the proportion of total hybrid fibres only demonstrated an increasing trend ($P<0.07$) (Figure 3.3).

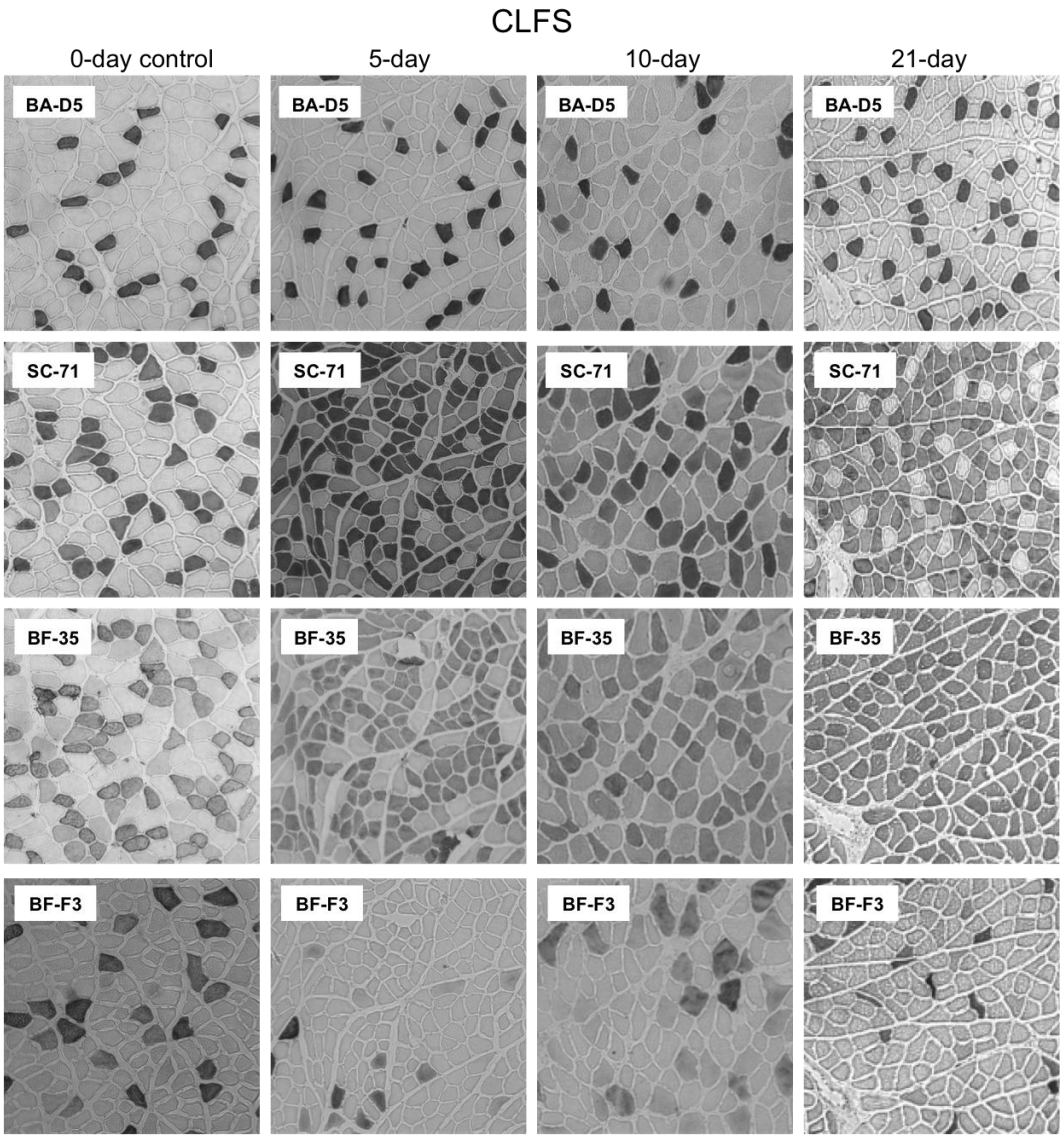

Figure 3.1 Representative photomicrographs of MyHC immunohistochemistry. 10 µm thick serial sections of *peroneus longus m.* were immunostained for MyHC-I (clone BA-D5), MyHC-IIa (clone SC-71), all MyHC's but not MyHC-IId(x) (clone BF-35), and MyHC-IIb (clone BF-F3). Columns are as labelled: 0-day Control, 5-days of CLFS, 10-days of CLFS, and 21-days of CLFS. Scale bar represents 100 µm.

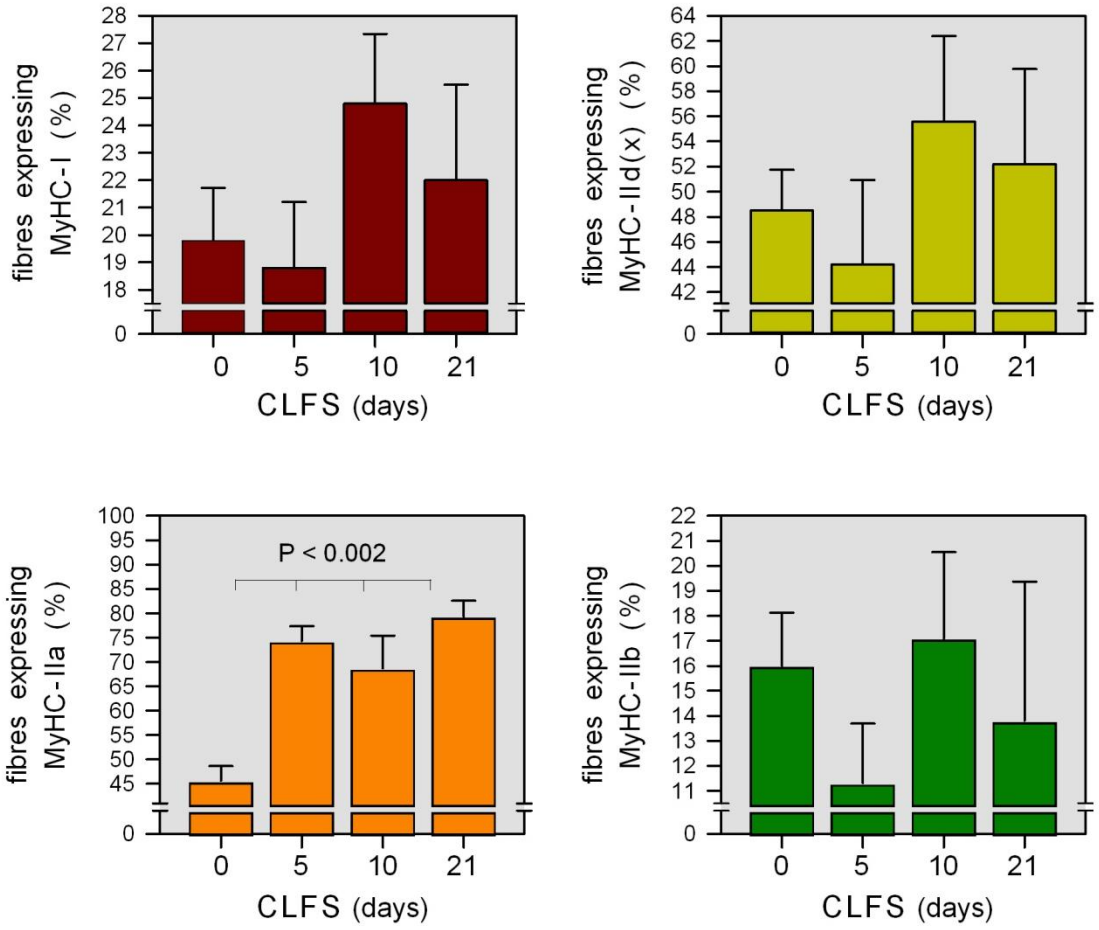

Figure 3.2 The proportion of muscle fibres expressing a MyHC isoform in the *peroneus longus m*. N = 6 at each time point. The number of fibres included in this analysis was 5,861. Data are mean ± SEM.

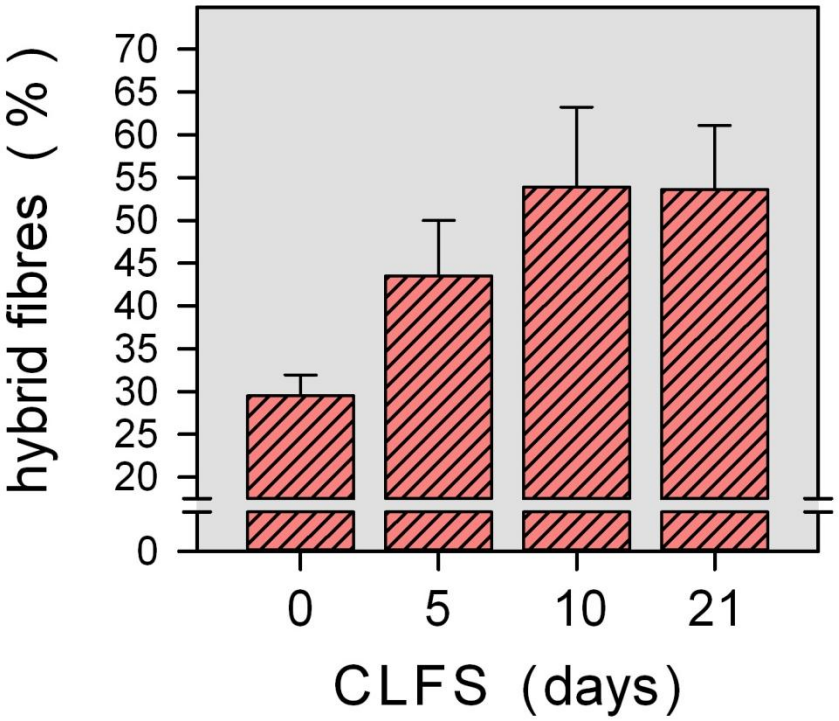

Figure 3.3 The proportion of hybrid muscle fibres simultaneously expressing two or more MyHC isoform within the *peroneus longus m.* N = 6 at each time point. The number of fibres included in this analysis was 5,861. Data are mean ± SEM.

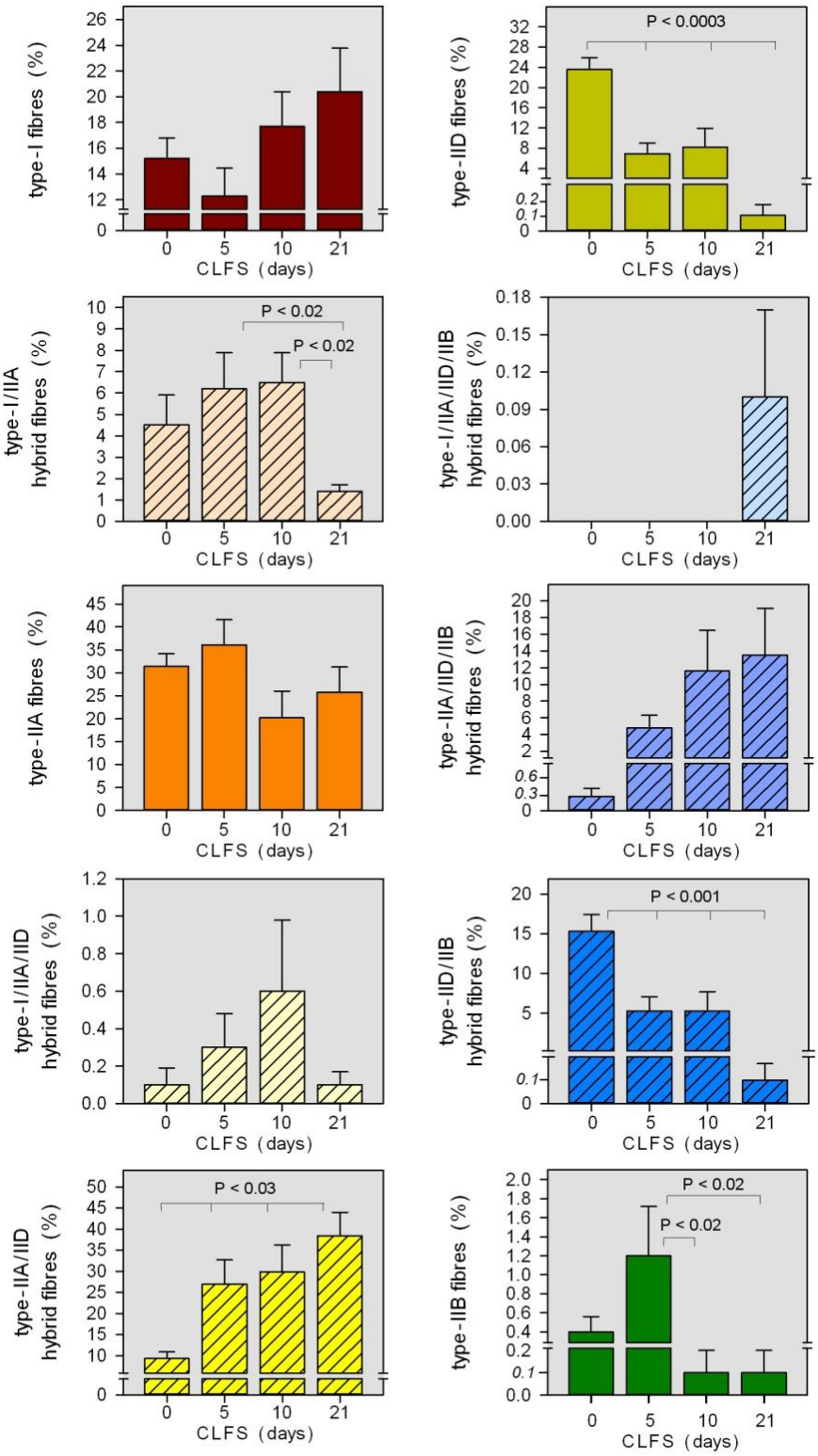

Figure 3.4 The proportion of individual hybrid muscle fibres within the *peroneus longus m.* N = 6 at each time point. The number of fibres included in this analysis was 5,861. Data are mean ± SEM.

3.3 Myonuclear Counts of NFAT-c1, -c2, -c3, -c4

The total myonuclear content was quantified on frozen sections of the *peroneus longus m.* that were immunohistochemically stained for the basement membrane protein laminin and counterstained with Hematoxylin, as shown in Figure 3.5. The corresponding data are summarized in Figure 3.7. An unexpected finding of this study was the approximate 2-fold greater number of myonuclei at 0-days when compared with the *tibialis anterior m.* (Martins*, et al.*, 2006; 2009; 2012) and the *extensor digitorum longus m. (Putman, et al., 1999; 2001)*. Additionally, unlike the previously mentioned studies, there were no significant time dependent changes in myonuclear content within the *peroneus longus m.* in response to CLFS. Collectively, the data show the *peroneus longus m.* already had a high myonuclear density than has been observed in muscle exposed to CLFS for 20- to 50-days (Putman*, et al.*, 1999; 2001). This seems especially relevant to the current data because the *peroneus longus m.* appears to inherently possess a myonuclear content that exceeds a suggested threshold thought to be necessary to support fibre type transition (Martins*, et al.*, 2009).

As hypothesized, NFAT-c4 positive nuclei remained constant over time. Interestingly, the absolute NFAT-c3 content (i.e., number/mm^2) increased from 0-day control to 5-day ($P<0.002$) and subsequently decreased at 10-day ($P<0.002$). The relative NFAT-c3 content displayed the same pattern, however did not reach significance. Since the overall myonuclear content of the *peroneus longus m.* did not change (Figure 3.7) the absolute data would be considered. The overall number of NFAT-c2 positive nuclei showed no significant change. Whereas, consistent with previous findings (Martins*, et al.*, 2012) NFAT-c1 significantly increased at the 5 day time point ($P<0.0001$) and then decreased at 10 days ($P<0.0001$) (Figure 3.7).

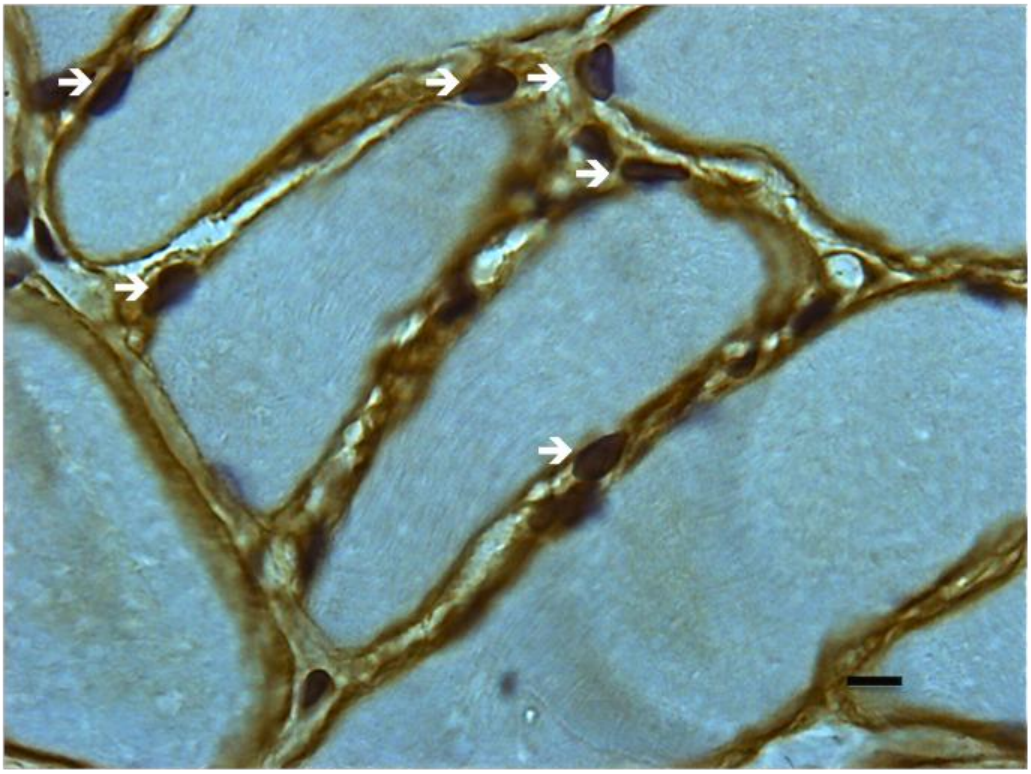

Figure 3.5 Representative micrograph of anti-laminin immunohistochemical staining, with a hemotoxylin counterstain. Myonuclei were identified as hemotoxylin positive within the circumference of the anti-laminin stain. Myonuclei are indicated by the white "➔". Scale bar represents 10μm.

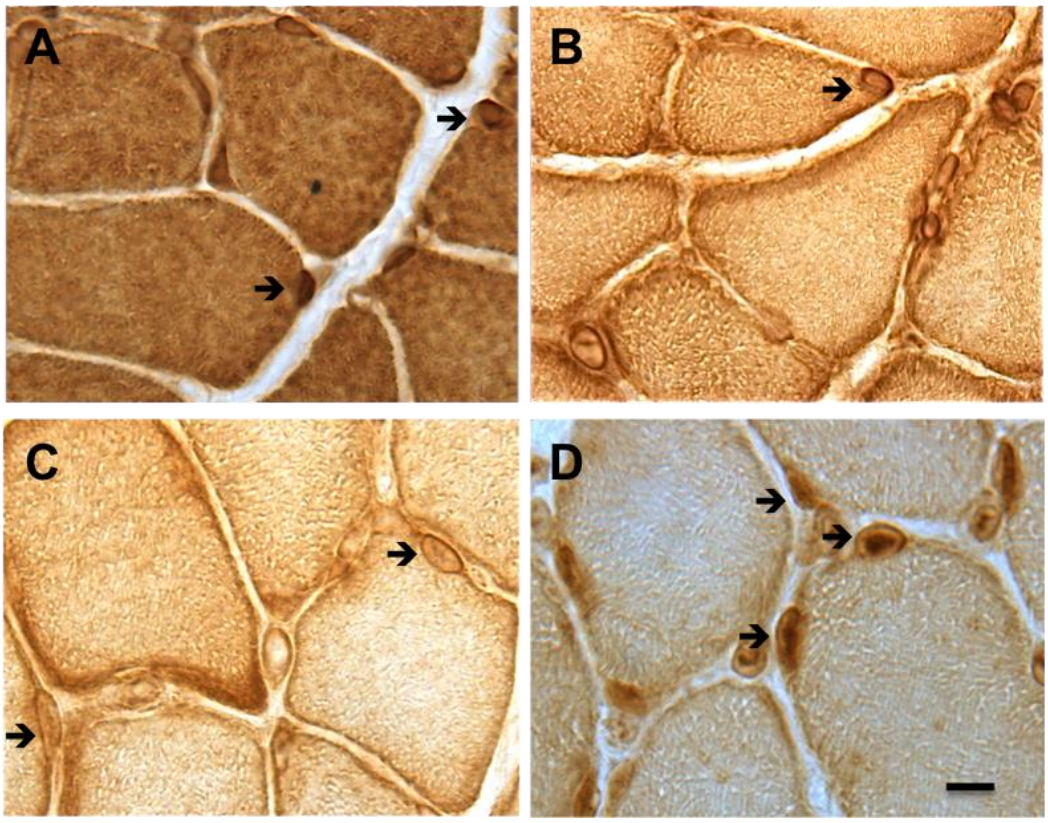

Figure 3.6 Representative micrographs of frozen sections immunohistochemically stained for the four NFAT isoforms. A) NFAT-c1, B) NFAT-c2, C) NFAT-c3, and D) NFAT-c4. Positive nuclear stains are indicated by "➔". Scale bar represents 10 μm.

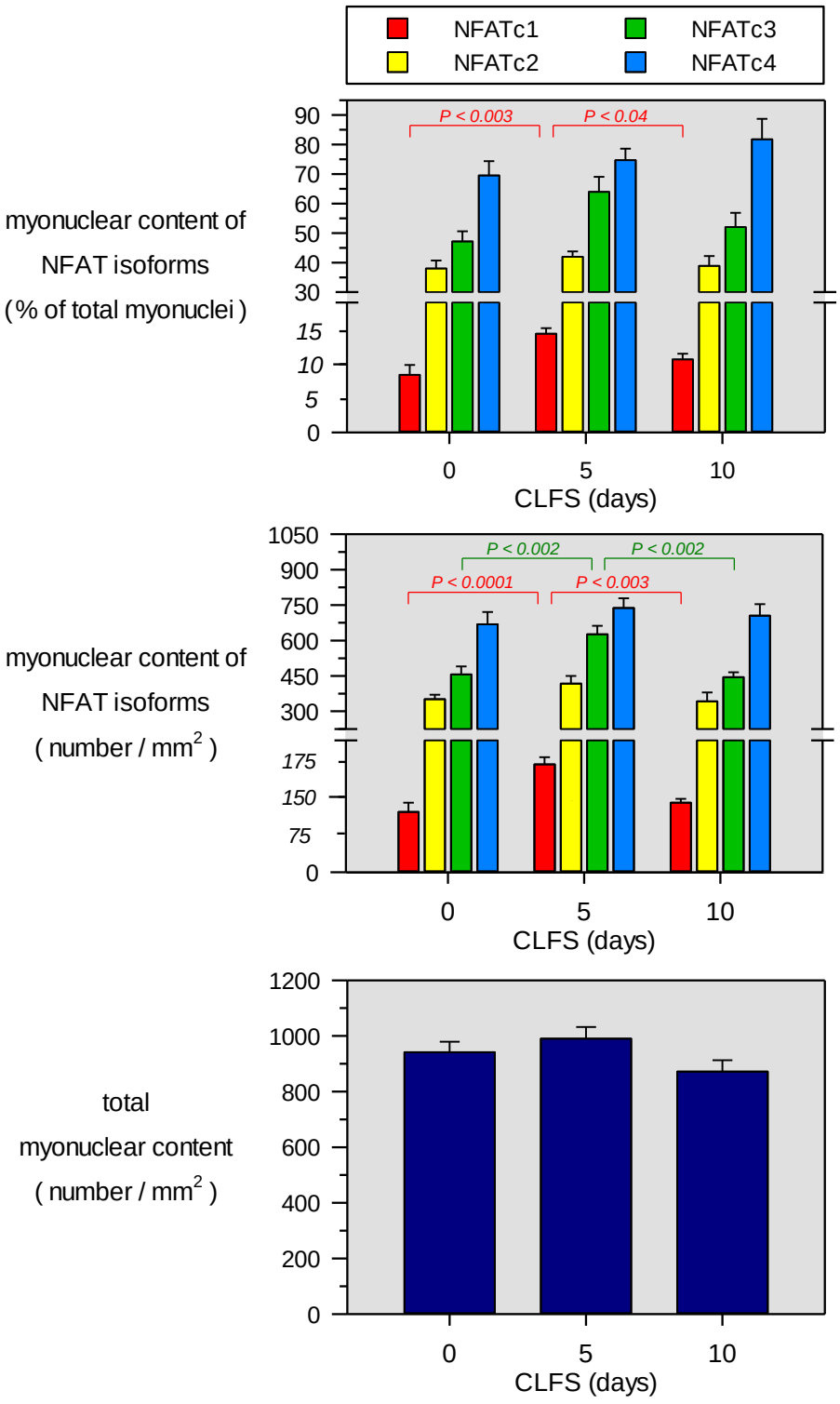

Figure 3.7 The relative (%) and absolute (number/mm²) myonuclear contents of NFAT isoforms, and total myonuclear content (number/mm²). Data are mean ± SEM.

3.3 Association of Fibre type and NFAT isoform

The patterns of NFAT isoform expression were examined on serial sections and quantified within all pure and hybrid fibre types (Figures 3.8, 3.9, 3.10 and 3.11). Criteria described in section 2.2.7 were set according to (Martins, *et al.*, 2012) and (Calabria, *et al.*, 2009).

The method used to analyze the fibre type specific pattern of NFAT-c1 expression is shown in Figure 3.8 and the corresponding data are summarized in Figures 3.12 and 3.13. The staining pattern of NFAT-c1 mirrored that of Martins *et al.* (2012), which was typically highly concentrated at the nuclear envelope (Figure 3.6A). When the nuclear localisation of NFAT-c1 was examined according to fibre types (Figure 3.12) a clear increase was observed within type-I ($P<0.02$) and type-IIA/D(X) ($P<0.005$) fibres at 5-days, which subsequently decreased at 10-days ($P<0.004$ and $P<0.003$, respectively) (Figure 3.12 and Figure 3.13). Interestingly, the type-IIA/D(X)/B fibres were rarely observed in control muscles (0.3% of fibres, Figure 3.4).

The method used to analyze the fibre type specific pattern of NFAT-c2 expression is shown in Figure 3.9. It is important to note that the staining pattern of NFAT-c2 (Figure 3.6B) was similar to that of NFAT-c1 but displayed a lower staining intensity that was still clearly detectable. This observation was consistent with the pattern shown by Calabria *et al.* (2009). The corresponding data for NFAT-c2 are summarized in Figures 3.12 and 3.13. There was a significant decrease in the nuclear localization of NFAT-c2 ($P<0.02$) in the type-IID(X) fibres (Figure 3.13), decreasing by 4-fold from 0- to 10-days (Figure 3.12).

The fibre type specific pattern of NFAT-c3 expression was analyzed using the method illustrated in Figure 3.10. The intensity and pattern of NFAT–c3 staining were similar to that of NFAT-c2 (Figure 3.6). The

corresponding data are summarized in Figures 3.12 and 3.14. NFAT-c3 nuclear localisation increased within type-I/IIA fibres ($P<0.02$) and type-IID/B fibres ($P<0.02$) after 10-days of CLFS (Figure 3.12). By comparison, NFAT-c3 nuclear localisation increased within type-IIA/D fibres after 5-days ($P<0.03$) and 10-days ($P<0.002$) of CLFS (Figure 3.12 and 3.14).

The method used to analyze the fibre type specific pattern of NFAT-c4 expression is shown in Figure 3.11 and the corresponding data are summarized in Figures 3.12 and 3.14. The staining pattern of NFAT-c4 was similar to that of NFAT-c1, with a slightly higher staining intensity. According to Calabria *et al.* (2009) NFAT-c4 is present in the nucleus at all exercise states and in all fibre types, therefore the darker staining would reflect that difference in expression. When the pattern of NFAT-c4 expression was examined according to all pure and hybrid fibre types (Figures 3.12 & 3.14) no changes in expression were detected in response to CLFS.

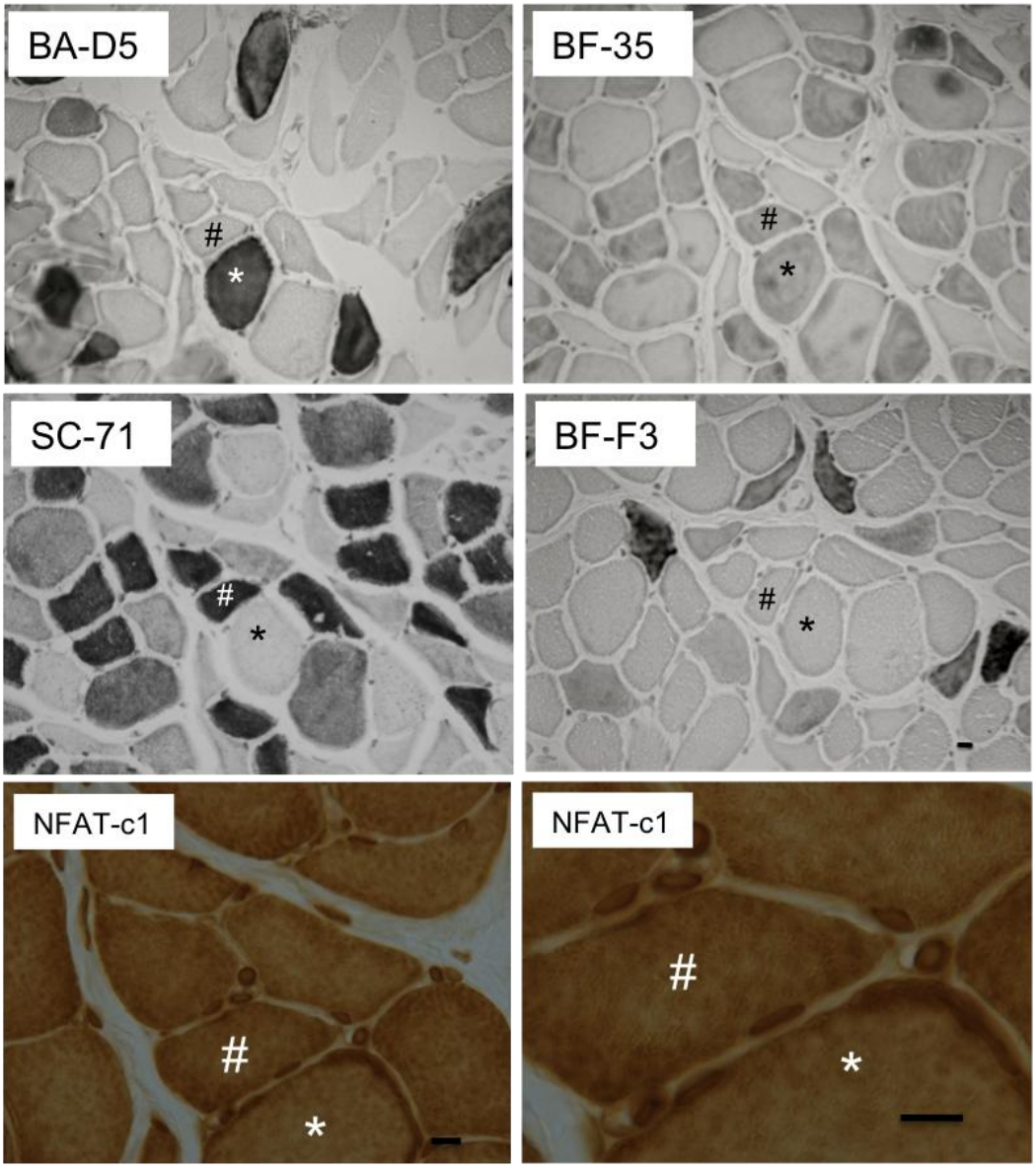

Figure 3.8 Representative micrographs of serial sections immunohistochemically stained to identify fibres expressing MyHC-I (BA-D5), MyHC-IIa (SC-71), all MyHC but not MyHC-IId(x) (BF-35) and MyHC-IIb (BF-F3), and to identify nuclear expression of NFAT-c1. * indicates a type-I fibre that is positive for NFAT-c1. # indicates a type-IIA fibre that is positive for NFAT-c1. Scale bar represents 10 μm.

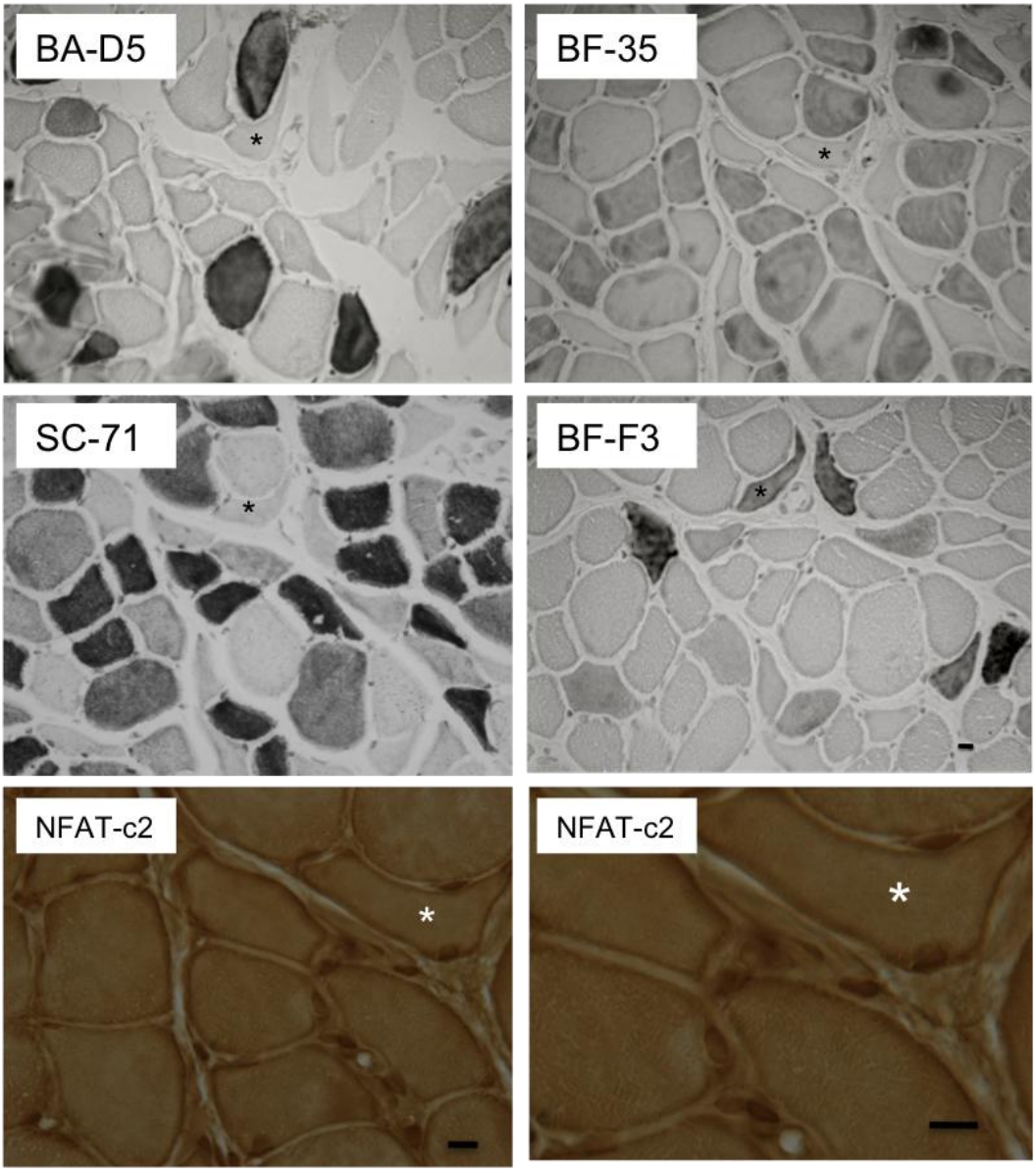

Figure 3.9 Representative micrographs of serial sections immunohistochemically stained to identify fibres expressing MyHC-I (BA-D5), MyHC-IIa (SC-71), all MyHC but not MyHC-IId(x) (BF-35) and MyHC-IIb (BF-F3), and to identify nuclear expression of NFAT-c2. * indicates a hybrid type-IID(X)/IIB fibre that is positive for NFAT-c2. Scale bar represents 10 μm.

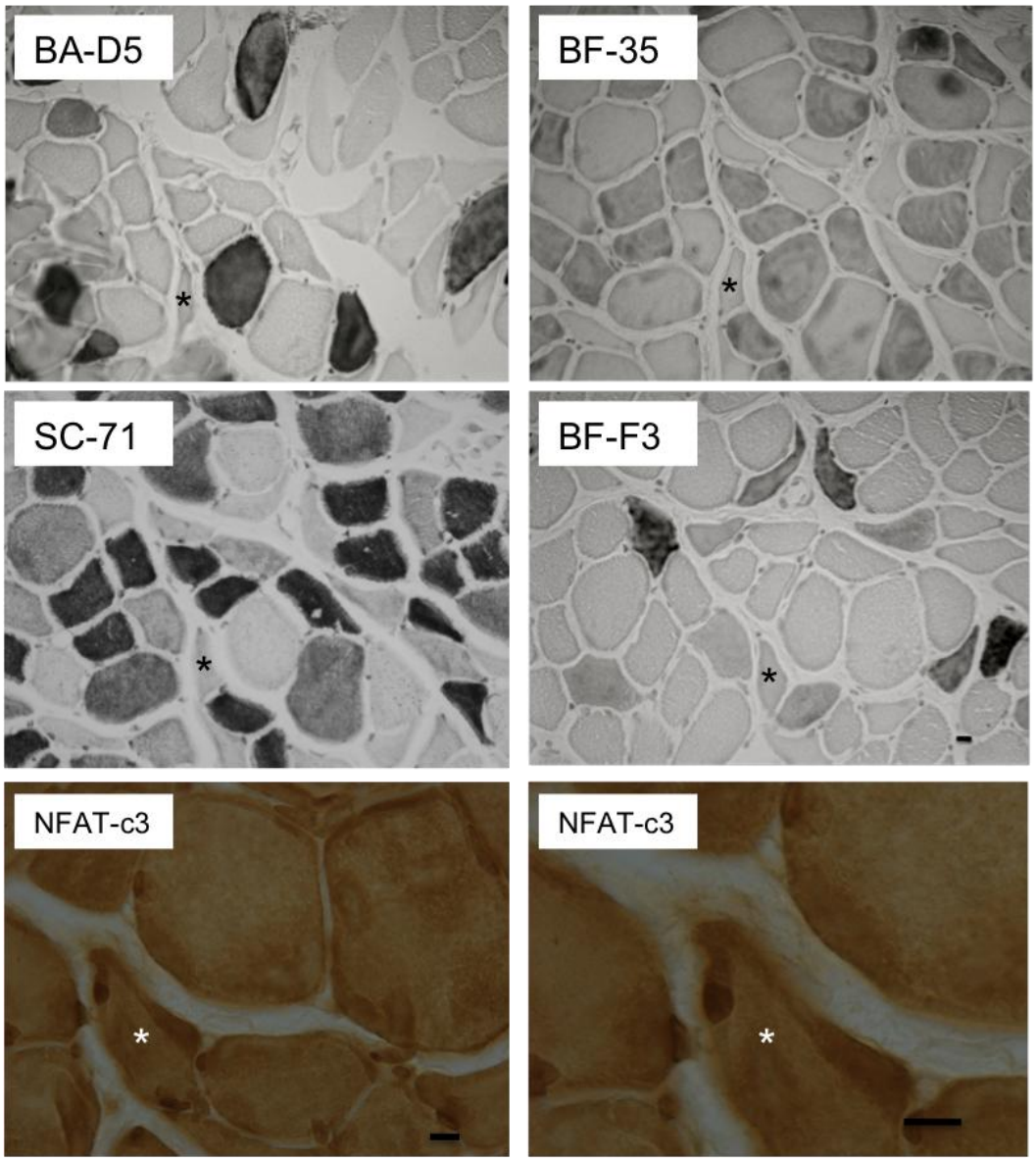

Figure 3.10 Representative micrographs of serial sections immunohistochemically stained to identify fibres expressing MyHC-I (BA-D5), MyHC-IIa (SC-71), all MyHC but not MyHC-IId(x) (BF-35) and MyHC-IIb (BF-F3), and to identify nuclear expression of NFAT-c3. * indicates a type-IID(X) fibre that is positive for NFAT-c3. Scale bar represents 10 μm.

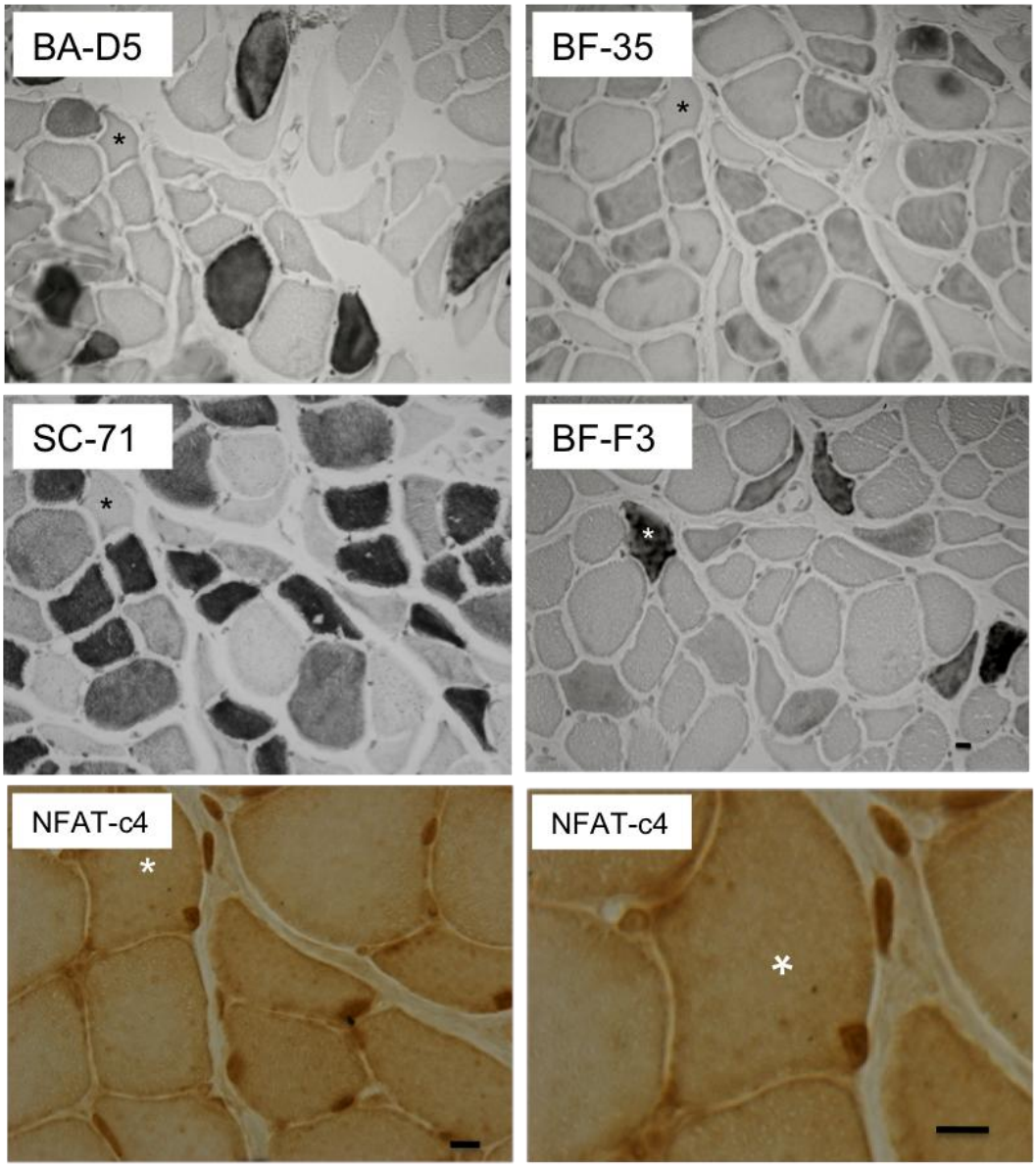

Figure 3.11 Representative micrographs of serial sections immunohistochemically stained to identify fibres expressing MyHC-I (BA-D5), MyHC-IIa (SC-71), all MyHC but not MyHC-IId(x) (BF-35) and MyHC-IIb (BF-F3), and to identify nuclear expression of NFAT-c4. * indicates a type-IIB fibre that is positive for NFAT-c4. Scale bar represents 10 μm.

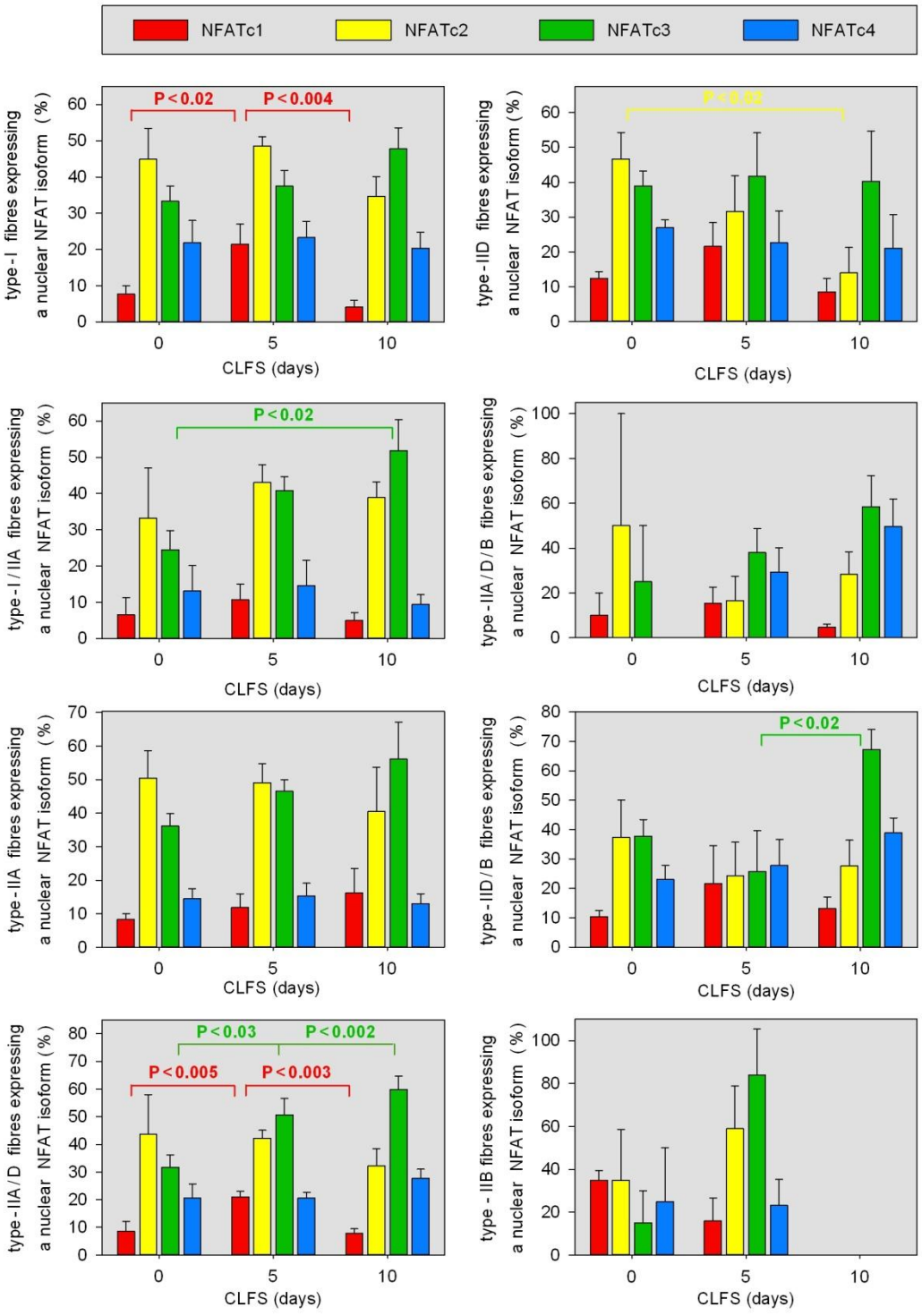

Figure 3.12 The proportion of individual hybrid muscle fibres within the *peroneus longus m.* expressing a particular NFAT isoform. N = 5 at 0-day time point, N = 5 at 5-day time point, and N = 6 at 10-day time point. The number of fibres included in this analysis was 3, 075. Data are mean ± SEM.

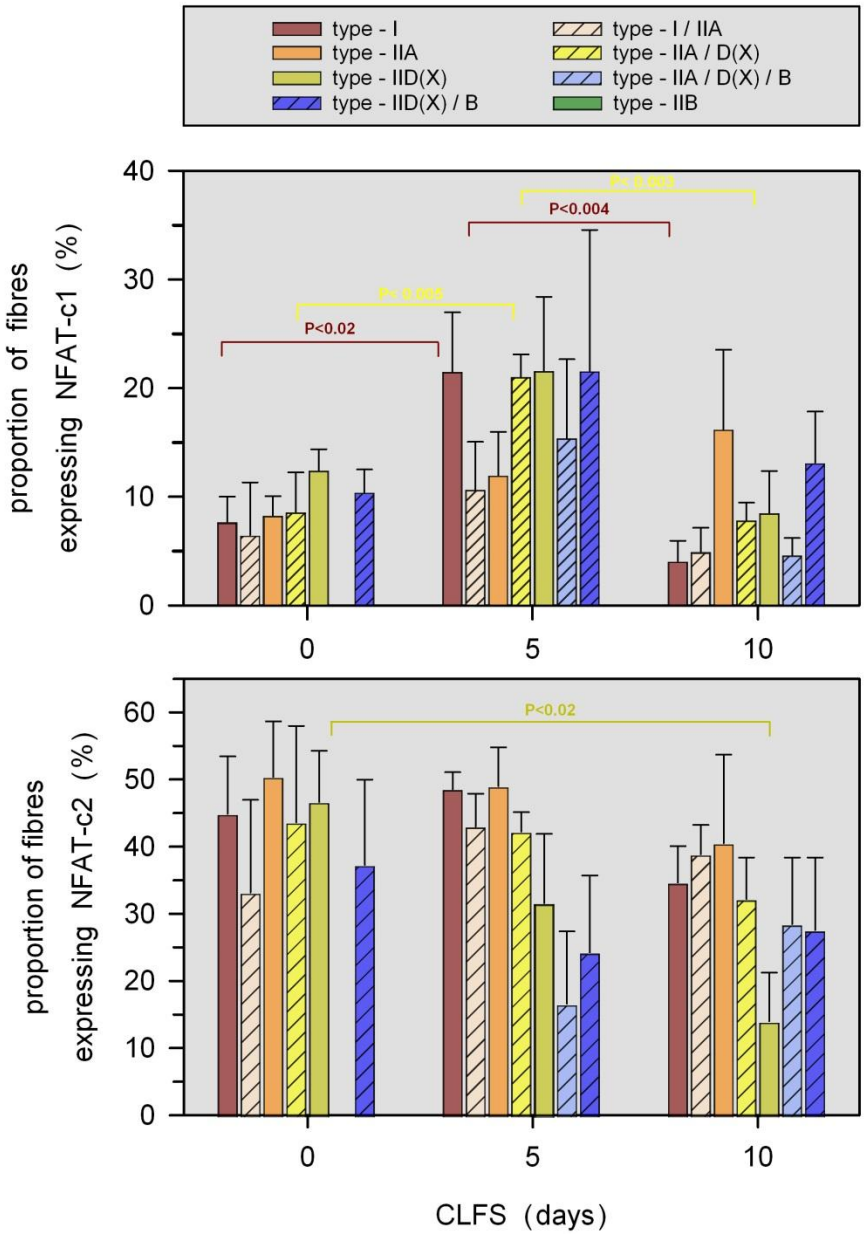

Figure 3.13 The proportion of individual hybrid muscle fibres within the *peroneus longus m*. expressing NFAT-c1 and -c2 isoforms. N = 5 at 0-day time point, N = 5 at 5-day time point, and N = 6 at 10-day time point. The number of fibres included in this analysis was 3, 034. Data are mean ± SEM. It is important to note that the hybrid type-IIA/D(X)/B fibres were rarely observed in the 0-day control muscles (see Figure 3.4); the frequency of NFAT-c1 and –c2 nuclear staining at 0-day within this fibre population was too low to conduct statistical analysis (i.e., the 4 type-IIA/D(X)/B fibres were not positive for NFAT-c1; One of the 4 type-IIA/D(X)/B fibres was positive for NFAT-c2). Similarly, the pure type-IIB fibres were rarely observed at all time points (see Figure 3.4). Thus the frequency of NFAT-c1 and –c2 nuclear staining within pure type-IIB fibres was too low to conduct statistical analysis. In the 0-day control muscles 1 out of 4 fibres was positive for NFAT-c1, at 5-days 2 out of 12 fibres were positive for NFAT-c1 and at 10-days the one pure type-IIB fibre observed did not express NFAT-c1. In the 0-day control muscles 2 out of 4 fibres were positive for NFAT-c2, at 5-days 9 out of 12 fibres were positive for NFAT-c2 and at 10-days the one pure type-IIB fibre observed did not express NFAT-c2.

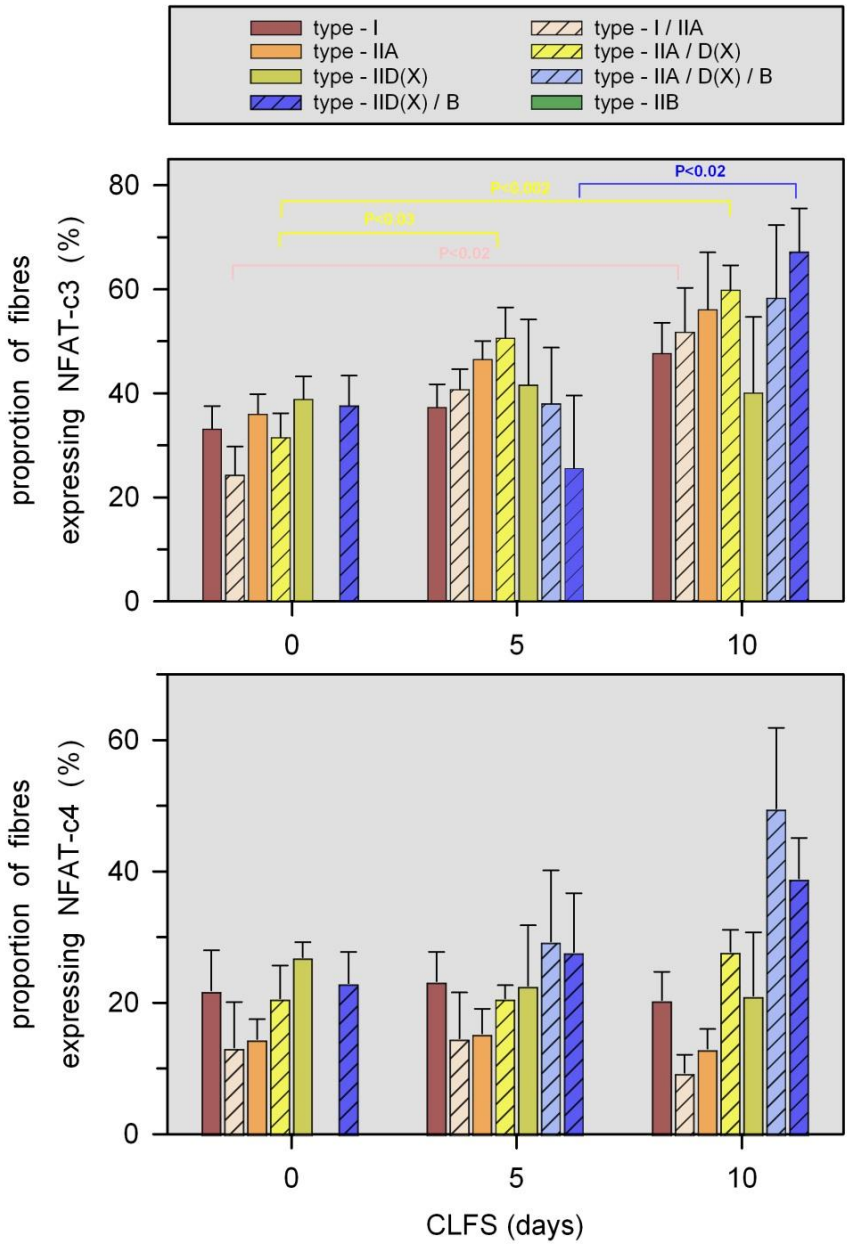

Figure 3.14 The proportion of individual hybrid muscle fibres within the *peroneus longus m.* expressing NFAT-c3 and -c4 isoforms. N = 5 at 0-day time point, N = 5 at 5-day time point, and N = 6 at 10-day time point. The number of fibres included in this analysis was 3, 034. Data are mean ± SEM. It is important to note that the hybrid type-IIA/D(X)/B fibres were rarely observed in the 0-day control muscles (see Figure 3.4); the frequency of NFAT-c3 and –c4 nuclear staining at 0-day within this fibre population was too low to conduct statistical analysis (i.e., one of the 4 type-IIA/D(X)/B fibres was positive for NFAT-c3; all of the 4 type-IIA/D(X)/B fibres were not positive for NFAT–c4). Similarly, the pure type-IIB fibres were rarely observed at all time points (see Figure 3.4). Thus the frequency of NFAT-c3 and –c4 nuclear staining within pure type-IIB fibres was too low to conduct statistical analysis. In the 0-day control muscles 3 out of 4 fibres was positive for NFAT-c3, at 5-days 10 out of 12 fibres were positive for NFAT-c3 and at 10-days the one pure type-IIB fibre observed did not express NFAT-c3. In the 0-day control muscles 1 out of 4 fibres were positive for NFAT-c4, at 5-days 4 out of 12 fibres were positive for NFAT-c4 and at 10-days the one pure type-IIB fibre observed did not express NFAT-c4.

CHAPTER FOUR

DISCUSSION

4.1 Introduction

The purpose of the present study was to investigate the relationship between the activity-induced transition of individual fibre types, and the preceding expression patterns of various NFAT-isoforms within mammalian skeletal muscle (*i.e.,* NFAT-c1, NFAT-c2, NFAT-c3 and NFAT-c4). Previous studies have reported correlations between muscle fibre types and the pattern of NFAT-isoform expression in normal control muscles (Calabria*, et al.*, 2009; Meissner, Umeda*, et al.*, 2007; Mutungi, 2007). However, the question remains as to whether muscle training can induce predictable changes in the patterns of NFAT-isoform expression, and associated nuclear translocation, which corresponds to the newly transformed muscle fibre phenotype.

A unique characteristic of this study is the comprehensive characterization of the immunohistochemically identified fibre type distribution of the *peroneus longus m*. at rest and with stimulation. Contrary to the current hypothesis, the proportion of fibres expressing each NFAT isoform at rest did not differ between fibre types. When stimulated with CLFS an overall shift toward a slower phenotype was observed. The proportion of fibres expressing NFAT-c1 and NFAT-c4 with CLFS happened as expected. Considerable transitions occurred within the fibre populations expressing MyHC-IIa and –IId(x). A corresponding increase in NFAT-c3 and decrease in NFAT-c2 nuclear localisation, respectively, suggests a role for NFAT-c2 in the maintenance of the IID(X) phenotype and a role for NFAT-c3 in the transition toward type-IIA fibres. Overall, changes in NFAT-c2 and -c3 were consistent with having important roles in the transformation and maintenance of the more oxidative fast fibre populations.

4.2 The Unique Composition of the Peroneus Longus m. at Rest

The rat *peroneus longus m.* is an infrequently studied rat mixed fast-twitch muscle in training adaptation research and as such, the fibre type composition has not been fully elucidated. Previous research has reported the composition to be 48±8% FG fibres (*i.e.,* type-IIB, type-IID(X)), 41±7% FOG fibres (*i.e.,* type-IIA, type-IID(X)), and 11±2% SO (*i.e.,* type-I) (Armstrong, R. B. & Phelps, 1984). In contrast, the current investigation has found 39±7% FG fibres, 46±3% FOG fibres, and 15±4% SO fibres. As discussed in section 1.3, the discovery of MyHC-IId(x) (Bar & Pette, 1988) and the corresponding type-IID(X) fibres (Schiaffino*, et al.*, 1989) occurred after the study of Armstrong and Phelps (1984). Therefore, the more precise immunohistochemical methods could partially account for the difference in proportions. Similar to current numbers, the proportion of type-I fibres in the *peroneus longus m.* in cat was reported to be 11.8 - 14.6% (Kernell & Hensbergen, 1998). In sheep, the *peroneus longus m*. is considered a locomotory muscle (Watanabe & Suzuki, 1999), if the same is true of rat it could explain the resting fibre type proportions. Kernell & Hensbergen (1998) measured daily muscle activity of cat muscles and found the *peroneus longus m.* was in use ≤9.5% of the day whilst, the *extensor digitorum longus m.* was only in use ≤1.9% of the day. Hence, the fibre type composition of the *peroneus longus m.* at rest is substantially different than the more commonly studied *tibialis anterior m.* and *extensor digitorum longus m.* The proportion of type-IIA fibres is substantially higher in the *peroneus longus m.*, while the proportion of type-IIB fibres is considerably lower. While the *peroneus longus m*. is described as a mixed fast-twitch muscle, but its composition is considerably slower than other mixed fast twitch muscles. Previous research has directly compared the *extensor digitorum longus m*. with the *peroneus longus m*. and found similar results. The area occupied by the type-IIB fibres was less than 5% in the *peroneus longus m*, whereas it was approximately 70% in the *extensor digitorum longus m.* (Ranatunga & Thomas, 1990).

A novel finding of the present study was the large proportion of hybrid fibres in control *peroneus longus m.* which was 30±6%. In contrast, Martins *et al.* (2009) found the proportion of hybrid fibres in control *tibialis anterior m.* was only 4%. Hybrid fibres are an indication of fibre type transition and are normally seen to increase in a time dependent manner with stimulation. This large discrepancy in hybrids between the *tibialis anterior m.* and *the peroneus longus m*. would suggest transition is happening at rest and being a locomotory muscle, transition at rest would not be totally unexpected. This constant state of plasticity would allow for a muscle that is more readily adaptive to stimulation.

There are many inherent differences between slow- and fast-twitch muscles at rest as discussed earlier. Major variations are present in Ca^{2+} concentration kinetics, including a higher resting cytosolic free [Ca^{2+}] in slower, than faster muscles (Carroll, S. L.*, et al.*, 1997; Carroll, S. L.*, et al.*, 1999; Fraysse*, et al.*, 2003; Fraysse*, et al.*, 2006); a larger sarcoplasmic reticulum in fast muscles (Trinh & Lamb, 2006); and a higher peak of Ca^{2+} transients and quicker rate of decline in fast muscles (Baylor & Hollingworth, 2003). Given the different traits in Ca^{2+} kinetics at rest and the mixed composition of the *peroneus longus m.,* early phenotypic transitions observed in the present study were not surprising.

4.3 CLFS INDUCED TRANSFORMATION OF THE PERONEUS LONGUS M.

CLFS is a well-characterized model of *fast-to-slow* fibre type transformation in rat that creates sustained low-amplitude increases in [Ca^{2+}] known to preferentially activate the Cn-NFAT pathway (Dolmetsch*, et al.*, 1997; Timmerman*, et al.*, 1996). Previously, our lab has analyzed the changes in the *tibialis anterior m*. with stimulation (Martins*, et al.*, 2006; 2009; 2012). At 21-days of stimulation a significant increase in MyHC-I and a concurrent decrease in MyHC-IIb and MyHC-IId(x) were observed (Martins*, et al.*, 2006),

with considerable fibre transformation occurring at the 10-day time point (Martins*, et al.*, 2009). Comparatively, in the *peroneus longus m*. substantial fibre type adaptation is noticed at the 5-day time point. The rapid transformation of the *peroneus longus m.* is most likely due to the unique plastic nature of this particular muscle. The large number (~30%) of hybrid fibres at rest indicates transformation was already occurring without any external stimuli, therefore it is not surprising that it adapted more readily to CLFS. Specific findings show a significant increase in fibres expressing MyHC-IIa throughout the time course (Figure 3.2), which is in agreement with Martins *et al.* (2009). An increase in type-IIA/D(X) fibres, along with a decrease in type-IID(X), and type-IID(X)/B fibres, indicates *fast-to-slow* fibre type transformation occurred.

4.4 NFAT-c2 and NFAT-c4 are Important for Cell Survival and Fibre Type Maintenance

NFAT-c2 has been found active in many tissues throughout the body in the regulation of cell size and/or number (Horsley & Pavlath, 2002; Ikeda*, et al.*, 2006; Perotti*, et al.*, 2012). In skeletal muscle Calabria *et al.* (2009) suggested that at rest NFAT-c2 nuclear localisation is imperative for the expression of MyHC-I, -IIa, and -IId(x), and with electrical stimulation NFAT-c2 is required for transition of the fastest type-IIB fibres into slower type-IID(X) and eventually type-IIA fibres. Findings of this investigation suggest a contrary role for NFAT-c2 with stimulation. The overall decrease in this particular isoform throughout the time course would seem to indicate a larger role for NFAT-c2 at rest than during transformation. Specifically, the proportion of NFAT-c2 positive nuclei significantly drops at 10-days in type-IID(X) fibres, this change coincides with a decrease in type-IID(X) fibres and a subsequent shift to a slower phenotype. NFAT-c2 plays a significant role during growth in the regulation of myoblast to myotube cell fusion (Horsley*, et al.*, 2001; Horsley*, et al.*, 2003; Horsley & Pavlath, 2003), which leads to

growth and maintenance of the muscle fibre. A similar function for NFAT-c2 could extend to adult skeletal muscle, suggesting NFAT-c2 has a larger role in fibre maintenance and cell survival, rather than transformation without injury.

In skeletal muscle, Calabria *et al.* (2009) reported NFAT-c4 to be required for the maintenance of all fibre types during rest and is involved in the suggested default type-IIB/IID(X) fibre type (Butler-Browne*, et al.*, 1982). Results of the present study support that proposition, with NFAT-c4 levels staying relatively consistent during stimulation. In other tissues, NFAT-c4 has been implicated in cell apoptosis (Li, L.*, et al.*, 2013), and may underlie activity-dependent neuronal plasticity throughout the adult brain (Bradley*, et al.*, 2005). NFAT-c4 has also been shown to be involved in cell survival (Vashishta*, et al.*, 2009), which could be the case in skeletal muscle as well. Overall, current findings as well as findings in other tissues support the notion that NFAT-c4 is involved in the maintenance of a "base fibre type."

4.5 NFAT-c1 and NFAT-c3 are Regulators of *fast-to-slow* Fibre Type Transition

NFAT-c1 is the most widely studied NFAT isoform in adult skeletal muscle to date. Previous research has focused on NFAT-c1 as a key regulator of the slow-gene program in adult muscle at rest (McCullagh*, et al.*, 2004; Mutungi, 2008; Shen*, et al.*, 2006), and with stimulation (Calabria*, et al.*, 2009; Martins*, et al.*, 2012; McCullagh*, et al.*, 2004; Tothova*, et al.*, 2006). The present study used Chronic Low-Frequency Stimulation, which induces the slow-gene program (Martins*, et al.*, 2012; Pette, 1991; Putman*, et al.*, 1999, 2000) to investigate NFAT-c1 activity. The pattern of stimulation is important in the activation and dephosphorylation of NFAT-c1 (Liu, J.*, et al.*, 2001; Martins*, et al.*, 2012; McCullagh*, et al.*, 2004; Tothova*, et al.*, 2006). As such, CLFS provides a slow, consistent increase in Ca^{2+} transients that have

been shown to activate the Cn-NFAT signalling pathway (Chin*, et al.*, 1998; Tothova*, et al.*, 2006).

Findings of the present study indicate a significant role for NFAT-c1 in the early transition from a *faster-to-slower* fibre type, evidenced by the overall increase in NFAT-c1 at 5-days of stimulation and subsequent decrease at 10-days. In particular, there is a substantial increase in NFAT-c1 nuclear localisation at 5-days in type-I and type-IIA/D(X) fibres. The subsequent increase in type-IIA/D(X) fibres along with a concurrent decrease in type-IID(X) and type-IID/B fibres, indicates *fast-to-slower* fibre type transformations occurred. These findings are in agreement with Martins *et al.* (2012), who showed a significant increase in NFAT-c1 nuclear localisation within the *tibialis anterior m*. after 5-days of CLFS and a decrease after 10-days.

In addition, Martins *et al.* (2012) demonstrated the hindrance of NFAT-c1 activity with the blockage Nitric Oxide and downstream GSK-3β dephosphorylation. This finding would implicate GSK-3β as a main export kinase of NFAT-c1, and in turn a regulator of NFAT-c1 activity. Confirming the postulation that differential regulation of the four calcium activated NFAT isoforms could be largely due to the different export and maintenance kinases, rather than activators. In T-cells, the domain of NFAT-c1 that is targeted by calcineurin is phosphorylated and inactivated by the c-Jun NH_2-terminal kinase (JNK) (Chow*, et al.*, 2000). Measuring levels of the other NFAT isoforms with Nitric Oxide blockade would provide insight into whether isoforms other that NFAT-c1 are exported by GSK-3β, another kinase, or a combination. Martins *et al.* (2012) and Calabria *et al.* (2009) both implicated NFAT-c1 in the final transition from type-IIA to type-I. The current data cannot undisputedly discern the function of each NFAT isoform independent of the others, however the significant amount of NFAT-c1 at 5 days in type-I fibres suggests it is the major isoform regulating MyHC-I.

NFAT-c3 seems to function somewhat differently than NFAT-c1. Calabria *et al.* (2009) used a model based on NFAT-isoform specific *si*RNAs and concluded that NFAT-c3 was important for the maintenance of MyHC-I, MyHC-IIa, and MyHC-IId(x), with a stronger influence on MyHC-IIa than MyHC-IId(x). With stimulation, NFAT-c3 translocated into the nucleus in response to slow and fast patterns of stimulation (Calabria*, et al.*, 2009). In this investigation, NFAT-c3 increased in hybrid type-I/IIA, type-IIA/D(X) and type-IID(X)/B fibres. Consistent with the hypothesis tested in this study the nuclear localisation of NFAT-c3 occurred within type-I/IIA and type-IIA/D(X) fibres, which are both transforming hybrid fibres expressing MyHC-IIa. Furthermore, NFAT-c3 appeared in the nuclei of type-IID(X)/B fibres, which are known to transform into type-IIA/D(X)/B fibres and then to type-IIA/D(X) fibres, which are also MyHC-IIa expressing hybrid fibre types (Figures 3.12 & 3.14).

Dephosphorylation and nuclear localization of NFAT-c3 appear to be activity dependent. Shen *et al.* (2006) found, in cultured CD-1 mice *flexor digitorum brevis* fibres, that NFAT-c3 did not shuttle in and out of the nucleus at rest even with the blockage of CRM1 (an export kinase) and suggested that stimulation is required for the nuclear localisation of NFAT-c3 (Shen*, et al.*, 2006). In neuronal cells, NFAT-c3 rapidly dephosphorylated and translocated to the nucleus in response to Ca^{2+} transients (Ulrich*, et al.*, 2012). Additionally, the present study found that NFAT-c3 is activity dependent due to the increase in nuclear localization in response to 10-days of CLFS. As for a role in resting fibre type maintenance, the proportion of NFAT-c3 positive nuclei is significant in all fibres not expressing MyHC-IIb when compared to NFAT-c1 levels. Overall, the results of this study indicate that NFAT-c3 is involved in the promotion of type-IIA fibres and is important for CLFS induced fibre type transitions.

4.6 CONCLUSIONS

The objective of this study was to better understand the mechanisms involved in skeletal muscle adaptation to environmental stimuli as well as the pathways that control fibre type transitions. This hypothesis driven basic study was designed to further characterize the cellular signals regulating activity-induced fibre type transitions. Results suggest that all four NFAT isoforms are involved in skeletal muscle in non-redundant roles. In contrast to the hypothesis, the proportion of fibres expressing a specific NFAT isoform at rest did not differ between fibre types. In response to CLFS, however, NFAT-c1 and NFAT-c3 were involved in the *fast-to-slow* fibre type transformation in *peroneus longus m*. Specifically, NFAT-c3 was involved in transformation surrounding type-IIA fibres. Concurrent data were consistent with NFAT-c2 being involved in determination of the type-IID(X) phenotype at rest. As expected, NFAT-c4 remained stable with stimulation, consistent with a role is in cell maintenance. Thus, CLFS-induced shifts in the nuclear localization of NFAT-isoforms within transforming muscle fibres provide new insights regarding the specific MyHC-isoform likely targeted.

Future investigations should include the earlier and later time points of CLFS. Since the fibre type transition in this analysis occurred more readily than some of the other mixed fast-twitch muscles, earlier time points (*i.e.,* 1- and 2-days of CLFS) would elucidate the preceding changes in NFAT. The later time point (*i.e.,* 21-days of CLFS) would provide insight into NFAT at rest in a phenotypically slower muscle. As well, valuable information could be gained through additional quantitative assays that would provide further insight as to the location of the 4 NFAT isoforms at rest and in response to stimulation (*e.g.,* Phosphorylation status of each NFAT isoform, and single fibre analysis). Lastly, further investigation into the many export and maintenance kinases that act on NFAT would provide insight into the overall balance of NFAT content in the nucleus.

REFERENCES

Abdelmalki, A., Fimbel, S., Mayet-Sornay, M. H., Sempore, B., & Favier, R. (1996). Aerobic capacity and skeletal muscle properties of normoxic and hypoxic rats in response to training. *Pflugers Arch, 431*(5), 671-679.

Al-Shanti, N., & Stewart, C. E. (2009). Ca2+/calmodulin-dependent transcriptional pathways: potential mediators of skeletal muscle growth and development. *Biol Rev Camb Philos Soc, 84*(4), 637-652.

Allen, D. L., & Leinwand, L. A. (2002). Intracellular Calcium and Myosin Isoform Transitions. *The Journal of Biological Chemistry, 277*(47), 7.

Allen, D. L., Sartorius, C. A., Sycuro, L. K., & Leinwand, L. A. (2001). Different Pathways Regulate Expression of the Skeletal Myosin Heavy Chain Genes. *The Journal of Biological Chemistry, 276*(47), 9.

Andersen, J. L., Klitgaard, H., & Saltin, B. (1994). Myosin heavy chain isoforms in single fibres from m. vastus lateralis of sprinters: influence of training. *Acta Physiol Scand, 151*(2), 135-142.

Armstrong, R. B., & Phelps, R. O. (1984). Muscle fiber type composition of the rat hindlimb. *Am J Anat, 171*(3), 259-272.

Armstrong, S. P., Caunt, C. J., Fowkes, R. C., Tsaneva-Atanasova, K., & McArdle, C. A. (2009). Pulsatile and sustained gonadotropin-releasing hormone (GnRH) receptor signaling: does the Ca2+/NFAT signaling pathway decode GnRH pulse frequency? *J Biol Chem, 284*(51), 35746-35757.

Ausoni, S., Gorza, L., Schiaffino, S., Gundersen, K., & Lomo, T. (1990). Expression of myosin heavy chain isoforms in stimulated fast and slow rat muscles. *J Neurosci, 10*(1), 153-160.

Bar, A., & Pette, D. (1988). Three fast myosin heavy chains in adult rat skeletal muscle. *FEBS Lett, 235*(1-2), 153-155.

Bass, A., Brdiczka, D., Eyer, P., Hofer, S., & Pette, D. (1969). Metabolic differentiation of distinct muscle types at the level of enzymatic organization. *Eur J Biochem, 10*(2), 198-206.

Bassel-Duby, R., & Olson, E. N. (2006). Signaling Pathways in Skeletal Muscle Remodeling. [Review]. *Annual Review of Biochemistry, 75*, 18.

Baylor, S. M., & Hollingworth, S. (2003). Sarcoplasmic reticulum calcium release compared in slow-twitch and fast-twitch fibres of mouse muscle. *J Physiol, 551*(Pt 1), 125-138.

Beals, C. R., Clipstone, N. A., Ho, S. N., & Crabtree, G. R. (1997). Nuclear localization of NF-ATc by a calcineurin-dependent, cyclosporin-sensitive intramolecular interaction. *Genes Dev, 11*(7), 824-834.

Beals, C. R., Sheridan, C. M., Turck, C. W., Gardner, P., & Crabtree, G. R. (1997). Nuclear export of NF-ATc enhanced by glycogen synthase kinase-3. *Science, 275*(5308), 1930-1934.

Bottinelli, R., Betto, R., Schiaffino, S., & Reggiani, C. (1994a). Maximum shortening velocity and coexistence of myosin heavy chain isoforms in single skinned fast fibres of rat skeletal muscle. *J Muscle Res Cell Motil, 15*(4), 413-419.

Bottinelli, R., Betto, R., Schiaffino, S., & Reggiani, C. (1994b). Unloaded shortening velocity and myosin heavy chain and alkali light chain isoform composition in rat skeletal muscle fibres. *J Physiol, 478 (Pt 2)*, 341-349.

Bottinelli, R., Canepari, M., Reggiani, C., & Stienen, G. J. (1994). Myofibrillar ATPase activity during isometric contraction and isomyosin

composition in rat single skinned muscle fibres. *J Physiol, 481 (Pt 3)*, 663-675.

Bottinelli, R., Schiaffino, S., & Reggiani, C. (1991). Force-velocity relations and myosin heavy chain isoform compositions of skinned fibres from rat skeletal muscle. *J Physiol, 437*, 655-672.

Bradley, K. C., Groth, R. D., & Mermelstein, P. G. (2005). Immunolocalization of NFATc4 in the adult mouse brain. *J Neurosci Res, 82*(6), 762-770.

Brooke, M. H., & Kaiser, K. K. (1970). Three "myosin adenosine triphosphatase" systems: the nature of their pH lability and sulfhydryl dependence. *J Histochem Cytochem, 18*(9), 670-672.

Brown, M. D., Cotter, M. A., Hudlicka, O., & Vrbova, G. (1976). The effects of different patterns of muscle activity on capillary density, mechanical properties and structure of slow and fast rabbit muscles. *Pflugers Arch, 361*(3), 241-250.

Buller, A. J., Eccles, J. C., & Eccles, R. M. (1960). Interactions between motoneurones and muscle in respect of the characteristic speeds of their responses. *The Journal of Physiology, 150*(February), 22.

Butler-Browne, G. S., Bugaisky, L. B., Cuenoud, S., Schwartz, K., & Whalen, R. G. (1982). Denervation of newborn rat muscle does not block the appearance of adult fast myosin heavy chain. *Nature, 299*(5886), 830-833.

Caiozzo, V. J., Baker, M. J., Huang, K., Chou, H., Wu, Y. Z., & Baldwin, K. M. (2003). Single-fiber myosin heavy chain polymorphism: how many patterns and what proportions? *Am J Physiol Regul Integr Comp Physiol, 285*(3), R570-580.

Calabria, E., Ciciliot, S., Moretti, I., Garcia, M., Picard, A., Dyar, K. A., Pallafacchina, G., Tothova, J., Schiaffino, S., & Murgia, M. (2009). NFAT isoforms control activity-dependent muscle fiber type specification. *Proc Natl Acad Sci U S A, 106*(32), 13335-13340.

Carrington, C. A., Fisher, W., & White, M. J. (1999). The effects of athletic training and muscle contractile character on the pressor response to isometric exercise of the human triceps surae. *Eur J Appl Physiol Occup Physiol, 80*(4), 337-343.

Carroll, S. L., Klein, M. G., & Schneider, M. F. (1997). Decay of calcium transients after electrical stimulation in rat fast- and slow-twitch skeletal muscle fibres. *Journal of Physiology, 501*(3), 15.

Carroll, S. L., Nicotera, P., & Pette, D. (1999). Calcium transients in single muscle fibres of low-frequency stimulated fast=twithc muscle of rat. *American Journal Physiology Cell Physiology, 277*(6 46-6), 7.

Carroll, T. J., Abernethy, P. J., Logan, P. A., Barber, M., & McEniery, M. T. (1998). Resistance training frequency: strength and myosin heavy chain responses to two and three bouts per week. *Eur J Appl Physiol Occup Physiol, 78*(3), 270-275.

Chin, E. R., Olson, E. N., Richardson, J. A., Yang, Q., Humphries, C., Shelton, J. M., Wu, H., Zhu, W., Bassel-Duby, R., & Williams, R. S. (1998). A calcineurin-dependent transcriptional pathway controls skeletal muscle fiber type. *Genes Dev, 12*(16), 2499-2509.

Chow, C. W., Dong, C., Flavell, R. A., & Davis, R. J. (2000). c-Jun NH(2)-terminal kinase inhibits targeting of the protein phosphatase calcineurin to NFATc1. *Mol Cell Biol, 20*(14), 5227-5234.

Chow, C. W., Rincon, M., Cavanagh, J., Dickens, M., & Davis, R. J. (1997). Nuclear accumulation of NFAT4 opposed by the JNK signal transduction pathway. *Science, 278*(5343), 1638-1641.

Chuvpilo, S., Jankevics, E., Tyrsin, D., Akimzhanov, A., Moroz, D., Jha, M. K., Schulze-Luehrmann, J., Santner-Nanan, B., Feoktistova, E., Konig, T., Avots, A., Schmitt, E., Berberich-Siebelt, F., Schimpl, A., & Serfling, E. (2002). Autoregulation of NFATc1/A expression facilitates effector T cells to escape from rapid apoptosis. *Immunity, 16*(6), 881-895.

Crabtree, G. R. (1999). Generic signals and specific outcomes: signaling through Ca2+, calcineurin, and NF-AT. *Cell, 96*(5), 611-614.

de la Pompa, J. L., Timmerman, L. A., Takimoto, H., Yoshida, H., Elia, A. J., Samper, E., Potter, J., Wakeham, A., Marengere, L., Langille, B. L., Crabtree, G. R., & Mak, T. W. (1998). Role of the NF-ATc transcription factor in morphogenesis of cardiac valves and septum. *Nature, 392*(6672), 182-186.

Delling, U., Tureckova, J., Lim, H. W., De Windt, L. J., Rotwein, P., & Molkentin, J. D. (2000). A calcineurin-NFATc3-dependent pathway regulates skeletal muscle differentiation and slow myosin heavy-chain expression. *Mol Cell Biol, 20*(17), 6600-6611.

Dolmetsch, R. E., Lewis, R. S., Goodnow, C. C., & Healy, J. I. (1997). Differential activation of transcription factors induced by Ca2+ response amplitude and duration. *Nature, 386*(6627), 855-858.

Dunn, S. E., Burns, J. L., & Michel, R. N. (1999). Calcineurin is required for skeletal muscle hypertrophy. *J Biol Chem, 274*(31), 21908-21912.

Dunn, S. E., Chin, E. R., & Michel, R. N. (2000). Matching of calcineurin activity to upstream effectors is critical for skeletal muscle fiber growth. *J Cell Biol, 151*(3), 663-672.

Dunn, S. E., & Michel, R. N. (1999). Differential sensitivity of myosin-heavy-chain-typed fibers to distinct aggregates of nerve-mediated activation. *Pflugers Arch, 437*(3), 432-440.

Dunn, S. E., Simard, A. R., Bassel-Duby, R., Williams, R. S., & Michel, R. N. (2001). Nerve activity-dependent modulation of calcineurin signaling in adult fast and slow skeletal muscle fibers. *J Biol Chem, 276*(48), 45243-45254.

Dunn, S. E., Simard, A. R., Prud'homme, R. A., & Michel, R. N. (2002). Calcineurin and skeletal muscle growth. *Nat Cell Biol, 4*(3), E46; author reply E46-47.

Esbjornsson, M., Hellsten-Westing, Y., Balsom, P. D., Sjodin, B., & Jansson, E. (1993). Muscle fibre type changes with sprint training: effect of training pattern. *Acta Physiol Scand, 149*(2), 245-246.

Esbjornsson, M., Jansson, E., Sundberg, C. J., Sylven, C., Eiken, O., Nygren, A., & Kaijser, L. (1993). Muscle fibre types and enzyme activities after training with local leg ischaemia in man. *Acta Physiol Scand, 148*(3), 233-241.

Fan, Y., Xie, P., Zhang, T., Zhang, H., Gu, D., She, M., & Li, H. (2008). Regulation of the stability and transcriptional activity of NFATc4 by ubiquitination. *FEBS Lett, 582*(29), 4008-4014.

Faulkner, J. A., Brooks, S. V., & Opiteck, J. A. (1993). Injury to skeletal muscle fibers during contractions: conditions of occurrence and prevention. *Phys Ther, 73*(12), 911-921.

Fraysse, B., Desaphy, J. F., Pierno, S., De Luca, A., Liantonio, A., Mitolo, C. I., & Camerino, D. C. (2003). Decrease in resting calcium and calcium entry associated with slow-to-fast transition in unloaded rat soleus muscle. *Faseb Journal, 17*(13), 1916-1918.

Fraysse, B., Desaphy, J. F., Rolland, J. F., Pierno, S., Liantonio, A., Giannuzzi, V., Camerino, C., Didonna, M. P., Cocchi, D., De Luca, A., & Conte Camerino, D. (2006). Fiber type-related changes in rat skeletal muscle calcium homeostasis during aging and restoration by growth hormone. *Neurobiol Dis, 21*(2), 372-380.

Frey, N., Frank, D., Lippl, S., Kuhn, C., Kogler, H., Barrientos, T., Rohr, C., Will, R., Muller, O. J., Weiler, H., Bassel-Duby, R., Katus, H. A., & Olson, E. N. (2008). Calsarcin-2 deficiency increases exercise capacity in mice through calcineurin/NFAT activation. *J Clin Invest, 118*(11), 3598-3608.

Frey, N., Richardson, J. A., & Olson, E. N. (2000). Calsarcins, a novel family of sarcomeric calcineurin-binding proteins. *Proc Natl Acad Sci U S A, 97*(26), 14632-14637.

Friedman, J. K., Nitta, C. H., Henderson, K. M., Codianni, S. J., Sanchez, L., Ramiro-Diaz, J. M., Howard, T. A., Giermakowska, W., Kanagy, N. L., & Gonzalez Bosc, L. V. (2013). Intermittent hypoxia-induced increases in reactive oxygen species activate NFATc3 increasing endothelin-1 vasoconstrictor reactivity. *Vascul Pharmacol*.

Gallo, M., Gordon, T., Syrotuik, D., Shu, Y., Tyreman, N., MacLean, I., Kenwell, Z., & Putman, C. T. (2006). Effects of long-term creatine feeding and running on isometric functional measures and myosin heavy chain content of rat skeletal muscles. *Pflugers Arch, 452*(6), 744-755.

Gallo, M., MacLean, I., Tyreman, N., Martins, K. J., Syrotuik, D., Gordon, T., & Putman, C. T. (2008). Adaptive responses to creatine loading and exercise in fast-twitch rat skeletal muscle. *Am J Physiol Regul Integr Comp Physiol, 294*(4), R1319-1328.

Glimcher, L. H., & Murphy, K. M. (2000). Lineage commitment in the immune system: the T helper lymphocyte grows up. *Genes Dev, 14*(14), 1693-1711.

Gomez del Arco, P., Martinez-Martinez, S., Maldonado, J. L., Ortega-Perez, I., & Redondo, J. M. (2000). A role for the p38 MAP kinase pathway in the nuclear shuttling of NFATp. *J Biol Chem, 275*(18), 13872-13878.

Graef, I. A., Chen, F., Chen, L., Kuo, A., & Crabtree, G. R. (2001). Signals transduced by Ca(2+)/calcineurin and NFATc3/c4 pattern the developing vasculature. *Cell, 105*(7), 863-875.

Green, H. J., Dusterhoft, S., Dux, L., & Pette, D. (1992). Metabolite patterns related to exhaustion, recovery and transformation of chronically stimulated rabbit fast-twitch muscle. *Pflugers Arch, 420*(3-4), 359-366.

Green, H. J., Grange, F., Chin, C., Goreham, C., & Ranney, D. (1998). Exercise-induced decreases in sarcoplasmic reticulum Ca(2+)-ATPase activity attenuated by high-resistance training. *Acta Physiol Scand, 164*(2), 141-146.

Green, H. J., & Pette, D. (1997). Early metabolic adaptations of rabbit fast-twitch muscle to chronic low-frequency stimulation. *Eur J Appl Physiol Occup Physiol, 75*(5), 418-424.

Gundersen, K., Leberer, E., Lomo, T., Pette, D., & Staron, R. S. (1988). Fibre types, calcium-sequestering proteins and metabolic enzymes in

denervated and chronically stimulated muscles of the rat. *J Physiol, 398*, 177-189.

Hämalainen, N., & Pette, D. (1993). The histochemical profiles of fast fiber types IIB, IID, and IIA in skeletal muscles of mouse, rat, and rabbit. *J Histochem Cytochem, 41*(5), 733-743.

Hämalainen, N., & Pette, D. (1995). Patterns of myosin isoforms in mammalian skeletal muscle fibres. *Microsc Res Tech, 30*(5), 381-389.

Harber, M., & Trappe, S. (2008). Single muscle fiber contractile properties of young competitive distance runners. *J Appl Physiol (1985), 105*(2), 629-636.

Hartner, K. T., Kirschbaum, B. J., & Pette, D. (1989). The multiplicity of troponin T isoforms. Distribution in normal rabbit muscles and effects of chronic stimulation. *Eur J Biochem, 179*(1), 31-38.

Hartner, K. T., & Pette, D. (1990). Fast and slow isoforms of troponin I and troponin C. Distribution in normal rabbit muscles and effects of chronic stimulation. *Eur J Biochem, 188*(2), 261-267.

Hather, B. M., Tesch, P. A., Buchanan, P., & Dudley, G. A. (1991). Influence of eccentric actions on skeletal muscle adaptations to resistance training. *Acta Physiol Scand, 143*(2), 177-185.

Healy, J. I., Dolmetsch, R. E., Timmerman, L. A., Cyster, J. G., Thomas, M. L., Crabtree, G. R., Lewis, R. S., & Goodnow, C. C. (1997). Different nuclear signals are activated by the B cell receptor during positive versus negative signaling. *Immunity, 6*(4), 419-428.

Henneman, E. (1985). The size-principle: a deterministic output emerges from a set of probabilistic connections. *J Exp Biol, 115*, 105-112.

Henneman, E., Clamann, H. P., Gillies, J. D., & Skinner, R. D. (1974). Rank order of motoneurons within a pool: law of combination. *J Neurophysiol, 37*(6), 1338-1349.

Hennig, R., & Lømo, T. (1985). Firing patterns of motor units in normal rats. *Nature, 314*(6007), 164-166.

Hermansen, L., & Wachtlova, M. (1971). Capillary density of skeletal muscle in well-trained and untrained men. *J Appl Physiol, 30*(6), 860-863.

Hicks, A., Ohlendieck, K., Gopel, S. O., & Pette, D. (1997). Early functional and biochemical adaptations to low-frequency stimulation of rabbit fast-twitch muscle. *Am J Physiol, 273*(1 Pt 1), C297-305.

Higginson, J., Wackerhage, H., Woods, N., Schjerling, P., Ratkevicius, A., Grunnet, N., & Quistorff, B. (2002). Blockades of mitogen-activated protein kinase and calcineurin both change fibre-type markers in skeletal muscle culture. *Pflugers Arch, 445*(3), 437-443.

Hogan, P. G., Chen, L., Nardone, J., & Rao, A. (2003). Transcriptional regulation by calcium, calcineurin, and NFAT. *Genes Dev, 17*(18), 2205-2232.

Holloszy, J. O. (1967). Biochemical adaptations in muscle. Effects of exercise on mitochondrial oxygen uptake and respiratory enzyme activity in skeletal muscle. *J Biol Chem, 242*(9), 2278-2282.

Hood, D. A., Zak, R., & Pette, D. (1989). Chronic stimulation of rat skeletal muscle induces coordinate increases in mitochondrial and nuclear mRNAs of cytochrome-c-oxidase subunits. *Eur J Biochem, 179*(2), 275-280.

Horsley, V., Friday, B. B., Matteson, S., Kegley, K. M., Gephart, J., & Pavlath, G. K. (2001). Regulation of the growth of multinucleated muscle cells by an NFATC2-dependent pathway. *J Cell Biol, 153*(2), 329-338.

Horsley, V., Jansen, K. M., Mills, S. T., & Pavlath, G. K. (2003). IL-4 acts as a myoblast recruitment factor during mammalian muscle growth. *Cell, 113*(4), 483-494.

Horsley, V., & Pavlath, G. K. (2002). NFAT: ubiquitous regulator of cell differentiation and adaptation. *J Cell Biol, 156*(5), 771-774.

Horsley, V., & Pavlath, G. K. (2003). Prostaglandin F2(alpha) stimulates growth of skeletal muscle cells via an NFATC2-dependent pathway. *J Cell Biol, 161*(1), 111-118.

Hu, P., Yin, C., Zhang, K. M., Wright, L. D., Nixon, T. E., Wechsler, A. S., Spratt, J. A., & Briggs, F. N. (1995). Transcriptional regulation of phospholamban gene and translational regulation of SERCA2 gene produces coordinate expression of these two sarcoplasmic reticulum proteins during skeletal muscle phenotype switching. *J Biol Chem, 270*(19), 11619-11622.

Ikeda, F., Nishimura, R., Matsubara, T., Hata, K., Reddy, S. V., & Yoneda, T. (2006). Activation of NFAT signal in vivo leads to osteopenia associated with increased osteoclastogenesis and bone-resorbing activity. *Journal of Immunology, 177*(4), 2384-2390.

Jain, J., Burgeon, E., Badalian, T. M., Hogan, P. G., & Rao, A. (1995). A similar DNA-binding motif in NFAT family proteins and the Rel homology region. *J Biol Chem, 270*(8), 4138-4145.

Jansson, E., Esbjornsson, M., Holm, I., & Jacobs, I. (1990). Increase in the proportion of fast-twitch muscle fibres by sprint training in males. *Acta Physiol Scand, 140*(3), 359-363.

Jaschinski, F., Schuler, M., Peuker, H., & Pette, D. (1998). Changes in myosin heavy chain mRNA and protein isoforms of rat muscle during forced contractile activity. *Am J Physiol, 274*(2 Pt 1), C365-370.

Kar, P., Nelson, C., & Parekh, A. B. (2011). Selective activation of the transcription factor NFAT1 by calcium microdomains near Ca2+ release-activated Ca2+ (CRAC) channels. *J Biol Chem, 286*(17), 14795-14803.

Kaufmann, M., Simoneau, J. A., Veerkamp, J. H., & Pette, D. (1989). Electrostimulation-induced increases in fatty acid-binding protein and myoglobin in rat fast-twitch muscle and comparison with tissue levels in heart. *FEBS Lett, 245*(1-2), 181-184.

Kegley, K. M., Gephart, J., Warren, G. L., & Pavlath, G. K. (2001). Altered primary myogenesis in NFATC3(-/-) mice leads to decreased muscle size in the adult. *Dev Biol, 232*(1), 115-126.

Kernell, D., & Hensbergen, E. (1998). Use and fibre type composition in limb muscles of cats. *Eur J Morphol, 36*(4-5), 288-292.

Klug, G. A., Leberer, E., Leisner, E., Simoneau, J. A., & Pette, D. (1988). Relationship between parvalbumin content and the speed of relaxation in chronically stimulated rabbit fast-twitch muscle. *Pflugers Arch, 411*(2), 126-131.

Lee, H., Chouinard, L., Bonin, M., & Michel, R. N. (2005). NFATc3 deficiency may contribute to the development of mammary gland adenocarcinoma in aging female mice. *Mol Carcinog, 44*(3), 219-222.

Lee, H. L., Bae, O. Y., Baek, K. H., Kwon, A., Hwang, H. R., Qadir, A. S., Park, H. J., Woo, K. M., Ryoo, H. M., & Baek, J. H. (2011). High extracellular

calcium-induced NFATc3 regulates the expression of receptor activator of NF-kappaB ligand in osteoblasts. *Bone, 49*(2), 242-249.

Leeuw, T., & Pette, D. (1993). Coordinate changes in the expression of troponin subunit and myosin heavy-chain isoforms during fast-to-slow transition of low-frequency-stimulated rabbit muscle. *Eur J Biochem, 213*(3), 1039-1046.

Leeuw, T., & Pette, D. (1996). Coordinate changes of myosin light and heavy chain isoforms during forced fiber type transitions in rabbit muscle. *Dev Genet, 19*(2), 163-168.

Li, H., Rao, A., & Hogan, P. G. (2011). Interaction of calcineurin with substrates and targeting proteins. *Trends Cell Biol, 21*(2), 91-103.

Li, L., Ke, K., Tan, X., Xu, W., Shen, J., Zhai, T., Xu, L., Rui, Y., Zheng, H., Zhai, P., Zhao, J., & Cao, M. (2013). Up-regulation of NFATc4 involves in neuronal apoptosis following intracerebral hemorrhage. *Cell Mol Neurobiol, 33*(7), 893-905.

Liu, J., Arai, K., & Arai, N. (2001). Inhibition of NFATx activation by an oligopeptide: disrupting the interaction of NFATx with calcineurin. *Journal of Immunology, 167*(5), 2677-2687.

Liu, Y., Shen, T., Randall, W. R., & Schneider, M. F. (2005). Signaling pathways in activity-dependent fiber type plasticity in adult skeletal muscle. *J Muscle Res Cell Motil, 26*(1), 13-21.

Ljubicic, V., Adhihetty, P. J., & Hood, D. A. (2005). Application of animal models: Chronic electrical stimulation-induced contractile activity. *Canadian Journal of Applied Physiology-Revue Canadienne De Physiologie Appliquee, 30*(5), 625-643.

Lopez-Rodriguez, C., Aramburu, J., Rakeman, A. S., Copeland, N. G., Gilbert, D. J., Thomas, S., Disteche, C., Jenkins, N. A., & Rao, A. (1999). NF-AT5: the NF-AT family of transcription factors expands in a new direction. *Cold Spring Harb Symp Quant Biol, 64*, 517-526.

Luo, C., Copeland, N. G., Jenkins, N. A., Edelhoff, S., Disteche, C., Hogan, P. G., & Rao, A. (1996). Normal function of the transcription factor NFAT1 in wasted mice. Chromosome localization of NFAT1 gene. *Gene, 180*(1-2), 29-36.

Lynch, G. S., Rodgers, B. J., & Williams, D. A. (1993). The effects of age and low-intensity endurance exercise on the contractile properties of single skinned fast- and slow-twitch skeletal muscle fibres. *Growth Dev Aging, 57*(3), 147-161.

Maffiuletti, N. A., Martin, A., Babault, N., Pensini, M., Lucas, B., & Schieppati, M. (2001). Electrical and mechanical H(max)-to-M(max) ratio in power- and endurance-trained athletes. *J Appl Physiol (1985), 90*(1), 3-9.

Martin, T. P., Vailas, A. C., Durivage, J. B., Edgerton, V. R., & Castleman, K. R. (1985). Quantitative histochemical determination of muscle enzymes: biochemical verification. *J Histochem Cytochem, 33*(10), 1053-1059.

Martins, K. J., Gordon, T., Pette, D., Dixon, W. T., Foxcroft, G. R., Maclean, I. M., & Putman, C. T. (2006). Effect of satellite cell ablation on low-frequency-stimulated fast-to-slow fibre-type transitions in rat skeletal muscle. *J Physiol, 572*(Pt 1), 281-294.

Martins, K. J., Murdoch, G. K., Shu, Y., Harris, R. L., Gallo, M., Dixon, W. T., Foxcroft, G. R., Gordon, T., & Putman, C. T. (2009). Satellite cell ablation attenuates short-term fast-to-slow fibre type transformations in rat fast-twitch skeletal muscle. *Pflugers Arch, 458*(2), 325-335.

Martins, K. J., St-Louis, M., Murdoch, G. K., MacLean, I. M., McDonald, P., Dixon, W. T., Putman, C. T., & Michel, R. N. (2012). Nitric oxide synthase inhibition prevents activity-induced calcineurin-NFATc1 signalling and fast-to-slow skeletal muscle fibre type conversions. *J Physiol, 590*(Pt 6), 1427-1442.

McCullagh, K. J., Calabria, E., Pallafacchina, G., Ciciliot, S., Serrano, A. L., Argentini, C., Kalhovde, J. M., Lomo, T., & Schiaffino, S. (2004). NFAT is a nerve activity sensor in skeletal muscle and controls activity-dependent myosin switching. *Proc Natl Acad Sci U S A, 101*(29), 10590-10595.

McKinsey, T. A., Zhang, C. L., & Olson, E. N. (2001). Identification of a signal-responsive nuclear export sequence in class II histone deacetylases. *Mol Cell Biol, 21*(18), 6312-6321.

Meissner, J. D., Chang, K. C., Kubis, H. P., Nebreda, A. R., Gros, G., & Scheibe, R. J. (2007). The p38alpha/beta mitogen-activated protein kinases mediate recruitment of CREB-binding protein to preserve fast myosin heavy chain IId/x gene activity in myotubes. *J Biol Chem, 282*(10), 7265-7275.

Meissner, J. D., Umeda, P. K., Chang, K. C., Gros, G., & Scheibe, R. J. (2007). Activation of the beta myosin heavy chain promoter by MEF-2D, MyoD, p300, and the calcineurin/NFATc1 pathway. *J Cell Physiol, 211*(1), 138-148.

Muller, M. R., & Rao, A. (2010). NFAT, immunity and cancer: a transcription factor comes of age. *Nat Rev Immunol, 10*(9), 645-656.

Muller, M. R., Sasaki, Y., Stevanovic, I., Lamperti, E. D., Ghosh, S., Sharma, S., Gelinas, C., Rossi, D. J., Pipkin, M. E., Rajewsky, K., Hogan, P. G., & Rao, A. (2009). Requirement for balanced Ca/NFAT signaling in

hematopoietic and embryonic development. *Proc Natl Acad Sci U S A, 106*(17), 7034-7039.

Mutungi, G. (2007). The expression of NFATc1 in adult rat skeletal muscle fibres. *Experimental Physiology, 93*(3), 7.

Mutungi, G. (2008). The expression of NFATc1 in adult rat skeletal muscle fibres. *Exp Physiol, 93*(3), 399-406.

Naya, F. J., Mercer, B., Shelton, J., Richardson, J. A., Williams, R. S., & Olson, E. N. (2000). Stimulation of slow skeletal muscle fiber gene expression by calcineurin in vivo. *J Biol Chem, 275*(7), 4545-4548.

Oh-hora, M., & Rao, A. (2009). The calcium/NFAT pathway: role in development and function of regulatory T cells. *Microbes Infect, 11*(5), 612-619.

Ohlendieck, K., Briggs, F. N., Lee, K. F., Wechsler, A. W., & Campbell, K. P. (1991). Analysis of excitation-contraction-coupling components in chronically stimulated canine skeletal muscle. *Eur J Biochem, 202*(3), 739-747.

Okamura, H., Aramburu, J., Garcia-Rodriguez, C., Viola, J. P., Raghavan, A., Tahiliani, M., Zhang, X., Qin, J., Hogan, P. G., & Rao, A. (2000). Concerted dephosphorylation of the transcription factor NFAT1 induces a conformational switch that regulates transcriptional activity. *Mol Cell, 6*(3), 539-550.

Parsons, S. A., Millay, D. P., Wilkins, B. J., Bueno, O. F., Tsika, G. L., Neilson, J. R., Liberatore, C. M., Yutzey, K. E., Crabtree, G. R., Tsika, R. W., & Molkentin, J. D. (2004). Genetic loss of calcineurin blocks mechanical overload-induced skeletal muscle fiber type switching but not hypertrophy. *J Biol Chem, 279*(25), 26192-26200.

Parsons, S. A., Wilkins, B. J., Bueno, O. F., & Molkentin, J. D. (2003). Altered skeletal muscle phenotypes in calcineurin Aalpha and Abeta gene-targeted mice. *Mol Cell Biol, 23*(12), 4331-4343.

Pavlath, G. K., Rich, K., Webster, S. G., & Blau, H. M. (1989). Localization of muscle gene products in nuclear domains. *Nature, 337*(6207), 570-573.

Peng, S. L., Gerth, A. J., Ranger, A. M., & Glimcher, L. H. (2001). NFATc1 and NFATc2 together control both T and B cell activation and differentiation. *Immunity, 14*(1), 13-20.

Perotti, V., Baldassari, P., Bersani, I., Molla, A., Vegetti, C., Tassi, E., Dal Col, J., Dolcetti, R., Anichini, A., & Mortarini, R. (2012). NFATc2 is a potential therapeutic target in human melanoma. *Journal of Investigative Dermatology, 132*(11), 2652-2660.

Pette, D. (1991). Effects of chronic electrostimulation on muscle gene expression. *Semin Thorac Cardiovasc Surg, 3*(2), 101-105.

Pette, D. (1997). Functional and biochemical adaptations to low-frequency stimulation: possible applications to microgravity. *Int J Sports Med, 18 Suppl 4*, S302-304.

Pette, D., Muller, W., Leisner, E., & Vrbova, G. (1976). Time dependent effects on contractile properties, fibre population, myosin light chains and enzymes of energy metabolism in intermittently and continuously stimulated fast twitch muscles of the rabbit. *Pflugers Arch, 364*(2), 103-112.

Pette, D., Ramirez, B. U., Muller, W., Simon, R., Exner, G. U., & Hildebrand, R. (1975). Influence of intermittent long-term stimulation on contractile,

histochemical and metabolic properties of fibre populations in fast and slow rabbit muscles. *Pflugers Arch, 361*(1), 1-7.

Pette, D., Sketelj, J., Skorjanc, D., Leisner, E., Traub, I., & Bajrovic, F. (2002). Partial fast-to-slow conversion of regenerating rat fast-twitch muscle by chronic low-frequency stimulation. *J Muscle Res Cell Motil, 23*(3), 215-221.

Pette, D., Smith, M. E., Staudte, H. W., & Vrbova, G. (1973). Effects of long-term electrical stimulation on some contractile and metabolic characteristics of fast rabbit muscles. *Pflugers Arch, 338*(3), 257-272.

Pette, D., & Staron, R. S. (1990). Cellular and molecular diversities of mammalian skeletal muscle fibers. *Rev Physiol Biochem Pharmacol, 116*, 1-76.

Pette, D., & Staron, R. S. (1997). Mammalian skeletal muscle fiber type transitions. *Int Rev Cytol, 170*, 143-223.

Pette, D., & Staron, R. S. (2000). Myosin isoforms, muscle fiber types, and transitions. *Microsc Res Tech, 50*(6), 500-509.

Pette, D., & Staron, R. S. (2001). Transitions of muscle fiber phenotypic profiles. *Histochem Cell Biol, 115*(5), 359-372.

Pette, D., & Vrbova, G. (1992). Adaptation of mammalian skeletal muscle fibers to chronic electrical stimulation. *Rev Physiol Biochem Pharmacol, 120*, 115-202.

Pette, D., & Vrbova, G. (1999). What does chronic electrical stimulation teach us about muscle plasticity? *Muscle Nerve, 22*(6), 666-677.

Putman, C. T., Dixon, W. T., Pearcey, J. A., Maclean, I. M., Jendral, M. J., Kiricsi, M., Murdoch, G. K., & Pette, D. (2004). Chronic low-frequency

stimulation upregulates uncoupling protein-3 in transforming rat fast-twitch skeletal muscle. *Am J Physiol Regul Integr Comp Physiol, 287*(6), R1419-1426.

Putman, C. T., Dusterhoft, S., & Pette, D. (1999). Changes in satellite cell content and myosin isoforms in low-frequency-stimulated fast muscle of hypothyroid rat. *J Appl Physiol, 86*(1), 40-51.

Putman, C. T., Dusterhoft, S., & Pette, D. (2000). Satellite cell proliferation in low frequency-stimulated fast muscle of hypothyroid rat. *Am J Physiol Cell Physiol, 279*(3), C682-690.

Putman, C. T., Jones, N. L., & Heigenhauser, G. J. (2003). Effects of short-term training on plasma acid-base balance during incremental exercise in man. *J Physiol, 550*(Pt 2), 585-603.

Putman, C. T., Kiricsi, M., Pearcey, J., MacLean, I. M., Bamford, J. A., Murdoch, G. K., Dixon, W. T., & Pette, D. (2003). AMPK activation increases uncoupling protein-3 expression and mitochondrial enzyme activities in rat muscle without fibre type transitions. *J Physiol, 551*(Pt 1), 169-178.

Putman, C. T., Sultan, K. R., Wassmer, T., Bamford, J. A., Skorjanc, D., & Pette, D. (2001). Fiber-type transitions and satellite cell activation in low-frequency-stimulated muscles of young and aging rats. *J Gerontol A Biol Sci Med Sci, 56*(12), B510-519.

Rana, Z. A., Gundersen, K., & Buonanno, A. (2008). Activity-dependent repression of muscle genes by NFAT. *Proc Natl Acad Sci U S A, 105*(15), 5921-5926.

Ranatunga, K. W., & Thomas, P. E. (1990). Correlation between shortening velocity, force-velocity relation and histochemical fibre-type composition in rat muscles. *J Muscle Res Cell Motil, 11*(3), 240-250.

Ranger, A. M., Grusby, M. J., Hodge, M. R., Gravallese, E. M., de la Brousse, F. C., Hoey, T., Mickanin, C., Baldwin, H. S., & Glimcher, L. H. (1998). The transcription factor NF-ATc is essential for cardiac valve formation. *Nature, 392*(6672), 186-190.

Ranvier, L. (1873). Propietés et structure différentes des muscles rouges et des muscles blancs chez les lapins et chezles raies. *C R Acad Sci Paris, 77*, 4.

Rao, A., Luo, C., & Hogan, P. G. (1997). Transcription factors of the NFAT family: regulation and function. *Annu Rev Immunol, 15*, 707-747.

Reid, B., Martinov, V. N., Nja, A., Lomo, T., & Bewick, G. S. (2003). Activity-dependent plasticity of transmitter release from nerve terminals in rat fast and slow muscles. *J Neurosci, 23*(28), 9340-9348.

Salmons, S. (1994). Exercise, stimulation and type transformation of skeletal muscle. *Int J Sports Med, 15*(3), 136-141.

Salmons, S. (2009). Adaptive change in electrically stimulated muscle: a framework for the design of clinical protocols. *Muscle Nerve, 40*(6), 918-935.

Salmons, S., & Vrbova, G. (1967). Changes in the speed of mammalian fast muscle following longterm stimulation. *J Physiol, 192*(2), 39P-40P.

Salmons, S., & Vrbova, G. (1969). The influence of activity on some contractile characteristics of mammalian fast and slow muscles. *J Physiol, 201*(3), 535-549.

Schachat, F., Williams, R. S., & Schnurr, C. A. (1988). Coordinate changes in fast thin filament and Z-line protein expression in the early response to chronic stimulation. *J Biol Chem, 263*(28), 13975-13978.

Schiaffino, S., Gorza, L., Sartore, S., Saggin, L., Ausoni, S., Vianello, M., Gundersen, K., & Lomo, T. (1989). Three myosin heavy chain isoforms in type 2 skeletal muscle fibres. *J Muscle Res Cell Motil, 10*(3), 197-205.

Schiaffino, S., & Reggiani, C. (2011). Fiber types in mammalian skeletal muscles. *Physiol Rev, 91*(4), 1447-1531.

Serrano, A. L., Murgia, M., Pallafacchina, G., Calabria, E., Coniglio, P., Lomo, T., & Schiaffino, S. (2001). Calcineurin controls nerve activity-dependent specification of slow skeletal muscle fibers but not muscle growth. *Proc Natl Acad Sci U S A, 98*(23), 13108-13113.

Shaw, J. P., Utz, P. J., Durand, D. B., Toole, J. J., Emmel, E. A., & Crabtree, G. R. (1988). Identification of a putative regulator of early T cell activation genes. *Science, 241*(4862), 202-205.

Shen, T., Liu, Y., Randall, W. R., & Schneider, M. F. (2006). Parallel mechanisms for resting nucleo-cytoplasmic shuttling and activity dependent translocation provide dual control of transcriptional regulators HDAC and NFAT in skeletal muscle fiber type plasticity. *J Muscle Res Cell Motil, 27*(5-7), 405-411.

Sheridan, C. M., Heist, E. K., Beals, C. R., Crabtree, G. R., & Gardner, P. (2002). Protein kinase A negatively modulates the nuclear accumulation of NF-ATc1 by priming for subsequent phosphorylation by glycogen synthase kinase-3. *J Biol Chem, 277*(50), 48664-48676.

Sitara, D., & Aliprantis, A. O. (2010). Transcriptional regulation of bone and joint remodeling by NFAT. *Immunol Rev, 233*(1), 286-300.

Sketelj, J., Crne-Finderle, N., Strukelj, B., Trontelj, J. V., & Pette, D. (1998). Acetylcholinesterase mRNA level and synaptic activity in rat muscles depend on nerve-induced pattern of muscle activation. *J Neurosci, 18*(6), 1944-1952.

Skorjanc, D., Heine, G., & Pette, D. (1997). Time-dependent increase of succinate dehydrogenase activity in low-frequency stimulated rabbit muscle: a comparison between microphotometric and biochemical methods. *Histochem Cell Biol, 107*(1), 47-55.

Skorjanc, D., Jaschinski, F., Heine, G., & Pette, D. (1998). Sequential increases in capillarization and mitochondrial enzymes in low-frequency-stimulated rabbit muscle. *Am J Physiol, 274*(3 Pt 1), C810-818.

Solymar, D. C., Agarwal, S., Bassing, C. H., Alt, F. W., & Rao, A. (2002). A 3' enhancer in the IL-4 gene regulates cytokine production by Th2 cells and mast cells. *Immunity, 17*(1), 41-50.

Staron, R. S., Hikida, R. S., Murray, T. F., Hagerman, F. C., & Hagerman, M. T. (1989). Lipid depletion and repletion in skeletal muscle following a marathon. *J Neurol Sci, 94*(1-3), 29-40.

Staron, R. S., Malicky, E. S., Leonardi, M. J., Falkel, J. E., Hagerman, F. C., & Dudley, G. A. (1990). Muscle hypertrophy and fast fiber type conversions in heavy resistance-trained women. *Eur J Appl Physiol Occup Physiol, 60*(1), 71-79.

Takayanagi, H., Kim, S., Koga, T., Nishina, H., Isshiki, M., Yoshida, H., Saiura, A., Isobe, M., Yokochi, T., Inoue, J., Wagner, E. F., Mak, T. W., Kodama, T., & Taniguchi, T. (2002). Induction and activation of the transcription factor NFATc1 (NFAT2) integrate RANKL signaling in terminal differentiation of osteoclasts. *Dev Cell, 3*(6), 889-901.

Talmadge, R. J., Otis, J. S., Rittler, M. R., Garcia, N. D., Spencer, S. R., Lees, S. J., & Naya, F. J. (2004). Calcineurin activation influences muscle phenotype in a muscle-specific fashion. *BMC Cell Biol, 5*, 28.

Timmerman, L. A., Clipstone, N. A., Ho, S. N., Northrop, J. P., & Crabtree, G. R. (1996). Rapid shuttling of NF-AT in discrimination of Ca2+ signals and immunosuppression. *Nature, 383*(6603), 837-840.

Torgan, C. E., & Daniels, M. P. (2001). Regulation of myosin heavy chain expression during rat skeletal muscle development in vitro. *Mol Biol Cell, 12*(5), 1499-1508.

Tothova, J., Blaauw, B., Pallafacchina, G., Rudolf, R., Argentini, C., Reggiani, C., & Schiaffino, S. (2006). NFATc1 nucleocytoplasmic shuttling is controlled by nerve activity in skeletal muscle. *J Cell Sci, 119*(Pt 8), 1604-1611.

Trinh, H. H., & Lamb, G. D. (2006). Matching of sarcoplasmic reticulum and contractile properties in rat fast- and slow-twitch muscle fibres. *Clin Exp Pharmacol Physiol, 33*(7), 591-600.

Tsytsykova, A. V., & Goldfeld, A. E. (2000). Nuclear factor of activated T cells transcription factor NFATp controls superantigen-induced lethal shock. *J Exp Med, 192*(4), 581-586.

Ulrich, J. D., Kim, M. S., Houlihan, P. R., Shutov, L. P., Mohapatra, D. P., Strack, S., & Usachev, Y. M. (2012). Distinct activation properties of the nuclear factor of activated T-cells (NFAT) isoforms NFATc3 and NFATc4 in neurons. *J Biol Chem, 287*(45), 37594-37609.

Vashishta, A., Habas, A., Pruunsild, P., Zheng, J. J., Timmusk, T., & Hetman, M. (2009). Nuclear factor of activated T-cells isoform c4 (NFATc4/NFAT3) as a mediator of antiapoptotic transcription in

NMDA receptor-stimulated cortical neurons. *J Neurosci, 29*(48), 15331-15340.

Vechetti-Junior, I. J., Aguiar, A. F., de Souza, R. W., Almeida, F. L., de Almeida Dias, H. B., de Aguiar Silva, M. A., Carani, F. R., Ferraresso, R. L., Carvalho, R. F., & Dal-Pai-Silva, M. (2013). NFAT Isoforms Regulate Muscle Fiber Type Transition without Altering CaN during Aerobic Training. *Int J Sports Med*.

Watanabe, K., & Suzuki, A. (1999). Distribution, density, and structure of muscle spindles in the vastus intermedius and the peroneus longus muscles of sheep. *Okajimas Folia Anat Jpn, 76*(5), 203-219.

Williamson, D. L., Gallagher, P. M., Carroll, C. C., Raue, U., & Trappe, S. W. (2001). Reduction in hybrid single muscle fiber proportions with resistance training in humans. *J Appl Physiol (1985), 91*(5), 1955-1961.

Wu, H., Naya, F. J., McKinsey, T. A., Mercer, B., Shelton, J. M., Chin, E. R., Simard, A. R., Michel, R. N., Bassel-Duby, R., Olson, E. N., & Williams, R. S. (2000). MEF2 responds to multiple calcium-regulated signals in the control of skeletal muscle fiber type. *EMBO J, 19*(9), 1963-1973.

Wu, H., Peisley, A., Graef, I. A., & Crabtree, G. R. (2007). NFAT signaling and the invention of vertebrates. *Trends Cell Biol, 17*(6), 251-260.

Yamaguchi, T., Omori, M., Tanaka, N., & Fukui, N. (2013). Distinct and additive effects of sodium bicarbonate and continuous mild heat stress on fiber type shift via calcineurin/NFAT pathway in human skeletal myoblasts. *Am J Physiol Cell Physiol, 305*(3), C323-333.

Zhou, B., Cron, R. Q., Wu, B., Genin, A., Wang, Z., Liu, S., Robson, P., & Baldwin, H. S. (2002). Regulation of the murine Nfatc1 gene by NFATc2. *J Biol Chem, 277*(12), 10704-10711.